

FINAL REPORT
California Air Resources Board
CONTRACT NO. 09-341

**Peripheral Blood Gene Expression in Subjects with Coronary Artery Disease
and Exposure to Particulate Air Pollutant Components and Size Fractions**

Submitted by

Ralph J. Delfino, MD, PhD

Department of Epidemiology, School of Medicine, University of California, Irvine, 92697-7550

Prepared for the California Air Resources Board and
the California Environmental Protection Agency.

Coinvestigators:

Constantinos Sioutas, ScD, Department of Civil and Environmental Engineering, Viterbi School of Engineering, University of Southern California, Los Angeles, CA.

James J. Schauer, PhD, University of Wisconsin-Madison, Environmental Chemistry and Technology Program, Madison, WI.

Daniel J. Gillen, PhD, Department of Statistics, UC Irvine School of Information and Computer Science.

Norbert Staimer, PhD, Department of Epidemiology, UCI School of Medicine

April 25, 2014

ACKNOWLEDGEMENTS

We thank staff from the Department of Epidemiology and General Clinical Research Center, University of California Irvine, the Department of Civil and Environmental Engineering, University of Southern California, the University of Wisconsin-Madison, Environmental Chemistry and Technology Program, Madison, Wisconsin, the California Air Resources Board, and the South Coast Air Quality Management District. Thomas Tjoa, MPH, MS, served as our SAS programmer analyst. We also thank the other coinvestigators from the parent study, especially, Sharine Wittkopp, who conducted doctoral thesis work on the project, Dr. Susan Neuhausen, who consulted on the GST genotyping work, and Timothy Stinchcombe of Intrexon Corp., Blacksburg, Virginia, who directed some of the gene expression laboratory work on the Sequenom system.

This project is funded under the ARB's Dr. William F. Friedman Health Research Program. During Dr. Friedman's tenure on the Board, he played a major role in guiding ARB's health research program. His commitment to the citizens of California was evident through his personal and professional interest in the Board's health research, especially in studies related to children's health. The Board is sincerely grateful for all of Dr. Friedman's personal and professional contributions to the State of California.

This project was additionally supported by the National Institutes of Health, including National Institute of Environmental Health Sciences grant nos. R01-ES012243 and R21-ES016420, and the National Center for Research Resources grant no. MO1 RR00827. Additional support was provided by the California Air Resources Board contracts nos. 03-329 and 08-307. Sharine Wittkopp's Medical Science Training Fellowship was supported in part by the National Institutes of Health, National Institute of Environmental Health Sciences grant no. F30-ES21107.

This Report was submitted in fulfillment of California Air Resources Board contract no. 09-341 by the University of California, Irvine under the sponsorship of the California Air Resources Board. Work was completed as of May 15, 2014.

CONTENTS

FINAL REPORT (Draft Nov 15, 2013)	<i>i</i>
Acknowledgements	<i>ii</i>
CONTENTS	<i>iii</i>
Disclaimer	<i>iv</i>
LIST OF FIGURES	<i>v</i>
LIST OF TABLES	<i>vi</i>
ABSTRACT	<i>vii</i>
EXECUTIVE SUMMARY	<i>viii</i>
BODY OF REPORT	<i>10</i>
1. Chapter One: Introduction	<i>10</i>
1.1 Background	<i>10</i>
1.2. Design of the Parent Project, and Scope and Purpose of the Present Project.....	<i>13</i>
1.3. Tasks.....	<i>16</i>
2. Chapter Two: Task 1	<i>21</i>
2.0 Overview of sampling method and chemical analyses	<i>21</i>
2.1 Organic speciation analysis	<i>21</i>
2.2 In vitro measurement of PM-related ROS production in alveolar macrophages.	<i>22</i>
References	<i>28</i>
3. Chapter Three: Task 2	<i>30</i>
3.0 Introduction	<i>30</i>
3.1 Materials and Methods	<i>30</i>
3.1.1 Sampling sites and schedule.....	<i>30</i>
3.1.2 Source apportionment.....	<i>31</i>
3.2. Results and Discussion	<i>32</i>
3.2.1 Infiltration ratios of tracer species	<i>32</i>
3.2.2 Source contribution estimates.....	<i>33</i>
3.4 Summary and Conclusions	<i>34</i>

References	44
4. Chapter four: Task 3	47
4.0 Introduction.....	47
4.1 Methods.....	49
4.1.1 Gene Expression Profiling.....	49
4.1.2 Air pollutant exposures.....	51
4.1.3 Analysis.....	54
4.2 Results.....	55
4.3 Discussion.....	70
4.4 Summary and Conclusions.....	73
References	74
5. Chapter 5. Supplemental Analyses: Gene-Environment Interactions	77
6. Chapter 6. Overall Summary and Conclusions.....	91
7. Chapter 7. Recommendations.....	91
8. Presentations and Publications	92
9. Abbreviations.....	92
10. Appendix. Permutation Analysis Results for NFE2L2.....	94

DISCLAIMER

The statements and conclusions in this report are those of the University and not necessarily those of the California Air Resources Board. The mention of commercial products, their source, or their use in connection with material reported herein is not construed as actual or implied endorsement of such products.

LIST OF FIGURES

- Figure 1.1. Known or Suspected Oxidative Stress Response Pathways.
- Figure 1.2. Panel Study Flow Chart.
- Figure 1.3. Hypothesized pathways from PM exposure to adverse cardiovascular health effects (in red) for evaluation in the present study.
- Figure 3.1. Average concentration of a) PAHs, b) hopanes, c) n-alkanes and d) organic acids at the indoor and outdoor sampling sites during the warm and cold phases.
- Figure 3.2. Average indoor-to-outdoor ratios and Pearson correlation coefficients between indoor and outdoor concentrations of (a) PAHs, (b) hopanes, (c) n-alkanes and (d) organic acids during the warm and cold phases.
- Figure 3.3. Average carbon preference index (CPI) of n-alkanes (C₁₉-C₄₀) at the indoor and outdoor sampling sites during the warm and cold phases.
- Figure 3.4. Contribution of different sources to fine PM mass at the sampling sites during the warm and cold phases.
- Figure 4.1. Candidate Genes grouped by biopathway.
- Figure 4.2. Fold-Change and 95% confidence interval for qPCR expression level of *CYP1B1*, *HMOX1*, *IL1B*, *NQO1*, *NFE2L2*, *SELP*, and *SOD2* in association with outdoor traffic-related air pollutants measured hourly (elemental carbon, black carbon, primary organic carbon, and NO_x).
- Figure 4.3. Fold-Change and 95% confidence interval for qPCR expression level of *CYP1B1*, *HMOX1*, *IL1B*, *NQO1*, *NFE2L2*, *SELP*, and *SOD2* in association with outdoor particulate matter size fractions, polycyclic aromatic hydrocarbons and oxidative potential (measured as macrophage ROS production *in vitro*).
- Figure 4.4. Fold-Change and 95% confidence interval for qPCR expression level of *CYP1B1*, *HMOX1*, *IL1B*, *NQO1*, *NFE2L2*, *SELP*, and *SOD2* in association with indoor traffic-related air pollutants measured hourly (elemental carbon, elemental carbon of outdoor origin, primary organic carbon of outdoor origin, and NO_x).
- Figure 4.5. Fold-Change and 95% confidence interval for qPCR expression level of *CYP1B1*, *HMOX1*, *IL1B*, *NQO1*, *NFE2L2*, *SELP*, and *SOD2* in association with indoor particulate matter size fractions, polycyclic aromatic hydrocarbons and oxidative potential (measured as macrophage ROS production *in vitro*).
- Figure 5.1. Relations between SELP gene expression and PM mass size fraction: effect modification by Nrf2 -617 A risk allele genotype.
- Figure 5.2. Relations between SELP gene expression and traffic-related air pollutants: effect modification by Nrf2 -617 A risk allele genotype.
- Figure 5.3. Relations between SELP gene expression and exposure to total organic carbon (OC), primary OC (OCpri), and secondary OC (SOC): effect modification by Nrf2 -617 A risk allele genotype.
- Figure 5.4. Relations between Nrf2 gene expression and PM mass size fraction: effect modification by Nrf2 -617 A risk allele genotype.
- Figure 5.5. Relations between Nrf2 gene expression and traffic-related air pollutants: effect modification by Nrf2 -617 A risk allele genotype.
- Figure 5.6. Relations between Nrf2 gene expression and exposure to total organic carbon (OC), primary OC (OCpri), and secondary OC (SOC): effect modification by Nrf2 -617 A risk allele genotype.

- Figure 5.7. Relations between SOD2 gene expression and PM mass size fraction: effect modification by Nrf2 -617 A risk allele genotype.
- Figure 5.8. Relations between SOD2 gene expression and traffic-related air pollutants: effect modification by Nrf2 -617 A risk allele genotype.
- Figure 5.9. Relations between SOD2 gene expression and exposure to total organic carbon (OC), primary OC (OCpri), and secondary OC (SOC): effect modification by Nrf2 -617 A risk allele genotype.
- Figure 5.10. Relations between IL1B gene expression and traffic-related air pollutants: effect modification by Nrf2 -617 A risk allele genotype.
- Figure 5.11. Relations between SELP gene expression and traffic-related air pollutants: effect modification by Nrf2 -617 A risk allele genotype.
- Figure 5.12. Relations between CYP1B1 gene expression and PM mass size fraction: effect modification by Nrf2 -617 A risk allele genotype.
- Figure 5.13. Relations between CYP1B1 gene expression and traffic-related air pollutants: effect modification by Nrf2 -617 A risk allele genotype.
- Figure 5.14. Relations between CYP1B1 gene expression and exposure to total organic carbon (OC), primary OC (OCpri), and secondary OC (SOC): effect modification by Nrf2 -617 A risk allele genotype.
- Figure 5.15. Relations between sP-selectin protein expression and selected air pollution exposures: effect modification by SOD2 Val16 risk allele genotype.

LIST OF TABLES

- Table 2.1. Organic Compounds Quantified and Selected QA/QC Results.
- Table 2.2. Average Indoor and Outdoor Accumulation Mode Organic Compound Concentrations by Season.
- Table 3.1. Contribution of mobile sources to PM_{2.5} in the co-linear cases, assuming that the OC apportioned to mobile sources is emitted from 1) only LDV, 2) only HDV, 3) 25% LDV, 75% HDV, 4) 75% LDV, 25% HDV.
- Table 3.2. Statistical parameters and weekly source contribution estimates (\pm standard error, in $\mu\text{g}/\text{m}^3$) to ambient fine PM mass at the indoor and outdoor sampling sites during the warm and cold phases.
- Table 4.1. Candidate Gene Names and NCBI identification numbers.
- Table 4.2. Characteristics of Subjects in the Gene Expression Analyses (N=43).
- Table 4.3. Descriptive statistics of outdoor air pollutant exposures in three retirement communities of the Los Angeles Air Basin.
- Table 4.4. Descriptive statistics of indoor air pollutant exposures in three retirement communities of the Los Angeles Air Basin.
- Table 4.5. Descriptive statistics of outdoor air pollutant exposures in 4 retirement communities of the Los Angeles Air Basin.
- Table 4.6. Descriptive statistics of indoor air pollutant exposures in 4 retirement communities of the Los Angeles Air Basin.
- Table 4.7. Spearman correlation matrix for air pollutants measured daily.
- Table 4.8. Spearman correlation matrix for PM air pollutants measured weekly.
- Table 4.9. Gene expression model estimates for markers of outdoor secondary organic aerosols. Fold change in gene expression (95% CI).

ABSTRACT

Background: Cardiovascular disease outcomes have been associated with exposure to ambient particulate matter (PM) air pollution in many epidemiological studies. Experimental studies have revealed potential mechanisms behind the epidemiological results and many of these studies have revealed changes in the expression of important genes in key biological pathways with exposure to air pollution from fossil fuel combustion. Few epidemiological studies have examined this. We hypothesized that blood cell gene expression levels along biological pathways relevant to cardiovascular outcomes would be associated with traffic-related air pollutant exposures in elderly subjects with coronary artery disease.

Methods: Available data were collected in a cohort panel study funded by the National Institutes of Health, National Institute of Environmental Health Sciences. Gene expression data were available for 43 subjects with up to 12 weekly repeated measures conducted in three of the four retirement communities in the Los Angeles Air basin where the exposure measurement work took place. Whole blood samples were collected weekly, RNA was isolated and then it was reversed transcribed into complementary DNA for subsequent gene expression analysis using the polymerase chain reaction method. Candidate genes (35) were selected *a priori* based on biological function and reported pollutant exposure effects. Exposure measurements were conducted in the indoor and outdoor environment of each community and included daily size-fractionated PM mass and PM organic chemical composition, including polycyclic aromatic hydrocarbons (PAH). We also measured hourly criteria pollutant gases, total particle number concentration, PM_{2.5} organic carbon (OC), and PM_{2.5} markers of primary combustion products, namely elemental carbon (EC), and black carbon (BC). The present ARB-funded study provided accumulation mode PM data for: 1) chemical composition; 2) *in vitro* generation of reactive oxygen species (ROS) by alveolar (lung) macrophages that were exposed to extracts of the weekly PM samples; and 3) source apportionment work, including estimations of photochemically-related secondary organic aerosols. Within-subject relations between air pollutant exposures and normalized gene expression levels were analyzed using mixed-effects regression models adjusted for weather, community and study season.

Results: Source apportionment results in the four retirement communities showed that although people spend most of their time indoors, this does not shield them from outdoor pollutants since a sizeable portion of indoor PM_{2.5} particles originate from outdoor mobile sources. Expression levels of 30 genes from the 43 subjects were suitable for analysis and provided around 360 samples. Results of regression models showed that traffic-related air pollutants were associated with the expression of 7 genes in important pathways including Nrf2-mediated oxidative stress response, xenobiotic response, inflammation, and platelet activation. Although many relationships were not statistically significant, associations were consistent with respect to their magnitude and direction (positive). PAH and/or ROS from quasi-ultrafine PM (<0.25 micrometers) generally showed stronger associations with gene expression than did accumulation mode PM (0.25-2.5 micrometers). In secondary analyses we found some evidence of effect modification of these and other associations by polymorphisms in selected candidate genes, including *NFE2L2*, *SELP*, and *SOD2*. Secondary air pollutant exposures were not associated with gene expression. Other air pollutants (metals, total OC and CO) were not associated with the expression of genes. Source-apportioned biomass smoke was positively associated with expression of the hemoxenase-1 gene and was positively, but not significantly, associated with expression of seven others. None of the air pollutant exposures were associated with expression of 15 genes linked to most of the biological pathways studied.

Conclusions: Results revealed numerous positive associations with gene expression among genes that are part of the Nrf2-mediated oxidative stress response, xenobiotic response, inflammation, and platelet activation pathways. This supports our hypothesis that traffic-related air pollutant exposures affect the expression of genes in pathways that are relevant to adverse cardiovascular effects. Our findings are relevant to ambient air quality standards, which do not include ultrafine PM or the general class of organic components from fossil fuel combustion sources that have been associated with gene expression outcomes in this study as well as with cardiovascular outcomes in other analyses involving the same cohort.

EXECUTIVE SUMMARY

Background: Cardiovascular disease outcomes have been associated with exposure to ambient particulate matter (PM) air pollution in many studies. However, there is a lack of knowledge about the health effects of various particle size fractions in ambient PM or their sources and components. A better understanding of mechanisms is also needed. To partly address this, *in vitro* experiments of the effects of air pollutants on cell cultures have shown gene expression changes in cells linked to cardiovascular disease progression, including endothelial cells, epithelial cells, monocytes and macrophages. Results of these and other experimental studies of potential mechanistic pathways through which air pollutants may cause adverse cardiovascular outcomes need to be tested in human populations at risk. We used repeated measures to evaluate gene expression changes in a well-characterized urban cohort panel to provide coherence with the toxicology literature. Few published studies in human subjects have examined associations of gene expression with exposure to air pollution from fossil fuel combustion or similar sources, and none have been panel studies to our knowledge. For the present analysis of our cohort panel we hypothesized that gene expression levels along biopathways relevant to cardiovascular outcomes would be associated with traffic-related air pollutant exposures.

Methods: We followed elderly subjects with coronary artery disease with up to 12 weekly repeated measures to evaluate acute cardiorespiratory health effects of exposure to PM with a focus on ultrafine particles. Included in the analysis of gene expression were 43 subjects living in three of four retirement communities in the Los Angeles Air basin that were in the parent study, the Cardiovascular Health and Air Pollution Study funded by the National Institutes of Health, National Institute of Environmental Health Sciences. Whole blood samples were collected weekly using a standardized collection method for stabilizing the RNA profile immediately after blood withdrawal. Total RNA was isolated and then reversed transcribed into first-strand cDNA for subsequent gene expression analysis using the polymerase chain reaction method. Gene expression normalization factors for each sample were generated from three stable reference genes. Thirty-five candidate genes were selected *a priori* based on biological function and reported pollutant exposure effects. Exposure measurements were conducted in the indoor and outdoor environment of each community and included daily size-fractionated PM mass for quasi-ultrafine particles, <0.25 μm in diameter ($\text{PM}_{0.25}$), accumulation mode particles, 0.25-2.5 μm in diameter ($\text{PM}_{0.25-2.5}$), and coarse mode particles, 2.5-10 μm in diameter ($\text{PM}_{2.5-10}$). PM organic chemical composition was measured for $\text{PM}_{0.25}$ and $\text{PM}_{0.25-2.5}$ for 5-day composites of the PM filters, including polycyclic aromatic hydrocarbons (PAH). We also measured hourly criteria pollutant gases, total particle number concentration, and $\text{PM}_{2.5}$ elemental carbon (EC), organic carbon (OC) and black carbon (BC). Primary OC and secondary OC were estimated using the EC tracer method. The present ARB-funded study provided accumulation mode PM data for: 1) chemical composition; 2) *in vitro* generation of reactive oxygen species (ROS) by alveolar (lung) macrophages that were exposed to extracts of the weekly composites of $\text{PM}_{0.25}$ and $\text{PM}_{0.25-2.5}$ filter samples; and 3) source apportionment work, including estimations of photochemically-related secondary organic aerosols (SOA). Within-subject relations between exposures and normalized gene expression levels were analyzed using mixed-effects regression models adjusted for weather, community and study period (warm or cool season).

Results: Source apportionment results in the four retirement communities demonstrated that mobile sources were the dominant contributor to both indoor and outdoor $\text{PM}_{2.5}$ at all sites. Indoor SOA formation, possibly resulting from the reaction of household products' emissions with ozone, was also evident at some of the sites.

In the analysis of gene expression, expression levels of five genes were too low for quantification. The remaining expression data for 30 genes from 43 subjects yielded 360 person-observations per gene on average. Results of the linear mixed-effects models showed that daily traffic-related air pollutants were associated with the expression of genes in several key *a priori*-selected pathways including Nrf2-mediated oxidative stress response, xenobiotic response,

inflammation, and platelet activation. Although many of the 95% CIs for the fold change estimates included 1.0, associations were consistent with respect to their magnitude and direction (positive) across each of the genes within the pathways. In particular, we found positive associations of primary pollutants (PAH, EC, BC, primary OC, and NO_x) with the Nrf2 gene (*NFE2L2*) as well as the Nrf2-mediated or linked genes (*HMOX1*, *NQO1*, and *SOD2*). Traffic-related air pollutants were also positively associated with increased expression of *IL1B* (inflammation), *SELP* (platelet activation), and *CYP1B1* (phase I enzyme, xenobiotic metabolism) whose transcription is not directly Nrf2-mediated. PM_{0.25} *in vitro* ROS was positively associated with expression of *NFE2L2*, *NQO1* and *CYP1B1* whereas PM_{0.25-2.5} ROS was only associated with *CYP1B1*. Overall, there were generally stronger associations for PM_{0.25} PAH and/or ROS than for PM_{0.25-2.5} PAH and ROS. PM from biomass burning was significantly associated with *HMOX1*, and was positively, but not significantly, associated with expression of seven others (*ATF4*, *ATF6*, *GCLM*, *IL1B*, *KLF2*, *MPO* and *XBP1*). Secondary air pollutant exposures were not associated with gene expression, including size-fractionated particle components (SOA and organic acids), PM_{2.5} SOC, and O₃. Other air pollutants measured (metals, total OC and CO) were not associated with the expression of genes. We also found no trends of association of any pollutants with down regulation of genes. None of the air pollutant exposures were associated with expression of the following 15 genes: *AHR*, *CCL2*, *CXCL1*, *DUSP1*, *F3*, *GCLC*, *GPX-1*, *GSTP1*, *HSPA8*, *IL6*, *IL6R*, *IL8*, *PTGS2*, *TNF*, *TNFRS1B*.

We found some evidence of effect modification of gene expression associations by polymorphisms in selected candidate genes, including *NFE2L2*, *SELP*, and *SOD2*. The effects were complex and suggested that multiple gene-gene interactions may be involved, including many genes we did not assess.

Conclusions: Results revealed numerous positive associations with gene expression among genes that are part of the Nrf2-mediated oxidative stress response pathway. This supports our hypothesis that traffic-related air pollutant exposures would be associated with the expression of genes in pathways that are relevant to adverse cardiovascular effects. Our novel findings for the Nrf2 gene itself are in agreement with the existing experimental literature that describes the Nrf2 protein as a master regulator of antioxidant response. The Nrf2 transcription factor regulates phase II and other antioxidant genes by binding to antioxidant response elements (ARE) of their promoter regions. The positive associations of *NFE2L2* expression with PAHs that we found are consistent with what would be expected based upon experimental data. We also found increases in gene expression of downstream genes in both Nrf2-ARE and AHR-XRE pathways consistent with recent experimental evidence suggesting crosstalk between the xenobiotic and antioxidant response pathways.

Other key findings are the positive associations of *IL1B* and *SELP* with traffic-related air pollutant exposure. IL-1 β contributes to atherosclerosis progression by mediating vascular injury responses. In the present panel we previously found positive associations between air pollution exposure and the circulating protein marker of platelet activation that is encoded by *SELP* (soluble platelet selectin). This finding is of clinical importance in that higher air pollution exposures may increase the potential for an acute thrombotic event.

The present hypothesis-driven analysis produced informative epidemiological results that support the experimental data (*in vivo* and *in vitro* toxicological studies). The involvement of the Nrf2 pathway in the associations we observed between gene expression and air pollution exposure supports the view that oxidative stress is a potential mode of action by which exposure to traffic-related air pollutants increases the risk of adverse cardiovascular responses we have previously observed in the CHAPS cohort panel.

Our findings are relevant to potential future regulations. Ambient air quality standards, do not include ultrafine PM or the general class of organic components from fossil fuel combustion sources that have been associated with gene expression outcomes in this study as well as with cardiovascular outcomes in other analyses involving the same cohort, although many of the regulation of the Air Resources Board are designed to reduce traffic pollution. This is important because we found that mobile sources were the dominant contributor to both indoor and outdoor PM_{2.5} at all community sites.

BODY OF REPORT

1. CHAPTER ONE: INTRODUCTION

1.1 Background

Gene Expression:

Cardiovascular disease outcomes have been associated with exposure to air pollution in many studies, both epidemiological and toxicological (Brook et al. 2010). In particular, increases in blood pressure, myocardial infarction, atherosclerotic progression, and other outcomes have been associated with traffic-related air pollution (Brook et al. 2010). The modes of action for these effects are still under investigation but are believed to include vascular dysfunction, thrombosis, coagulation, increases in oxidative stress and inflammation, and autonomic dysregulation (Brook et al. 2010). In previous studies, using the same elderly coronary artery disease (CAD) cohort panel examined in the current research, we showed a positive association between circulating inflammatory biomarker levels and exposure to traffic-related air pollutants (Delfino et al. 2009, 2010a). However, cellular mechanisms behind these findings are not completely understood. For the present analysis of our cohort panel we hypothesized that gene expression levels along biopathways relevant to the above outcomes would be associated with traffic-related air pollutant exposures. Figure 1.1 illustrates how gene expression responses are involved in selected known or suspected biopathways of air pollutant exposure-response relations.

In vitro experiments of the effects of air pollutants have shown gene expression changes in cells linked to cardiovascular disease progression, including endothelial cells, epithelial cells, monocytes and macrophages. Gong et al. (2007) found human endothelial cells exposed to diesel exhaust particles demonstrated increased expression levels of genes linked to vascular inflammation (*IL8*, *CXCL1*, and *DUSP1*), antioxidant genes (*SOD1*, *HMOX1* and *NQO1*), and unfolded protein response (UPR) genes (*HSPA8*, *XBP1*, *ATF4*, and *ATF6*). The unfolded protein response is also referred to as endoplasmic reticulum (ER) stress. Gargalovic et al. (2006) studied human endothelial cells *in vitro* and identified UPR genes as mediators of vascular inflammation and atherosclerosis, supporting the potential that UPR genes may be important in air pollution effects on cardiovascular outcomes. Huang et al. 2011 found that genes from the Nrf2-mediated oxidative stress response pathway were upregulated in airway epithelial cells after exposure to particulate matter (PM) from ambient outdoor air pollution. Oxidative stress is an important factor in the progression of cardiovascular disease, including atherosclerotic plaques (Lee et al. 2012). Oxidative stress has been shown to be increased with particulate air pollution exposure in several studies reviewed by Delfino et al. (2011). Therefore, it is likely that Nrf2-mediated oxidative stress response genes are important in adverse cardiovascular responses in humans exposed to elevated levels of air pollution.

Wu et al. (2011) showed decreased expression of Kruppel-like factor 2 (Klf2) with PM exposure in inflammation-prone Sirt1 knock-out mice (Wu et al. 2012). Klf2 is a key transcription factor for proper coagulation and thrombotic function and down-regulates pro-inflammatory genes (Das et al. 2006; Lin et al. 2005). Klf2 expression levels are reduced in circulating monocytes from patients with CAD compared with age-matched controls (Das et al. 2006). Therefore, it is possible that in our cohort panel of subjects with CAD, cardiovascular responses to air pollution exposure may be mediated by *KLF2* expression changes.

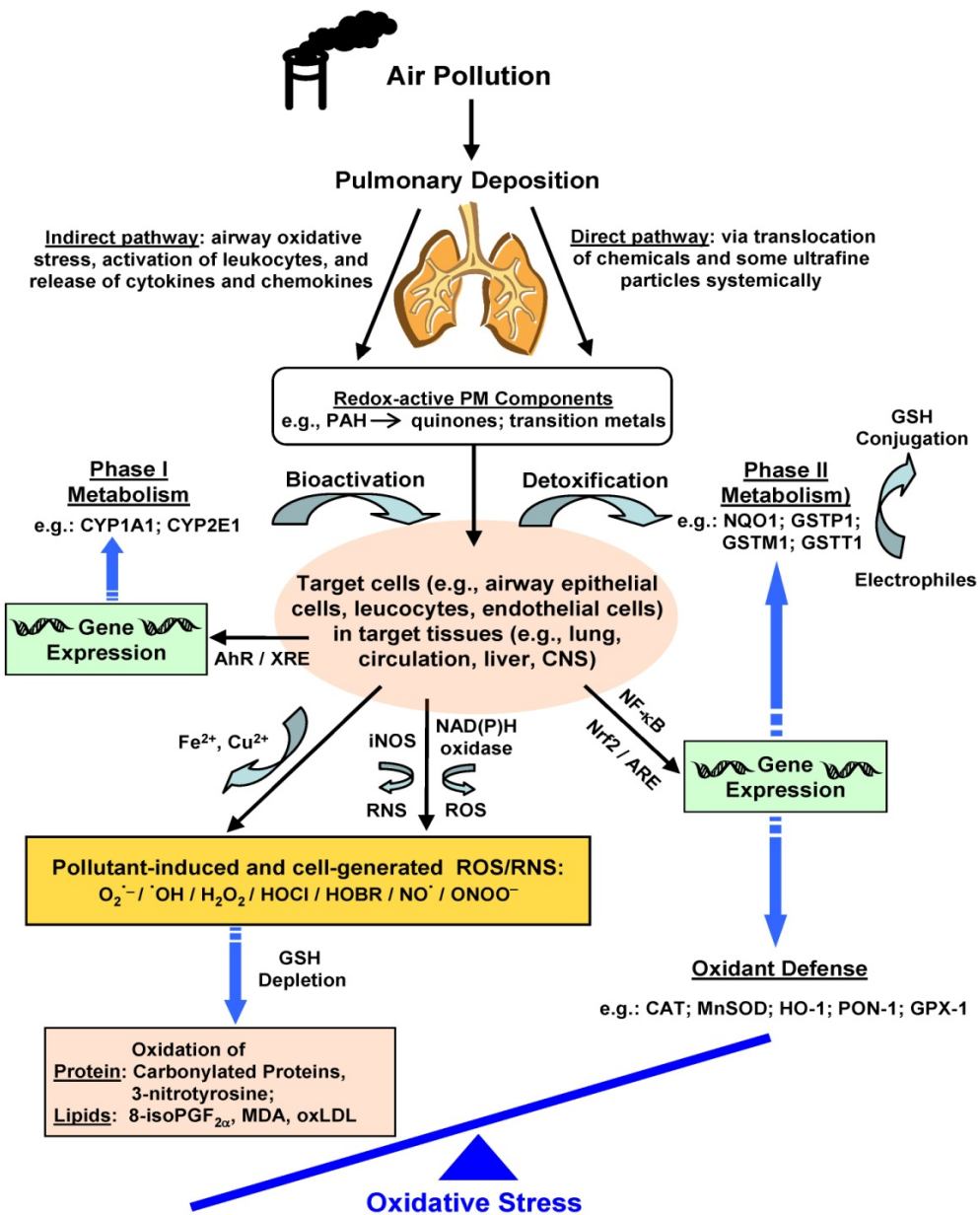


Figure 1.1 Known or Suspected Oxidative Stress Response Pathways. Many effects of air pollutant exposures may occur through the generation of reactive oxygen and nitrogen species (ROS/RNS) from organic chemicals acting either directly or through activation of bronchial epithelial cells, macrophages, neutrophils, and endothelial cells. Relevant pollutant components are emitted from fossil fuel combustion and include polycyclic aromatic hydrocarbons (PAH), quinones, and transition metals (e.g. Fe). These components have pro-oxidant properties and can induce oxidative stress through the production of free radicals and subsequent activation of redox-sensitive signaling pathways (e.g., Nrf2, ARE, and NF-κB). Activation of these pathways may underlie findings that indicate exposures to fine particles trigger inflammatory and cytotoxic responses in the human lung as well as systemic inflammation and thrombosis. This is most likely when oxidant defenses are inadequate. Systemic oxidative stress and inflammation may occur as a result of effects of air pollutants deposited on the airways

(indirect pathway) or from the direct systemic distribution of pollutant chemicals following pulmonary deposition (direct pathway). Adapted from: Delfino RJ, Staimer N, Vaziri ND. Air pollution and circulating biomarkers of oxidative stress. *Air Qual Atmos Health*, 2011;4:37-52.

We used repeated measures to evaluate gene expression changes in a well-characterized urban cohort panel to provide coherence with studies of potential mechanistic pathways through which air pollutants may cause adverse cardiovascular outcomes. To our knowledge, there have been only five published studies in human subjects examining associations of gene expression with exposure to air pollution from fossil fuel combustion or similar sources, but none have been panel studies (Peretz et al. 2007; van Leeuwen et al. 2006, 2008; Wang et al. 2005; Wu et al. 2011) (see McHale et al. 2010 for review of human genome-wide studies of other inhaled exposures). All have been exploratory microarray studies. Two small studies with limited results evaluated changes in peripheral-blood mRNA levels in occupational settings, one with metal fumes exposure in welders (Wang et al. 2005) and another in coke oven workers exposed to polycyclic aromatic hydrocarbons (Wu et al. 2011). Two small studies with limited or no ambient air pollution exposure data evaluated cross-sectional differences in mRNA levels (van Leeuwen et al. 2006, 2008). Peretz et al. (2007) conducted an experimental human clinical chamber study and found gene expression changes using microarray analysis of peripheral blood mononuclear cells in only 5 healthy subjects. They showed that 1290 probe sets were > 1.5-fold up- or down-regulated at $p < .05$ following 6h and 22h after exposure to 200 $\mu\text{g}/\text{m}^3$ diesel exhaust compared to clean air. Genes included those involved in inflammation and oxidative stress, as well as vascular homeostasis.

Air Pollutant Particle Characteristics:

A lack of knowledge about the health effects of various particle size fractions in ambient PM or their sources and components has limited the ability of regulatory agencies to established protective exposure limits (NRC 2004; U.S. EPA 2009). In this regard, there are two important classes of organic aerosols for which little are known regarding differences in their health effects in human populations, namely:

- 1) Primary organic aerosols (POA) from combustion sources, which are primarily traffic-related in the Los Angeles air basin;
- 2) Secondary organic aerosols (SOA), which are photochemically-produced from combustion-related, industrial, and biogenic volatile or semi-volatile precursors.

These particle types have different spatial and temporal variability and are thus minimally or not correlated (Delfino et al. 2008, 2009). The organic component mix and size distribution in ambient PM differs as well between these classes of particulate organic matter, with POA being the predominant mass fraction in ultrafine particles and SOA generally predominant in accumulation mode particles. In addition, POA components are more hydrophobic, and SOA components are more hydrophilic. These characteristics will likely determine their toxicity, their ability to enter the circulation, and pathophysiological mechanisms of effect. However, to our knowledge, data on the direct relevance of this in human populations is limited to our previous research (Delfino et al. 2008, 2009, 2010a, 2010b). Furthermore, there is little data in humans on whether increased exposure to urban air pollution is associated with changes in mRNA expression reflecting biological processes linked to oxidative stress and inflammation.

For our panel study, the Cardiovascular Health and Air Pollution Study (CHAPS), we previously reported that associations with biomarkers of inflammation in the blood were stronger with mass concentrations of quasi-ultrafine particles $<0.25 \mu\text{m}$ ($\text{PM}_{0.25}$) compared with larger particles that make up most of the accumulation mode of $\text{PM}_{2.5}$ ($\text{PM}_{0.25-2.5}$) (Delfino et al. 2008, 2009). We then reassessed these biomarker associations with indoor and outdoor home $\text{PM}_{0.25}$ mass using the new particle organic composition data from $\text{PM}_{0.25}$ filter extracts (Arhami et al. 2009a; Delfino et al. 2010a, 2010b). We found indoor and outdoor PAH in $\text{PM}_{0.25}$, followed by hopanes (a tracer of vehicular emissions), were most strongly positively associated with inflammatory biomarkers as compared with little to no associations for SOA tracers (organic acids, water soluble organic carbon) or transition metals (Delfino et al. 2010a, 2010b). Using source apportionment data from chemical mass balance models (Arhami et al. 2009a), we found that only vehicular emission sources and hopanes were strongly correlated with PAH ($R = 0.71$). To further elucidate our earlier findings, we present herein new particle composition data from archived frozen accumulation mode filter samples, and then an analysis of repeated measures using available gene expression data from CHAPS. PM composition and source tracers were used to detect differences in associations between POA and SOA, as well as between particle size fractions carrying these organic aerosol types.

1.2. Design of the Parent Project, and Scope and Purpose of the Present Project

Briefly, in the parent study (CHAPS) we followed subjects longitudinally with repeated measures of health outcomes and exposures across 12 weeks in each subject to evaluate acute cardiorespiratory health effects of exposure to PM with a focus on ultrafine particles. Recruited subjects were elderly individuals with a diagnosis of CAD to ensure that clinically relevant changes in cardiovascular outcomes would occur during the study. CHAPS is a cohort panel study, which is a design that is well suited to the study of acute-on-chronic patterns of change in physiologic factors important to cardiovascular diseases. The main analytic focus is on within-subject exposure-response relationships, with each subject serving as his/her own control over time modeled by the use of a random effect term for each subject. The design is statistically efficient because: 1) multiple exposure conditions and time frames are studied in each subject, and 2) response variability due to between-subject characteristics is reduced by repeated measurements without reductions in the magnitude of exposure-response relationships, thereby enhancing power and precision (Weiss and Ware 1996).

Study subjects were nonsmokers and lived in retirement communities prohibiting indoor tobacco smoke at shared locations and in buildings with common ventilation systems. We completed follow-up in four targeted communities in the LA air basin. Three were in the San Gabriel Valley and one in Riverside County. These communities are located in inland urban areas of the basin considered to be down-wind smog receptor sites with aged PM, but also affected by local traffic with freshly emitted PM. Our research as well as others has shown that size-fractionated PM concentrations and components vary across the sites because of traffic density and transport, and between our two seasonal study periods described below (Fine et al. 2004a, 2004b; Kim et al. 2002; Polidori et al. 2007; Zhu et al. 2002a, 2002b, 2004).

Over a seven month period, subjects were followed in two 6-week blocks with blood draws at the end of each week for circulating biomarkers of inflammation, platelet activation, and antioxidant activity (Figure 1.2). Two 6-week periods of follow-up in each subject were separated by around a two-month rest period. In each community, we collected 6 weeks of data during a warmer period of higher photochemical activity (Phase 1: Jul to early Oct), and 6 weeks of data during a cooler period of higher air stagnation (Phase 2: late Oct through Feb). This was

intended to enhance contrasts in PM composition (including POA and SOA), particle number, and size distribution in each community (Sioutas et al. 2005). In 2005-2006, two retirement communities were followed in four alternating six-week phases. Again in 2006-2007, another two retirement communities were followed in four alternating six-week phases.

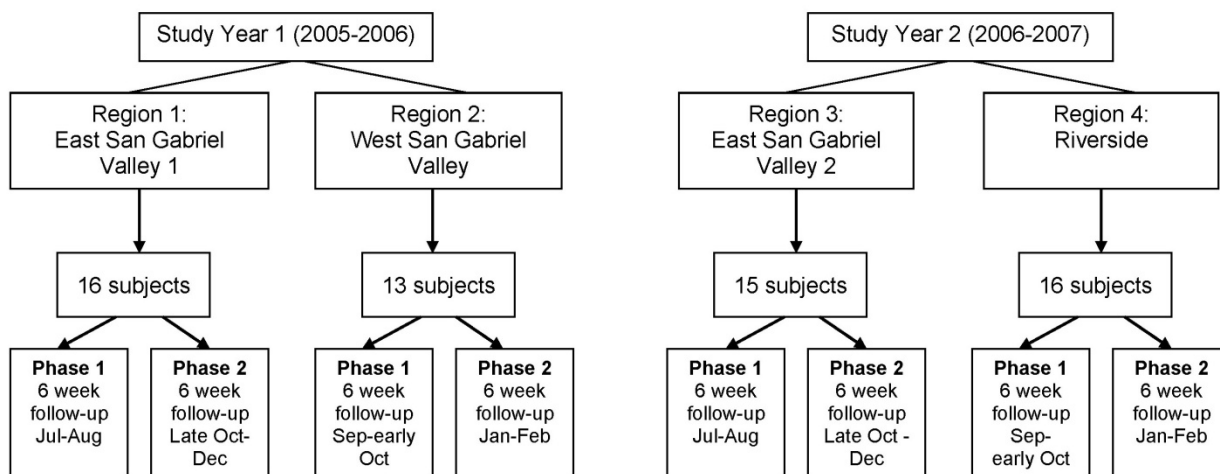


Figure 1.2. Panel Study Flow Chart.

Subjects completed a baseline questionnaire with items from our previous work, the Multiethnic Study of Atherosclerosis, and the Atherosclerosis Risk in Communities study. This data was used to assess demographic characteristics, lifestyle and environmental risk factors, personal and family history of cardiovascular and pulmonary conditions, other comorbidities, and home environment. Subject-specific characteristics that are time invariant over the daily periods of interest such as socioeconomic status or race-ethnicity are controlled for by the repeated measures (within-subject) design. A clinical work-up was done once only at baseline and included an intake history and physical by study cardiologists, 12-lead ECG, pulmonary function tests, blood tests including CBC, fasting lipid profile and fasting glucose. Confirmation of CAD diagnosis was made with a medical records review (e.g. positive stress test, MI history). In Chapter 4, we describe the complete exposure measurements from funded work in CHAPS that are available to enhance the present measurements of additional accumulation mode exposures.

Population and Recruitment

Inclusion criteria included age ≥ 65 , history of CAD, which could include a history of myocardial infarction and bypass surgery but not within the preceding 12 months. Subjects also had to be sufficiently ambulatory to perform sit-to-stand transfers over short distances.

Exclusion criteria included the following: employment outside of the monitored home; exposure to environmental tobacco smoke at home (all communities had to prohibit smoking in common areas as well); active smoking within the preceding 12 months; psychiatric disorders; dementia; Parkinson's or other debilitating neuromuscular diseases; alcohol or drug abuse; dialysis treatment; daily oral corticosteroids; or medical conditions that would place the subject or staff at risk from the blood donations.

We recruited four retirement communities with an average of 365 residents (range 182 to 575). We recruited 102 subjects who underwent baseline clinical evaluations on site at the UC Irvine Mobile Medicine unit. Twenty-one were not eligible and 21 dropped out prior to or after

the start of the panel study, or had too few biomarker observations (< 5 of 12 weeks), in part due to exclusions for frequent infections. This left 60 subjects for the analysis of circulating protein biomarker data for use in supplemental studies of gene variants, (Figure 1.2).

Enrolled subjects in CHAPS were investigated in this study of gene expression (Task 3, described below). Subject samples for the gene expression assay came from a subset of 43 subjects living in three of the four parent-study retirement communities. These three were in the San Gabriel Valley region of the Los Angeles Air Basin (Figure 1.2). This was necessary given the available funds from NIH NIEHS who funded the gene expression assay work (R21ES016420). The three communities located in the San Gabriel Valley were selected rather than the semi-rural Riverside community since these were closest to the Los Angeles metro area, and thus more likely to experience higher exposures to traffic-related air pollutants. Exposure measurements at all four communities was intensive and included daily PM mass (ultrafine, accumulation and coarse modes), PM chemical composition, and hourly measurements of indoor and outdoor home pollutant gases, EC, OC, BC, and total particle number concentration. Tasks 1 and 2 (described below) were to utilize PM filter samples and data from all four communities.

The informative nature of this panel study prior to the present analysis is evidenced in our previous papers (Bartell, et al. 2013; Delfino et al. 2008, 2009, 2010a, 2010b, 2010c, 2011). Their overall findings combined with the current literature (Brook et al. 2010; Link and Dockery 2010; Mills et al. 2009) support the following hypothesized pathways to cardiovascular health effects (Figure 1.3): Redox-active and other components in particles from fossil fuel combustion affect airway and cardiovascular target sites leading to oxidative stress, as well as systemic inflammation and thrombosis that were measured as both protein expression (Delfino et al. 2008, 2009, 2010a, 2010b) and gene expression (present study). Other gene expression changes we measured include endoplasmic reticulum (ER) stress and changes in phase I and II enzymes. ER stress is also called the unfolded protein response (UPR) functions to restore cells to normal function where cells have accumulated unfolded or misfolded proteins in the ER. This is done by stopping the translation of protein as well as activating the production of chaperones that carry out the folding of protein. If unsuccessful, the ER stress response then moves the cell towards apoptosis.

Resultant clinical effects that were previously measured in this cohort include the adverse cardiovascular responses of increased blood pressure (Delfino et al. 2010c), cardiac ischemia (Delfino et al. 2011), and occurrence of ventricular arrhythmias (Bartel et al., 2013), all of which enhance the risk of myocardial infarction.

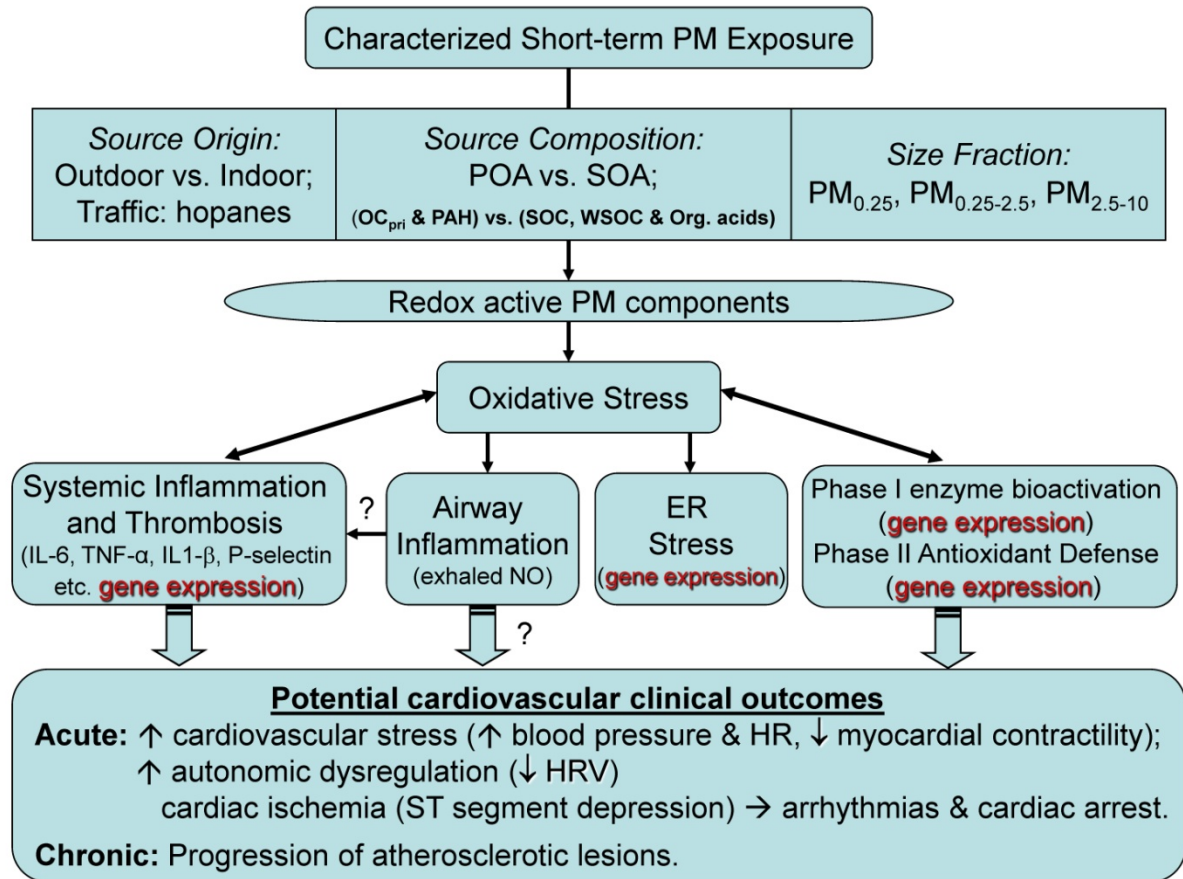


Figure 1.3. Hypothesized pathways from PM exposure to adverse cardiovascular health effects (in red) for evaluation in the present study. Adapted from: Delfino RJ, Staimer N, Tjoa T, Gillen D, Polidori A, Arhami M, Kleinman MT, Vaziri N, Longhurst J, Sioutas C. Air pollution exposures and circulating biomarkers of effect in a susceptible population: clues to potential causal component mixtures and mechanisms. *Environ Health Perspect*, 2009;117:1232–1238.

1.3. Tasks

This study expands upon and further elucidates our earlier findings in CHAPS showing associations between traffic-related air pollutants and systemic inflammation, platelet activation, increased ambulatory blood pressure, and ischemic ST-segment depression and ventricular arrhythmias from ambulatory electrocardiographs. We produced new particle composition data from archived frozen accumulation mode filter samples from CHAPS, and then conducted a repeated measures analysis using available gene expression data from CHAPS. We first measured organic components in indoor and outdoor accumulation modes and performed a source apportionment. We then investigated effects of POA and SOA on peripheral blood gene (mRNA) expression reflecting biological processes linked to oxidative stress and inflammation. Composition and source tracers were used to detect differences between POA and SOA in associations with gene expression. We also compared associations for different particle size fractions carrying these organic aerosol types as well as with transition metals in those PM fractions.

We expected that gene expression measurements from whole blood would enhance understanding of the biological basis for exposure-related impacts on systemic mediators of oxidative stress, inflammation and thrombosis that likely play a role in air pollutant-mediated acute cardiovascular events. Primary *Research Questions* of this study include the following:

- Are expression levels of key genes more strongly associated with markers of primary (combustion-related) organic aerosols than with secondary (photochemically-related) organic aerosols?
- Are there differences in associations of gene expression with POA, SOA, and particle components such as PAH and transition metals across different particle size fractions?
- What are the sources of key particle component classes and size fractions in both indoor and outdoor environments of study subjects?

The following tasks were completed to address the above research questions:

- Task 1.** To conduct a chemical speciation of organic components in indoor and outdoor accumulation mode filters (47 weeks) collected at retirement communities of 60 study subjects in CHAPS. (Dr. James J. Schauer)
- Task 2.** To use the accumulation mode composition data from Task 1 and existing metals data to conduct exposure analysis and source apportionment using chemical mass balance models. (Dr. Constantinos Sioutas, USC). This was combined with existing metals data to extend the indoor-outdoor exposure analysis and source apportionment work already completed using the quasi-ultrafine PM ($PM_{0.25}$) data in a chemical mass balance (CMB) model.
- Task 3.** To conduct an epidemiologic analysis of the relations between gene expression and exposure to particle mass, components, and source tracers of $PM_{0.25}$ and $PM_{0.25-2.5}$ from Tasks 1 and 2 as well as to PM mass and metal content in $PM_{2.5-10}$ (Dr. Ralph Delfino and colleagues, UCI). Gene expression data for 35 genes selected *a priori* were available from NIH, NIEHS-funded work. This includes genes involved in oxidative stress, antioxidant defense, xenobiotic metabolism, inflammation, coagulation, and endoplasmic reticulum stress.

The following chapters reports on the methods, results and conclusions of each of these three tasks (Chapters 2-4) as well as a supplemental analyses to evaluate gene expression models for the modifying effects of potentially important genetic variants of selected genes (Chapter 5). Chapter 5 will also include supplemental analyses of genetic polymorphisms to evaluate effect modification of relations between air pollution exposures and protein expression (e.g., soluble platelet selectin) that utilized exposure and outcome data from all four communities. This will be followed by an overall summary and conclusions (Chapter 6), and recommendations (Chapter 7).

References:

- Bartell S, Tjoa T, Longhurst J, Sioutas C, Delfino RJ. Particulate air pollution, ambulatory heart rate variability and cardiac arrhythmia in retirement community residents with coronary artery disease. *Environ Health Perspect* in press 3-2013.
- Brook RD, Rajagopalan S, Pope CA 3rd, Brook JR, Bhatnagar A, Diez-Roux AV, et al. 2010. Particulate matter air pollution and cardiovascular disease: An update to the scientific statement from the American Heart Association. *Circulation* 2010;121(21):2331-78.
- Das H, Kumar A, Lin Z, et al. Kruppel-like factor 2 (KLF2) regulates proinflammatory activation of monocytes. *Proc Natl Acad Sci U S A* 2006;103(17):6653-8.
- Delfino RJ, Gillen DL, Tjoa T, Staimer N, Polidori A, Arhami M, Sioutas C, Longhurst J. Electrocardiographic ST segment depression and exposure to traffic-related aerosols in elderly subjects with coronary artery disease. *Environ Health Perspect* 2011;119:196–202. PMID: 20965803.
- Delfino RJ, Sioutas C, Malik S, Potential role of ultrafine particles in associations between airborne particle mass and cardiovascular health. *Environ Health Perspect*, 2005; 113:934-46.
- Delfino RJ, Staimer N, Tjoa T, Arhami M, Polidori A, Gillen D, Kleinman MT, Schauer J, Sioutas C. Association of biomarkers of systemic effects with organic components and source tracers in quasi-ultrafine particles. *Environ Health Perspect*, 2010a;118:756-762.
- Delfino RJ, Staimer N, Tjoa T, Arhami M, Polidori A, Gillen DL, George SC, Shafer MM, Schauer J, Sioutas C. Associations of primary and secondary organic aerosols with airway and systemic inflammation in an elderly panel cohort. *Epidemiology* 2010b;21:892-902. PMID: 20811287
- Delfino RJ, Staimer N, Tjoa T, Gillen D, Polidori A, Arhami M, Kleinman MT, Vaziri N, Longhurst J, Sioutas C. Air pollution exposures and circulating biomarkers of effect in a susceptible population: clues to potential causal component mixtures and mechanisms. *Environ Health Perspect*, 2009;117:1232–1238. PMID: 19672402
- Delfino RJ, Staimer N, Tjoa T, Polidori A, Arhami M, Gillen D, Kleinman MT, Vaziri N, Zaldivar F, Longhurst J, Sioutas C. Circulating biomarkers of inflammation, antioxidant activity, and platelet activation are associated with urban air pollution in elderly subjects with a history of coronary artery disease. *Env Health Perspect*, 2008; 116:898–906. PMID: 18629312.
- Delfino RJ, Staimer N, Vaziri ND. Air pollution and circulating biomarkers of oxidative stress. *Air Quality, Atmosphere & Health* 2011;4(1):37-52.
- Delfino RJ, Tjoa T, Gillen D, Staimer N, Polidori A, Arhami M, Jamner L, Sioutas C, Longhurst J. Traffic-related air pollution and blood pressure in elderly subjects with coronary artery disease. *Epidemiology*, 2010c;21:396-404. PMID: 20335815.
- Fine PM, Si S, Geller MG, Sioutas C. Inferring the sources of fine and ultrafine PM at downwind receptor areas in the Los Angeles Basin using multiple continuous monitors. *Aerosol Science and Technology*, 2004a; 38:182-195.
- Fine PM, Chakrabarti B, Krudysz M, Schauer JJ, Sioutas C. 2004b. Seasonal, spatial, and diurnal variations of individual organic compound constituents of ultrafine and accumulation mode PM in the Los Angeles Basin. *Environmental Science and Technology*, 38:1296-304.

- Gargalovic PS, Gharavi NM, Clark MJ, et al. The unfolded protein response is an important regulator of inflammatory genes in endothelial cells. *Arterioscler Thromb Vasc Biol* 2006;26(11):2490-6.
- Gong KW, Zhao W, Li N, et al. Air-pollutant chemicals and oxidized lipids exhibit genome-wide synergistic effects on endothelial cells. *Genome biology* 2007;8(7):R149.
- Huang YC, Karoly ED, Dailey LA, et al. Comparison of gene expression profiles induced by coarse, fine, and ultrafine particulate matter. *Journal of toxicology and environmental health Part A* 2011;74(5):296-312.
- Kim S, Shi S, Zhu Y, Hinds WC, Sioutas C. 2002. Size distribution, diurnal and seasonal trends of ultrafine particles in source and receptor sites of the Los Angeles Basin. *J Air Waste Manage Assoc* 52:174-185.
- Lee R, Margaritis M, Channon KM, et al. Evaluating oxidative stress in human cardiovascular disease: methodological aspects and considerations. *Curr Med Chem* 2012;19(16):2504-20.
- Lin Z, Kumar A, SenBanerjee S, Staniszewski K, Parmar K, Vaughan DE, Gimbrone MA Jr, Balasubramanian V, García-Cardeña G, Jain MK. Kruppel-like factor 2 (KLF2) regulates endothelial thrombotic function. *Circ Res*. 2005;96:e48-57.
- Link MS, Dockery DW. 2010. Air pollution and the triggering of cardiac arrhythmias. *Curr Opin Cardiol* 25:16–22.
- McHale CM, Zhang L, Hubbard AE, et al. Toxicogenomic profiling of chemically exposed humans in risk assessment. *Mutat Res* 2010;705(3):172-83.
- Mills NL, Donaldson K, Hadoke PW, Boon NA, MacNee W, Cassee FR, Sandström T, Blomberg A, Newby DE. Adverse cardiovascular effects of air pollution. *Nat Clin Pract Cardiovasc Med*. 2009;6:36-44.
- National Research Council, Committee on Research Priorities for Airborne Particulate Matter. *Research Priorities for Airborne Particulate Matter: IV. Continuing Research Progress*. National Academies Press, 2004.
- Peretz A, Peck EC, Bammler TK, et al. Diesel exhaust inhalation and assessment of peripheral blood mononuclear cell gene transcription effects: an exploratory study of healthy human volunteers. *Inhal Toxicol* 2007;19(14):1107-19.
- Polidori A, Arhami M, Delfino RJ, Allen R, Sioutas C. 2007. Indoor-outdoor relationships, trends and carbonaceous content of fine particulate matter in retirement communities of the Los Angeles basin. *J Air Waste Manage Assoc* 57:366-379.
- Sioutas C, Delfino RJ, Singh M. 2005. Exposure assessment for atmospheric ultrafine particles (UFP) and implications in epidemiological research. *Environ Health Perspect*, 113:947-55.
- U.S. EPA. *Integrated Science Assessment for Particulate Matter (Final Report)*. U.S. Environmental Protection Agency, Washington, DC, EPA/600/R-08/139F, 2009. Available at: <http://cfpub.epa.gov/ncea/cfm/recordisplay.cfm?deid=216546>
- van Leeuwen DM, Pedersen M, Hendriksen PJ, et al. Genomic analysis suggests higher susceptibility of children to air pollution. *Carcinogenesis* 2008;29(5):977-83.
- van Leeuwen DM, van Herwijnen MH, Pedersen M, et al. Genome-wide differential gene expression in children exposed to air pollution in the Czech Republic. *Mutat Res* 2006;600(1-2):12-22.

- Wang Z, Neuburg D, Li C, et al. Global gene expression profiling in whole-blood samples from individuals exposed to metal fumes. *Environ Health Perspect* 2005;113(2):233-41.
- Weiss ST, Ware JH. Overview of issues in the longitudinal analysis of respiratory data. *Am J Respir Crit Care Med* 1996; 154:S208-S211.
- Wu MT, Lee TC, Wu IC, et al. Whole genome expression in peripheral-blood samples of workers professionally exposed to polycyclic aromatic hydrocarbons. *Chem Res Toxicol* 2011;24(10):1636-43.
- Wu Z, Liu MC, Liang M, et al. Sirt1 protects against thrombomodulin down-regulation and lung coagulation after particulate matter exposure. *Blood* 2012;119(10):2422-9.
- Zhu Y, Hinds WC, Kim S, Sioutas C. 2002a. Concentration and size distribution of ultrafine particles near a major highway. *J Air Waste Manage Assoc* 52:1032-42.
- Zhu Y, Hinds WC, Kim S, Shen S, Sioutas C. 2002b. Study on ultrafine particles and other vehicular pollutants near a busy highway. *Atmos Environ* 36:4375-4383.
- Zhu Y, Hinds, WC, Kim S, Shen S, Sioutas C. 2004. Seasonal trends of concentration and size distributions of ultrafine particles near major freeways in Los Angeles. *Aerosol Science and Technology*, 38(Suppl 1):5-13.

2. CHAPTER TWO: TASK 1

Task 1. To conduct a chemical speciation of organic components in indoor and outdoor accumulation mode filters (47 weeks) collected at retirement communities of 60 study subjects in CHAPS. (Dr. James J. Schauer)

2.0 Overview of sampling method and chemical analyses

24-h size segregated PM samples were collected prior to the project by USC investigators using the Personal Cascade Impactor Sampler (PCIS, SKC Inc., Eighty Four, Pennsylvania, USA). Coarse, accumulation, and quasi-ultrafine particle (UFP) mode PM were collected on Zefluor filters (3 μm pore-size, Pall Life Sciences, Ann Arbor MI); however, the present Task 1 focused on the accumulation PM fraction. The PM mass concentrations had been already determined gravimetrically by weighing filters in a controlled temperature and relative humidity room using a microbalance (Mettler-Toledo, Columbus, OH; weight uncertainty $\pm 2 \mu\text{g}$).

For the present study, PM filter substrates from the PCIS were composited weekly for chemical analyses (including 5 daily collected samples, from Monday to Friday). Chemical speciation of quasi-UFP had already been reported prior to the study in a number of publications resulting from our previous ARB- and NIH-funded CHAPS study (Polidori et al 2007; Arhami et al 2009; 2010).

Similar to the quasi-UFP samples that had already been speciated, composites were sectioned for chemical analysis. The remaining 1/4 sections of the Accumulation Mode particles were analyzed as part of the present study for more than 80 different organic compounds using Gas Chromatography/Mass Spectrometry (GC/MS). A previous section of the composited filters had already been digested with concentrated acid using microwave digestion and then analyzed by high resolution Inductively Coupled Plasma Mass Spectrometer (HR-ICPMS, Finnigan Element 2) to determine transition metals (Herner et al., 2006). Another section had already been analyzed for water soluble organic carbon (WSOC).

2.1 Organic speciation analysis

Due to the limited mass on the remaining portion of the filters, a high volume injection version of the standard organic speciation method for primary and secondary organic compounds was employed for the accumulation mode POA and SOA tracers, which were mathematically added to the existing ultrafine particle organics data that was completed as part of the earlier project. The organic analysis employed the methods used in earlier studies by Prof. Schauer's research group at the University of Wisconsin-Madison (Schauer et al., 1996; Lewandowski et al. 2008; Stone et al., 2009). More than 80 organic compounds were quantified including the key source tracers shown in Table 2.1. The methods of analysis to quantify individual organic compounds in the collected aerosol samples were based on earlier established solvent extraction methods (Sheesley et al. 2004), and was modified to increase analytical sensitivity by increasing the sample injection volume for the GCMS analysis to 30 μl from the standard 3 μl using a Agilent Programmable Temperature Vaporization (PVT) inlet (Agilent G2888A). Procedures for sample extraction and molecular quantification for the organic tracers have been described in detail by Phuleria et al. (2006) and only a brief summary is presented here. The impactor samples were spiked with known amounts of isotope labeled internal standard compounds, including three deuterated PAH, three deuterated alkanic acids, four deuterated alkanes, deuterated cholestane, deuterated cholesterol, and C13 labeled

levoglucosan. Samples were extracted in dichloromethane and methanol, combined, and reduced in volume to 100 μ L by rotary evaporation followed by pure nitrogen evaporation. The final target volume was determined based on the amount of organic carbon mass in each sample (Phuleria et al. 2006). The extracts were derivatized using diazomethane to convert organic acids to their methyl esters and run on the GCMS. An aliquot of the sample extract was then silylated and run on the GC-PCI-MS to measure levoglucosan and other polar organic compounds (Lewandowski et al. 2008; Stone et al., 2009).

The methylated and silylated samples were analyzed by auto-injection into a GC/MSD system (GC model 5890, MSD model 5973, Agilent). A 30 m \times 0.25 mm DB-5MS capillary column (Agilent) is used with a splitless injection. Along with the samples, six dilutions of authentic quantification standard solutions were also injected and used to determine calibration curves for the compounds of interest. While some compounds are quantified based on the response of a matching compound in the standard mixtures, others for which matching standards were not available were quantified using the response factors of compounds with similar structures and retention times.

Field blanks, laboratory blanks, spiked samples, and small aliquots of standard reference material (NIST Urban Dust SRM 1649a) were analyzed along with the composite $PM_{0.25-2.5}$ samples used for organic tracer compound analysis by GC/MS. Table 2.1 summarizes the recovery of spikes for the spiked samples. Analytical errors for these methods were calculated by compound using spike recovery and the standard deviation of blank filter analysis. All measurements were blank corrected using the average of the blanks. Point-wise estimates of uncertainties for each measurement, which were based on analytical uncertainties and uncertainties associated with blank correction, were used to determine if each measurement were statistically different from zero. Although duplicate samples were not available to evaluate method precision based on our experimental protocol of the study, the precision of the spike and standard reference material analyses were used to estimate method precision. Table 2.1 also show which compounds were used in the chemical mass balance (CMB) model (Task 2, Chapter 3). Table 2.2 shows mean concentrations for the various organic compounds.

2.2 In vitro measurement of PM-related ROS production in alveolar macrophages

We measured the potential biological production of ROS using an *in vitro* system of rat alveolar macrophage cells (NR8383, American Type Culture Collection) that were exposed to aqueous extracts of PM filters. Details of the method can be found in Landerman et al. (2008) including the assay validation study. The rationale for using murine cell line NR8383 is outlined in Landreman et al. (2008). Briefly, well-characterized human alveolar macrophage cell lines are not available. Hence, we selected NR8383 because it exhibits all the functional characteristics of normal primary human alveolar macrophages. These cells are highly responsive to microbial, particulate, and soluble stimuli with phagocytosis and killing. NR8383 cells produce an oxidative burst and secrete relevant cytokines (e.g. IL-1, IL-6, TNF- α , β). Importantly, NR8383 cells express a functional mannose receptor, which is a phagocytic and endocytic receptor critical for immune response and host defense. This cell line has been used in studies of the health impacts of environmental particles; it has proven robust and consistent in its cellular responses, allowing for accurate comparisons between studies and environmental samples.

Cells were exposed to aqueous extracts of PM filters for either $PM_{0.25}$ (previously performed under separate funding) or $PM_{0.25-2.5}$ particles (funded under the present ARB study) as previously described (Hu et al. 2008, Verma et al. 2009). We present laboratory results of the $PM_{0.25-2.5}$ assay here and data from both size fractions are used in the epidemiologic analysis in Task 3. Extracts were collected from composited $PM_{0.25}$ and $PM_{0.25-2.5}$ samples using

purified water. Dissolved, colloidal, and small insoluble species were collected after filtration with a 0.22 μm pore size filter. A dilution series of salt- and glucose- buffered filtrate in medium was prepared for cell exposures. The NR8383 cells were exposed in triplicate to $\text{PM}_{0.25}$ or $\text{PM}_{0.25-2.5}$ extracts and 2'7'-dichlorohydrofluorescein diacetate (DCFH-DA) in 96-well plates, and incubated at 37°C for 2.5 hours. After incubation, a Cytoflour II automated fluorescence plate reader was used to read fluorescence intensity; increased fluorescence (from the oxidized product, DCF) represented increased ROS production and therefore increased oxidative generating capacity of extracts. Un-opsionized Zymosan (a β -1,3-polysachharide of D-glucose) was used as the positive control because, by binding to TLR-2 receptors on macrophage cells, it causes a strong respiratory burst and reproducibly increases ROS production. Results are filter blank (negative control) subtracted and reported in units μg Zymosan equivalents/ m^3 air (μg Zymosan/ μg PM in extract multiplied by 5-day average PM $\mu\text{g}/\text{m}^3$ air).

The mean ROS activity of 6 filter blanks and 24 method blanks was not significantly greater than zero (mean filter blank activity was <1% of average PM sample activity). Positive controls were consistent within repetitions ($\pm 20\%$). Overall assay precision (based on intra- and inter-batch results) averaged 11% (without Zymosan normalization) and 7.2% with Zymosan normalization. We assessed cell viability by (a) running a dilution series of each extract, and (b) measuring lactate dehydrogenase release. Cell damage/toxicity, revealed as non-linearity in dose-response curves and/or increased lactate dehydrogenase release, was not detected. Descriptive statistics of the ROS data are presented later in Chapter 4 (Tables 4.3 and 4.4).

Table 2.1 Organic Compounds Quantified and Selected QA/QC Results.

Compound	Compound Class	Used In CMB Model	Spike Recovery (n=10)
Fluoranthene	Low MW PAH		115 \pm 7
Acephenanthrylene	Low MW PAH		105 \pm 6
Pyrene	Low MW PAH		NQ
Benzo(ghi)fluoranthene	Low MW PAH		126 \pm 9
Benz(a)anthracene	Low MW PAH		102 \pm 6
Chrysene	Low MW PAH		120 \pm 11
1-Methylchrysene	Low MW PAH		NQ
Benzo(b)fluoranthene	Medium MW PAH	X	127 \pm 10
Benzo(k)fluoranthene	Medium MW PAH	X	125 \pm 4
Benzo(j)fluoranthene	Medium MW PAH		NQ
Benzo(e)pyrene	Medium MW PAH	X	NQ

Table 2.1 (cont.)

Compound	Compound Class	Used In CMB Model	Spike Recovery (n=10)
Benzo(a)pyrene	Medium MW PAH		NQ
Indeno(1,2,3-cd)pyrene)	High MW PAH		89 ± 20
Benzo(ghi)perylene	High MW PAH		106 ± 13
Dibenz(ah)anthracene	High MW PAH		NQ
Picene	High MW PAH		NQ
Coronene	High MW PAH		103 ± 11
17 α (H)-22,29,30-Trisnorhopane	Hopanes	X	111 ± 14
17 β (H)-21 α (H)-30-Norhopane	Hopanes		115 ± 14
17 α (H)-21 β (H)-Hopane	Hopanes		120 ± 14
22S-Homohopane	Hopanes	X	105 ± 8
22R-Homohopane	Hopanes	X	NQ
22S-Bishomohopane	Hopanes		NQ
22R-Bishomohopane	Hopanes		NQ
22S-Trishomohopane	Hopanes		NQ
22R-Trishomohopane	Hopanes		NQ
n-Decanoic acid	Organic Acids		NQ
n-Dodecanoic acid	Organic Acids		NQ
n-Tetradecanoic acid	Organic Acids		NQ
n-Pentadecanoic acid	Organic Acids		NQ
n-Hexadecanoic acid	Organic Acids		NQ
n-Heptadecanoic acid	Organic Acids		NQ
n-Octadecanoic acid	Organic Acids		NQ
Palmitoleic acid	Organic Acids		115 ± 16
Oleic acid	Organic Acids		95 ± 13
Phthalic acid	Organic Acids		NQ
n-Tetracosane	n-Alkanes		109 ± 7
n-Pentacosane	n-Alkanes		94 ± 7
n-Hexacosane	n-Alkanes		89 ± 7

Table 2.1 (cont.)

Compound	Compound Class	Used In CMB Model	Spike Recovery (n=10)
n-Heptacosane	n-Alkanes		86 ± 7
n-Octacosane	n-Alkanes		106 ± 9
n-Nonacosane	n-Alkanes	X	109 ± 6
n-Triacontane	n-Alkanes		118 ± 9
n-Hentriacontane	n-Alkanes	X	107 ± 5
n-Dotriacontane	n-Alkanes		118 ± 9
n-Tritriacontane	n-Alkanes	X	NQ
n-Tetratriacontane	n-Alkanes		NQ
n-Pentatriacontane	n-Alkanes		NQ
n-Hexatriacontane	n-Alkanes		NQ
n-Heptatriacontane	n-Alkanes		NQ
n-Octatriacontane	n-Alkanes		NQ
n-Nonatriacontane	n-Alkanes		NQ
n-Tetracontane	n-Alkanes		NQ
αββ-20R-C ₂₇ -Cholestane	Steranes		105 ± 8
αββ-20S-C ₂₇ -Cholestane	Steranes		103 ± 9
ααα-20S-C ₂₇ -Cholestane	Steranes		NQ
αββ-20R-C ₂₈ -Ergostane	Steranes		105 ± 7
αββ-20S-C ₂₈ -Ergostane	Steranes		NQ
αββ-20R-C ₂₉ -Sitostane	Steranes		106 ± 6
αββ-20S-C ₂₉ -Sitostane	Steranes		NQ
Levoglucosan	Levoglucosan	X	NQ

Abbreviations: CMB, chemical mass balance; MW: molecular weight; NQ, not quantified

Table 2.2. Average Indoor and Outdoor Accumulation Mode Organic Compound Concentrations by Season.

Concentration (ng/m3)	Indoor Phase 1	Indoor Phase 2	Outdoor Phase 1	Outdoor Phase 2
Fluoranthene	0.032	0.033	0.032	0.033
Acephenanthrylene	0.032	0.033	0.032	0.033
Pyrene	0.024	0.024	0.024	0.025
Benzo(ghi)fluoranthene	0.008	0.009	0.008	0.008
Cyclopenta(cd)pyrene	0.032	0.033	0.032	0.033
Benz(a)anthracene	0.032	0.033	0.032	0.033
Chrysene	0.016	0.025	0.017	0.038
1-Methylchrysene	0.008	0.011	0.008	0.009
Retene	0.024	0.026	0.024	0.025
Benzo(b)fluoranthene	0.032	0.051	0.032	0.077
Benzo(k)fluoranthene	0.008	0.017	0.008	0.029
Benzo(j)fluoranthene	0.008	0.008	0.008	0.008
Benzo(e)pyrene	0.024	0.034	0.024	0.045
Benzo(a)pyrene	0.016	0.017	0.016	0.016
Indeno(1,2,3-cd)pyrene	0.018	0.046	0.025	0.056
Perylene	0.016	0.016	0.016	0.016
Benzo(ghi)perylene	0.029	0.057	0.038	0.066
Dibenz(ah)anthracene	0.032	0.037	0.032	0.033
Picene	0.024	0.027	0.024	0.025
Coronene	0.024	0.026	0.024	0.026
Dibenzo(ae)pyrene	0.024	0.032	0.024	0.024
17A(H)-22,29,30-Trisnorhopane	0.017	0.021	0.025	0.032
17B(H)-21A(H)-30-Norhopane	0.032	0.044	0.054	0.066
17A(H)-21B(H)-Hopane	0.041	0.061	0.075	0.086
22S-Homohopane	0.050	0.063	0.082	0.087
22R-Homohopane	0.051	0.056	0.078	0.080
22S-Bishomohopane	0.012	0.016	0.032	0.026
22R-Bishomohopane	0.012	0.014	0.027	0.021
22S-Trishomohopane	0.008	0.008	0.012	0.008
22R-Trishomohopane	0.008	0.008	0.011	0.008
ABB-20R-C27-Cholestane	0.020	0.027	0.023	0.028
ABB-20S-C27-Cholestane	0.023	0.032	0.029	0.033
AAA-20S-C27-Cholestane	0.017	0.022	0.021	0.024
ABB-20R-C28-Ergostane	0.010	0.012	0.012	0.011
ABB-20S-C28-Ergostane	0.010	0.012	0.012	0.011
ABB-20R-C29-Sitostane	0.020	0.028	0.029	0.033
ABB-20S-C29-Sitostane	0.016	0.021	0.024	0.024
Norpristane	0.049	0.049	0.048	0.049
Heptadecane	0.040	0.041	0.040	0.041
Pristane	0.032	0.033	0.032	0.033
Octadecane	0.032	0.033	0.032	0.033
Phytane	0.024	0.024	0.024	0.024
Nonadecane	0.042	0.024	0.024	0.024
Eicosane	0.197	0.008	0.042	0.008

Table 2.2 (cont.)

Concentration (ng/m3)	Indoor Phase 1	Indoor Phase 2	Outdoor Phase 1	Outdoor Phase 2
Heneicosane	0.11	0.14	0.08	0.10
Docosane	0.26	0.21	0.06	0.27
Tricosane	0.89	0.96	0.67	1.48
Tetracosane	1.03	1.12	0.77	2.04
Pentacosane	0.50	0.54	0.47	1.67
Hexacosane	0.93	0.89	0.87	2.03
Heptacosane	0.58	0.56	0.46	1.47
Octacosane	0.80	0.81	0.62	1.53
Nonacosane	0.80	0.85	0.77	1.45
Triacontane	0.99	0.89	0.79	1.39
Hentriacontane	0.83	0.79	0.69	1.13
Dotriacontane	1.03	0.85	0.80	1.20
Tritriacontane	0.68	0.60	0.58	0.81
Tetratriacontane	0.90	0.77	0.72	1.07
Pentatriacontane	0.35	0.36	0.28	0.42
Hexatriacontane	0.56	0.46	0.41	0.55
Heptatriacontane	0.24	0.24	0.23	0.26
Octatriacontane	0.40	0.34	0.30	0.43
Nonatriacontane	0.29	0.29	0.28	0.29
Tetracontane	0.47	0.45	0.36	0.50
Decylcyclohexane	0.04	0.04	0.04	0.04
Pentadecylcyclohexane	0.02	0.02	0.02	0.02
Hexadecylcyclohexane	0.04	0.04	0.04	0.04
Heptadecylcyclohexane	0.04	0.04	0.04	0.04
Octadecylcyclohexane	0.04	0.04	0.04	0.04
Nonadecylcyclohexane	0.01	0.01	0.01	0.02
Squalane	0.04	0.04	0.04	0.04
Decanoic acid	0.85	0.30	0.54	0.32
Dodecanoic acid	0.83	0.75	0.62	0.82
Tetradecanoic acid	1.19	1.35	1.48	0.98
Pentadecanoic acid*	0.49	0.38	0.56	0.27
Hexadecanoic acid	4.00	8.54	7.40	11.47
Heptadecanoic acid*	0.39	0.42	0.46	0.48
Octadecanoic acid	4.06	6.04	6.04	6.91
Nonadecanoic acid*	0.17	0.13	0.16	0.33
Pinonic acid	1.01	0.38	0.53	0.83
Palmitoleic acid	0.28	0.21	0.37	0.31
Oleic acid	1.56	1.54	0.65	2.16
Linoleic acid	0.68	0.82	0.32	2.20
Linolenic acid	0.24	0.24	0.24	0.31
Eicosanoic acid	0.91	0.98	0.89	1.14
Heneicosanoic acid	0.24	0.25	0.27	0.33
Docosanoic acid	0.34	0.39	0.47	0.63
Tricosanoic acid	0.23	0.26	0.27	0.33
Tetracosanoic acid	0.59	0.73	0.97	0.88
Pentacosanoic acid	0.17	0.18	0.19	0.19

Table 2.2 (cont.)

Concentration (ng/m3)	Indoor Phase 1	Indoor Phase 2	Outdoor Phase 1	Outdoor Phase 2
Hexacosanoic acid	0.21	0.27	0.36	0.40
Heptacosanoic acid	0.16	0.16	0.19	0.18
Octacosanoic acid	0.45	0.58	0.66	0.70
Nonacosanoic acid	0.21	0.19	0.27	0.29
Triacosanoic acid	0.38	0.52	0.64	0.65
Dehydroabietic acid	0.53	2.10	0.59	2.93
7-oxodehydroabietic acid	0.21	0.33	0.23	0.40
Phthalic acid	25.71	13.83	22.90	18.51
Isophthalic acid	1.05	1.22	1.93	1.83
Terephthalic acid	3.98	5.91	4.58	5.89
1,2,4-Benzenetricarboxylic acid	1.88	1.81	2.96	2.79
1,2,3-Benzenetricarboxylic acid	0.30	0.30	0.29	0.31
1,3,5-Benzenetricarboxylic acid	0.16	0.16	0.16	0.16
1,2,4,5-Benzenetetracarboxylic acid	0.23	0.23	0.22	0.22
Methylphthalic acid	5.21	4.96	7.63	7.04
Levogluconan	12.50	14.19	10.01	19.03
Glutaric acid	0.16	0.16	0.16	0.16
Adipic acid	0.16	0.44	0.23	0.22
Pimelic acid	0.25	0.16	0.39	0.16
Suberic acid	1.04	0.89	0.84	0.65
Azelaic acid	3.20	3.24	3.53	4.00

References

- Arhami M, Minguillón MC, Polidori A, Schauer JJ, Delfino RJ, Sioutas C. 2010. Organic compound characterization and source apportionment of indoor and outdoor quasi-ultrafine PM in retirement homes of the Los Angeles basin. *Indoor Air* 20: 17–30
- Arhami M, Polidori A., Tjoa T., Delfino R.J., and Sioutas C. 2009. Associations Between Personal, Indoor and outdoor Pollutant Concentration; Implications for Exposure Assessment to Size – Fractionated PM. *J Air Waste Manage Assoc* 59:392–404.
- Herner, J.D., Green, P.G. and Kleeman, M.J. 2006. Measuring the trace elemental composition of size-resolved airborne particles. *Environ Sci Technol* 40:1925–1933.
- Hu S, Polidori A, Arhami M, Shafer MM, Schauer JJ, Cho A, Sioutas C. Redox activity and chemical speciation of size-fractionated PM in the communities of the Los Angeles-Long Beach harbor. *Atmos Chem Physics*. 2008;8:6439-6451.

- Landerman AP, Shafer MM, Hemming JC, Hannigan MP, Schauer JJ. A macrophage-based method for the assessment of the oxidative stress activity of atmospheric particulate matter (PM) and application to routine (daily 24-hour) aerosol monitoring studies. *Aerosol Science and Technology*. 2008;42:946-957.
- Lane KB, Egan B, Vick S, Abdolrasulnia R, Shepherd VL. Characterization of a rat alveolar macrophage cell line that expresses a functional mannose receptor. *J Leukoc Biol*. 1998;64:345-350.
- Lewandowski M, Jaoui M, Offenberg JH, Kleindienst TE, Edney EO, Sheesley RJ, Schauer JJ. 2008. Primary and Secondary Contributions to Ambient PM_{2.5} in the Midwestern United States. *Environ Sci Technol* 42, 3303-3309.
- Phuleria, H. C., M. D. Geller, P. M. Fine and C. Sioutas. 2006. Size-resolved emissions of organic tracers from light-and heavy-duty vehicles measured in a California roadway tunnel. *Environ Sci Technol* 40: 4109-4118.
- Polidori A, Arhami M, Delfino RJ, Allen R, Sioutas C. 2007. Indoor-outdoor relationships, trends and carbonaceous content of fine particulate matter in retirement communities of the Los Angeles basin. *J Air Waste Manage Assoc* 57:366-379.
- Schauer JJ, Rogge WF, Hildemann LM, Mazurek MA, Cass GR. 1996. Source apportionment of airborne particulate matter using organic compounds as tracers. *Atmos Environ* 30:3837-3855.
- Sheesley RJ, Schauer JJ, Bean E, Kenski D. 2004. Trends in secondary organic aerosol at a remote site in Michigan's upper peninsula. *Environ Sci Technol* 38: 6491-6500.
- Stone EA, Zhou J, Snyder DC, Rutter AP, Mieritz M, Schauer JJ. 2009. A Comparison of Summertime Secondary Organic Aerosol at Contrasting Urban Locations. *Environ Sci Technol* 43:3448-3454.
- Verma V, Polidori A, Schauer JJ, Shafer MM, Cassee FR, Sioutas C. Physicochemical and toxicological profiles of particulate matter (PM) from the October 2007 Southern California Wildfires. *Environ Sci Technol*. 2009;43:954-960.

3. CHAPTER THREE: TASK 2

Task 2: To use the accumulation mode composition data from Task 1 and existing metals data to conduct exposure analysis and source apportionment using chemical mass balance models (Dr. Constantinos Sioutas). This was combined with existing metals data to extend the indoor-outdoor exposure analysis and source apportionment work already completed using the quasi-ultrafine PM ($PM_{0.25}$) data in a chemical mass balance (CMB) model.

3.0 Introduction

This task focused on source apportionment of fine PM ($PM_{2.5}$, particles with an aerodynamic diameter smaller than $2.5 \mu m$) in indoor and outdoor environments of four retirement communities in the Los Angeles Basin, which constitute the study sites of CHAPS.

The main objectives of this task were:

- a) To determine the degree to which outdoor fine mode PM infiltrates indoors (following a similar process to that used for $PM_{0.25}$ in our previously published work, described by Arhami et al. (2010).
- b) To identify major sources of $PM_{2.5}$ at the indoor and outdoor environments throughout the two study years.
- c) To quantify source contributions to $PM_{2.5}$ mass concentration at the indoor and outdoor environments.

The results described in this task were used by the CHAPS investigators to evaluate associations between indoor and outdoor PM sources and health outcomes.

3.1 Materials and Methods

3.1.1 Sampling sites and schedule

At each of the four retirement community sites that were monitored sequentially for 12 weeks each across a two-year period, 24-hour size-segregated PM samples were collected daily from Monday to Friday by means of Sioutas Personal Cascade Impactor Sampler (PCIS, SKC Inc., Eighty Four, Pennsylvania, USA). Coarse, accumulation, and quasi-UF mode PM were sampled on Zefluor filters ($3 \mu m$ pore-size, Pall Life Sciences, Ann Arbor, Michigan, USA). However, the present study focuses only on fine PM ($PM_{2.5}$), where data for accumulation ($PM_{0.25-2.5}$) and quasi-ultrafine ($PM_{0.25}$) PM modes were combined to derive data for $PM_{2.5}$. PM mass concentrations were determined gravimetrically by weighing filters using a microbalance (Mettler-Toledo, Columbus, Ohio, USA; weight uncertainty $\pm 2 \mu g$) following equilibration under controlled temperature and relative humidity conditions ($22-24^\circ C$ and $40-50\%$, respectively).

Filters were composited weekly (including five daily collected samples – from Monday to Friday) for chemical analyses, which are described in Chapter 2 (Task 1) of this report. Briefly, samples were analyzed for water-soluble organic carbon (WSOC), total metals, organic tracer compounds and reactive oxygen species (ROS). A description of ROS data is presented in Chapter 2 (Task 1) of this report. The WSOC content of the samples was evaluated using a Sievers 900 Total Organic Carbon Analyzer (Zhang et al., 2008). The total elemental mass of

the samples was measured using a high resolution magnetic sector Inductively Coupled Plasma Mass Spectrometry (Thermo-Finnigan Element 2) (Herner et al. 2006). For this analysis filter substrates were digested in a mixture of 1 mL of 16 M nitric acid, 0.25 mL of 12 M hydrochloric acid, and 0.10 mL of hydrofluoric acid, which is typically referred to the “microwave-aided Teflon bomb digestion”. Finally, organic speciation was conducted using gas chromatography mass spectrometry (GC-6980, quadrupole MS-5973, Agilent Technologies). Details of this method can be found in Stone et al. (2008). All measurements were blank corrected using the average and standard deviation of the blanks. Finally, hourly PM_{2.5} elemental and organic carbon (EC and OC, respectively) levels in the PM_{2.5} fraction have already been measured using two semi-continuous OC-EC analyzers (Model 3F, Sunset Laboratory Inc), one located indoors and one outdoors at the four retirement community sites or groups (G1, G2, G3 and G4). G1 and G3 were in the east San Gabriel Valley, G2 in the west San Gabriel Valley, and G4 in Riverside CA.

3.1.2 Source apportionment

Source apportionment of fine PM (PM_{2.5}) was conducted using combined data for accumulation (PM_{0.25-2.5}) and quasi-ultrafine PM (PM_{0.25}) modes. Primary source contributions to weekly ambient fine organic carbon (OC) were estimated using a molecular marker-based chemical mass balance model (CMB) that was mathematically solved with the US Environmental Protection Agency CMB software (EPA-CMB8.2) by applying the effective variance weighted least squares algorithm to apportion the receptor data to the source profiles (Watson 1984). Molecular marker compounds that are chemically stable during transport from source to receptor and that were detected in the PM samples were selected as fitting species (Schauer, Rogge et al. 1996). These included EC, 22S-homohopane, 22R-homohopane, 17 α (H)-21 β (H)-hopane, 17 α (H)-22,29,30-trisnorhopane, benzo(e)pyrene, benzo(b)fluoranthene, benzo(k)fluoranthene, benzo(ghi)perylene, levoglucosan, indeno(1, 2, 3-cd)pyrene, nonacosane, hentriacontane, tritriacontane, vanadium, nickel and aluminum. The model input source profiles were based on the observed primary tracers. These profiles included light-duty and heavy-duty vehicles (LDV and HDV, respectively) (Kam, Liacos et al. 2012; Liacos, Kam et al. 2012), biomass burning in Western US (Fine, Cass et al. 2004; Sheesley, Schauer et al. 2007), ship emissions (Rogge, Hildemann et al. 1997; Agrawal, Malloy et al. 2008), paved road dust for the Los Angeles area (Schauer 1998) and vegetative detritus (Rogge, Hildemann et al. 1993). Markers used to apportion vegetative detritus included nonacosane, hentriacontane and tritriacontane.

Mobile source profiles were derived from on-road measurements of PM_{0.25-2.5} and PM_{0.25} conducted at CA-110 and I-710 freeways in Los Angeles (Kam, Liacos et al. 2012), and thus, suitably represent vehicular emissions at the study sites. Kam et al. (2012) reported an HDV composition of 3.9% and 11.3% for I-110 and I-710, respectively. However, inclusion of both LDV and HDV vehicular profiles led to co-linearity problems in some CMB runs (29 cases). For these samples, the “estimable linear combinations of inestimable sources” was considered as the contribution from mobile sources (Watson, Robinson et al. 1997). Whereas, mobile source contribution was determined as the sum of both LDV and HDV source contributions for the remaining samples (Lough et al., 2007). Other OC sources, including coal soot and natural gas, were found to be non-statistically significant and were therefore excluded from the model.

Source contributions to total PM_{2.5} were evaluated by converting CMB apportionment results for fine OC to those of PM_{2.5} using fine OC-to-PM mass ratios for each source (Rogge, Hildemann et al. 1993; Rogge, Hildemann et al. 1997; Schauer 1998; Fine, Cass et al. 2004; Sheesley, Schauer et al. 2007; Agrawal, Malloy et al. 2008; Kam, Liacos et al. 2012). For samples displaying a co-linearity in mobile sources, we assumed that mobile source contribution

to OC is entirely derived from LDVs. OC/PM ratio for the LDV source profile was therefore used to convert OC mobile source apportionment results to mass apportionment results for these co-linear samples. To evaluate the variation in the mass apportionment of mobile sources for these co-linear cases, we conducted a sensitivity analysis by considering three different cases. The OC apportionment results were converted to PM mass-based assuming that the OC apportioned to mobile sources is emitted from 1) only HDV, 2) 25% LDV/75% HDV, 3) 75% LDV/25% HDV. Results were then compared to our prior assumption that OC from mobile sources is only emitted from LDVs. As can be seen in Table 3.1, results are about 25, 18, and 8% higher when assuming that OC apportioned to mobile sources is from only LDVs, compared to cases 1, 2 and 3, respectively. In addition to the sources identified in OC apportionment, other water-insoluble organic matter (“other WIOM”), secondary organic aerosol (SOA) and sulfate concentrations were considered in PM_{2.5} apportionment. In anthropogenic-influenced regions, water-soluble organic carbon (WSOC) is mainly emitted from biomass burning sources or formed through photochemical reactions (Weber, Sullivan et al. 2007). Since tracers of secondary sources were not included in the CMB model, SOA was estimated by multiplying the difference between measured WSOC and WSOC from biomass burning by a factor of 1.8 (µgOM/µgOC) (Turpin and Lim 2001). This ratio, which is the average molecular weight per carbon weight for the organic aerosols, varies from 1.4 to 1.8 for urban aerosols and 1.9 to 2.3 for non-urban aerosols. Biomass burning, determined from CMB output, was estimated as 71% water-soluble (Sannigrahi et al. 2006). “Other WIOM” corresponds to water-insoluble organic matter that could not be apportioned to the considered primary sources. It was estimated by multiplying “other water-insoluble organic carbon (WIOC)” by a factor of 1.8 (Turpin and Lim 2001). “Other WIOC” was determined as the difference between the total concentration of WIOC (OC-WSOC) and the sum of all primary source contribution estimates (excluding biomass burning), plus the concentration of WIOC from biomass burning. Sulfate was determined from S concentration assuming that all measured S by ICPMS is in the form of ammonium sulfate (Arhami et al. 2009). Lastly, we should note that samples collected at G4 were excluded from the CMB analysis because they were affected by organic adsorption artifacts.

Table 3.2 presents the results from the CMB model including R^2 , χ^2 and source contribution estimates (\pm standard error) to PM_{2.5}. R^2 corresponds to the variance in ambient species concentrations explained by their calculated concentration. χ^2 represents the weighted sum of squares of the differences between calculated and measured fitting species concentrations.

3.2. Results and Discussion

3.2.1 Infiltration ratios of tracer species

Figure 3.1a-d shows the average indoor and outdoor levels of PAHs, hopanes and steranes, n-alkanes and organic acids at each site and phase of the study. To investigate the influence of outdoor and indoor sources on PM_{2.5} levels inside the retirement communities, weekly average indoor-to-outdoor (I/O) mass ratios and their standard deviations were determined for the speciated organics, as shown in Figure 3.2a-d. I/O Pearson correlation coefficients (R) were also evaluated to determine whether an indoor species is attributable to infiltration from outdoors.

During both phases, the average outdoor level of total PAHs was lowest at G4 while the highest was at the G2 site (Figure 3.1a). The Riverside site (G4) was the most distant from primary combustion sources (i.e. freeways and busy roadways) while G2 (west San Gabriel Valley) was the closest to a major freeway (within 300 m). The average concentration of the sum of all measured PAHs was slightly lower indoors than outdoors, suggesting a possible

contribution from outdoor sources to indoor particle levels. This was further corroborated by the I/O ratios and indoor-to-outdoor correlation coefficients for individual PAHs (Figure 3.2a). PAH components displayed average I/O ratios close to unity, with generally high and positive correlation coefficients (median R across components is 0.64 and 0.50 during the warm and cold phase, respectively), indicating a strong impact from outdoor sources (e.g. motor vehicle emissions) on indoor PAHs. PAHs generated by tobacco smoke were not expected indoors, as all of the considered retirement communities were non-smoking residences. Similarly to PAHs, the cumulative concentration of select hopanes was slightly higher outdoors than indoors at all sites (Figure 3.1b). Average I/O ratios of individual hopanes were close to unity (ranging from a minimum of 0.76 to a maximum of 1.20, across phases) and were accompanied by relatively high R-values, highlighting the possible influence of outdoor sources on indoor levels of hopanes (Figure 3.2b). Unlike PAHs and hopanes, the average cumulative concentration of measured n-alkanes was higher indoors than outdoors, with significantly high indoor levels during the cold phase at G3 and G4 sites (Figure 3.1c). Furthermore, individual n-alkanes displayed I/O ratios exceeding unity (up to 12 during the cold phase) and overall low or negative I/O correlation coefficients, implying a considerable influence from indoor sources on n-alkanes levels inside the retirement communities (Figure 3.2c). Potential indoor sources include cooking, household products, dust, smoking and candle burning (Fine, Cass et al. 1999; Schauer 1999; Kleeman 2008). To further investigate the origin of these n-alkanes, the carbon preference index (CPI), defined as the concentration ratio of their odd-to-even numbered homologues, was estimated (Figure 3.3). A CPI about 1 indicates a dominance of anthropogenic sources, whereas a CPI greater than 2 indicates a prevalence of biogenic sources (Simoneit 1986). Both indoor and outdoor n-alkanes did not exhibit a discernible odd-to-even carbon number preference (CPI ranging from 0.78 to 1.02), indicating their anthropogenic source. Similarly to n-alkanes, the average total concentration of measured organic acids (n-alkanoic acids (C10-C18), palmitoleic acid and oleic acid) was overall substantially higher indoors than outdoors for all sites and phases (Figure 3.1d). Individual organic acids were also poorly or negatively correlated with their outdoor components and displayed I/O ratios greater than unity, indicating their predominantly indoor origin (Figure 3.2d). Potential indoor sources include cooking. Oleic and palmitoleic acids have often been used as biomarkers of food cooking (Robinson 2006). Other significant sources of organic acids include human skin emissions (Nicolaidis 1974).

3.2.2 Source contribution estimates

Results of the source apportionment of fine PM mass are shown in Figure 3.4. Mobile sources overall contributed the most to both indoor and outdoor $PM_{2.5}$ at all sites and during all phases ($7.9 \pm 3.7 \mu\text{g}/\text{m}^3$, $42.7 \pm 18.7\%$, on average \pm standard deviation). Furthermore, contribution of outdoor mobile sources to indoor $PM_{2.5}$ was 0.72 times those outdoors, on average across sites and phases, indicating a significant influence on indoor fine PM levels from outdoor mobile source emissions. "Other WIOM", which represents uncharacterized primary sources such as food cooking, was generally the next most abundant source, contributing to $25.3 \pm 21.1\%$ of $PM_{2.5}$ on average across all sites and phases. At all sites, sulfate displayed greater contributions during the warm phase ($23.3 \pm 6.0\%$, $4.4 \pm 1.2 \mu\text{g}/\text{m}^3$) than cold phase ($9.5 \pm 2.7\%$, $1.9 \pm 0.5 \mu\text{g}/\text{m}^3$), consistent with its outdoor secondary origin (Rodhe 1999). Soil source contribution estimates averaged $1.8 \pm 1.6 \mu\text{g}/\text{m}^3$ ($10.7 \pm 8.1\%$ of $PM_{2.5}$) at all indoor sites while they accounted for $2.5 \pm 2.2 \mu\text{g}/\text{m}^3$ at all outdoor sites ($11.4 \pm 8.8\%$ of $PM_{2.5}$). Indoor activities likely contributed to re-suspension of dust. SOA contributed significantly to $PM_{2.5}$, accounting for 8.0 ± 2.0 and $5.6 \pm 4.5\%$ of its mass across all sites during the warm (summer and early fall) and cold (late fall and winter) phases, respectively. Its concentration was higher during the warm phase than cold period at both indoor and outdoor sites, most likely due to increased

photochemical activity during warm months. SOA source estimates during the warm phase averaged 1.76 ± 0.18 and $1.40 \pm 0.70 \mu\text{g}/\text{m}^3$ at the outdoor and indoor sites, respectively. On the other hand, source contributions from SOA accounted for 0.84 ± 0.55 and $1.4 \pm 1.16 \mu\text{g}/\text{m}^3$ at the outdoor and indoor sites during the cold phase, respectively. We should note that the greater SOA concentrations at indoor than outdoor locations at some of the sites, such as G1, can be attributed to indoor SOA formation from the reaction of household products' emissions with ozone and to a lesser extent with hydroxyl radicals (Destailats, Lunden et al. 2006; Weschler and Nazaroff 2008). It is noteworthy that outdoor ozone concentrations are typically the dominant source of ozone at indoor environments; nonetheless, many indoor source of ozone exist such as laser printers, photocopiers, and ion generators. Contribution of biomass burning to fine PM mass was on average 1.8 times higher during the cold phase than warm period, likely due to increased emissions from domestic heating. However, contributions of biomass burning to $\text{PM}_{2.5}$ were overall low, accounting for $2.5 \pm 2.3\%$ of its mass, on average across all sites and phases. The high biomass burning concentration seen at G2 indoor during the warm phase was driven by high levoglucosan concentration at this site during this period and while the reason for this increase was unclear, this result is consistent with that reported by Arhami et al. (2010) for ultrafine PM at the same site and for the same sampling period. Ships emissions were minor contributors to fine PM, respectively accounting for <1 and 2% of its mass, on average. The concentrations apportioned to vegetative detritus at indoor site G3 during the cold phase are substantially higher than at other locations. This was possibly due to the impact of small local sources other than vegetative detritus on n-alkanes concentration (and therefore the contribution of vegetative detritus) at G3 indoor, including synthetic fireplace logs, if used. Unapportioned PM mass accounted for less than 15% of $\text{PM}_{2.5}$. This discrepancy in mass apportionment could be associated with ammonium nitrate, which was not measured in this study, but could constitute a major component of $\text{PM}_{2.5}$ (Hughes, Allen et al. 2002). Additionally, uncertainties in the source profiles composition and multiplication factor used to estimate water-insoluble organic matter (WIOM) and SOA could lead to this discrepancy.

3.4 Summary and Conclusions

$\text{PM}_{2.5}$ and its components were concurrently measured at indoor and outdoor locations of four retirement communities in the Los Angeles air basin. Indoor PAHs and hopanes were generally strongly correlated with their outdoor counterparts and displayed indoor/outdoor ratios close to unity, highlighting the possible influence of outdoor sources (mainly vehicular emissions) on their indoor levels. On the other hand, concentrations of n-alkanes and organic acids inside the retirement communities were dominated by indoor sources (e.g. cooking). Source apportionment results showed that mobile sources were the dominant contributor to both indoor and outdoor $\text{PM}_{2.5}$ at all sites ($42.7 \pm 18.7\%$, of fine PM mass, on average across sites and phases). Moreover, the contribution of vehicular sources to indoor levels was generally comparable to their corresponding outdoor estimates, illustrating the strong influence of these sources on indoor PM concentrations. "Other WIOM", which represents uncharacterized primary sources (e.g. food cooking) was generally the next most abundant source, accounting for $25.3 \pm 21.1\%$ of $\text{PM}_{2.5}$ across all sites and phases, on average. Furthermore, indoor SOA formation, possibly resulting from the reaction of household products' emissions with ozone, was also evident at some of the sites.

In conclusion, these findings suggest that although the elderly retirees of the studied communities generally spend most of their time indoors (Jenkins et al. 1992), a sizeable portion of $\text{PM}_{2.5}$ particles to which they are exposed likely originated from outdoor mobile sources.

Table 3.1. Contribution of mobile sources to PM_{2.5} in the co-linear cases, assuming that the OC apportioned to mobile sources is emitted from 1) only LDV, 2) only HDV, 3) 25% LDV, 75% HDV, 4) 75% LDV, 25% HDV. The units are in µg/m³.

Co-linear cases (site, phase, indoor/outdoor, week)	only LDV	only HDV	25% LDV, 75% HDV	75% LDV, 25% HDV
G1P1INW4	10.22	8.16	8.68	9.71
G1P2INW1	6.11	4.88	5.18	5.80
G1P2INW2	10.67	8.52	9.06	10.13
G1P2INW3	6.52	5.21	5.54	6.19
G2P1INW2	4.02	3.21	3.41	3.82
G2P2INW1	14.19	11.34	12.05	13.48
G2P2INW2	7.12	5.68	6.04	6.76
G2P2INW3	7.77	6.21	6.60	7.38
G2P2INW5	11.88	9.49	10.09	11.29
G3P1INW1	6.03	4.81	5.12	5.72
G3P1INW2	9.60	7.67	8.15	9.12
G3P1INW3	7.50	5.99	6.37	7.12
G3P1INW4	5.24	4.18	4.45	4.98
G3P1INW5	6.56	5.24	5.57	6.23
G1P1OUTW1	10.95	8.74	9.29	10.40
G1P1OUTW2	13.33	10.64	11.31	12.66
G1P1OUTW5	8.85	7.07	7.52	8.41
G1P1OUTW6	8.91	7.12	7.57	8.46
G1P2OUTW2	11.78	9.41	10.00	11.19
G1P2OUTW3	10.43	8.33	8.86	9.91
G1P2OUTW4	10.81	8.63	9.18	10.27
G1P2OUTW5	16.00	12.78	13.58	15.19
G1P2OUTW6	13.00	10.38	11.04	12.34
G2P1OUTW2	6.93	5.53	5.88	6.58
G2P1OUTW3	14.42	11.52	12.24	13.70
G2P2OUTW2	11.86	9.47	10.07	11.26
G2P2OUTW3	11.57	9.24	9.83	10.99
G3P1OUTW2	10.80	8.63	9.17	10.26
G3P1OUTW4	7.09	5.66	6.02	6.73

Table 3.2. Statistical parameters and weekly source contribution estimates (\pm standard error, in $\mu\text{g}/\text{m}^3$) to ambient fine PM mass at the indoor and outdoor sampling sites during the warm and cold phases. * indicates samples affected by adsorption artifacts. Source apportionment results for these samples were excluded from the calculations. **uncertainty quantified by propagation of the uncertainties of the measurements and CMB output results.

Indoor warm phase											
Site	Week	R ²	χ^2	Vegetative Detritus	Wood smoke	Ship Emissions	Soil	Mobile sources	SOA**	Other WIOM**	Sulfate
G1	1	0.86	2.59	0 \pm 0.09	0.19 \pm 0.11	-	-	4.17 \pm 5.22	2.49 \pm 0.15	4.22 \pm 2.47	-
	2	0.93	2.26	0 \pm 0.09	0.18 \pm 0.11	0.25 \pm 0.03	4.29 \pm 0.77	5.69 \pm 4.27	2.57 \pm 0.16	2.71 \pm 2.04	4.77 \pm 0.04
	3	0.97	2.49	0 \pm 0.08	0.11 \pm 0.1	0.16 \pm 0.02	1.29 \pm 0.59	16.86 \pm 3.6	2.08 \pm 0.14	0 \pm 1.69	3.87 \pm 0.04
	4	0.9	2.85	0 \pm 0.1	0.14 \pm 0.11	0.4 \pm 0.05	8.44 \pm 1.32	10.22 \pm 0.85	2.73 \pm 0.16	1.1 \pm 0.64	7.54 \pm 0.06
	5	0.7	10.27	0.14 \pm 0.09	0.15 \pm 0.1	0.24 \pm 0.04	2.04 \pm 0.52	3.46 \pm 4.09	1.12 \pm 0.15	4.89 \pm 1.93	4.24 \pm 0.06
	6										
G2	1	0.63	9.95	0.08 \pm 0.09	0.98 \pm 0.26	0.26 \pm 0.04	1.8 \pm 0.53	0	1.48 \pm 0.33	7.21 \pm 2.28	3.65 \pm 0.09
	2	0.84	3.51	0.1 \pm 0.08	1.24 \pm 0.32	0.25 \pm 0.03	2.17 \pm 0.48	4.02 \pm 0.65	1.12 \pm 0.39	3.21 \pm 0.77	2.81 \pm 0.04
	3	0.91	2.53	0.31 \pm 0.11	1.75 \pm 0.4	0.35 \pm 0.04	3.25 \pm 0.71	1.5 \pm 5.59	1.49 \pm 0.49	4.82 \pm 2.75	4.66 \pm 0.07
	4	0.89	3.96	0 \pm 0.09	1.4 \pm 0.35	0.15 \pm 0.02	2.29 \pm 0.58	5.72 \pm 4.65	0.8 \pm 0.44	6.12 \pm 2.35	1.71 \pm 0.03
	5	0.91	3.41	0 \pm 0.08	1.04 \pm 0.3	0.17 \pm 0.02	2.2 \pm 0.57	7.73 \pm 4.14	0.31 \pm 0.37	3.29 \pm 2.03	1.92 \pm 0.03
	6	0.9	3.03	0.31 \pm 0.11	1.9 \pm 0.38	0.23 \pm 0.03	1.03 \pm 0.53	3.83 \pm 5.25	0 \pm 0.47	5.91 \pm 2.54	2.23 \pm 0.04
G3	1	0.87	2.05	0 \pm 0.09	0.34 \pm 0.13	0.09 \pm 0.01	1.29 \pm 1.72	6.03 \pm 0.73	0.93 \pm 0.19	3.31 \pm 0.67	2.39 \pm 0.05
	2	0.89	2.27	0 \pm 0.11	0.22 \pm 0.11	0.1 \pm 0.02	1.01 \pm 1.73	9.6 \pm 0.89	1.37 \pm 0.18	1.88 \pm 0.67	3.31 \pm 0.11
	3	0.84	3.15	0.09 \pm 0.09	0.14 \pm 0.1	0.1 \pm 0.02	0.97 \pm 1.72	7.5 \pm 0.83	1.37 \pm 0.17	4.11 \pm 0.67	4.18 \pm 0.09
	4	0.87	2.25	0 \pm 0.08	0.19 \pm 0.1	0.13 \pm 0.02	1.08 \pm 1.72	5.24 \pm 0.58	0.7 \pm 0.17	1.94 \pm 0.55	5.73 \pm 0.03
	5	0.85	2.58	0 \pm 0.08	0.14 \pm 0.1	0.1 \pm 0.02	1.01 \pm 1.65	6.56 \pm 0.74	1.36 \pm 0.16	3.48 \pm 0.6	2.12 \pm 0.03
	6	0.91	1.79	0 \pm 0.07	0.16 \pm 0.1	0.14 \pm 0.02	0.71 \pm 1.63	0.68 \pm 3.13	1.14 \pm 0.16	5.09 \pm 1.53	3.12 \pm 0.03

Indoor cold phase											
Site	Week	R ²	χ ²	Vegetative Detritus	Wood smoke	Ship Emissions	Soil	Mobile sources	SOA**	Other WIOM**	Sulfate
G1	1	0.91	2.56	0.03±0.08	0.07±0.09	0.11±0.01	1.51±0.38	6.11±0.49	1.21±0.16	2.34±0.55	2.31±0.03
	2	0.94	2.28	0±0.09	0.24±0.12	0.16±0.02	3.24±0.65	10.67±0.67	1.94±0.2	0±0.55	3.17±0.04
	3	0.94	2.61	0.14±0.08	0.45±0.13	0.18±0.02	0.65±0.4	6.52±0.46	1.19±0.18	0.6±0.52	3.54±0.06
	4	0.89	4.28	0.15±0.1	0.18±0.11	0.11±0.02	11±1.63	7.34±3.94	0.89±0.17	1.99±1.91	1.64±0.04
	5	0.94	2.98	0.11±0.11	0.51±0.16	0.15±0.02	0.46±0.56	14.48±4.88	1.21±0.23	1.66±2.3	1.49±0.03
	6										
G2	1	0.97	1.1	0±0.1	0.94±0.24	0.09±0.02	0±1.7	14.19±0.91	0±0.3	1.94±0.79	0.88±0.03
	2	0.9	2.39	0.01±0.08	0.36±0.13	0.02±0	0±1.67	7.12±0.57	0±0.17	2.2±0.59	0.34±0.03
	3	0.88	3.34	0±0.07	0.97±0.28	0.04±0.01	0±1.7	7.77±0.64	0.08±0.35	3.21±1.03	1.16±0.04
	4	0.93	2.68	0.04±0.08	1.41±0.33	0.17±0.02	0±1.72	11.63±4.36	1.46±0.41	6.28±2.55	2.62±0.03
	5	0.95	1.56	0±0.09	1.13±0.26	0.08±0.01	0±1.69	11.88±0.82	0±0.32	1.97±0.87	1.12±0.03
	6	0.85	2.92	0±0.07	0.19±0.1	0.06±0.01	0±0.27	2.49±2.67	0.23±0.14	4.77±1.26	0.94±0.03
G3	1	0.82	4.78	2.3±0.43	0.12±0.09	0.05±0.01	0.73±0.58	1.3±4.87	1.75±0.15	11.47±2.31	1.62±0.03
	2	0.9	2.47	3.44±0.58	0.3±0.14	0.1±0.02	0.38±0.78	0.64±6.29	3.47±0.21	10.01±2.97	3.22±0.04
	3										
	4*	0.89	2.49	2.53±0.45	0.07±0.09	0.02±0.01	0.52±0.61	0	0.67±0.15	15.62±2.46	0.43±0.01
	5*	0.91	1.97	0.14±0.09	0.17±0.09	0.02±0	0.43±0.31	2.04±2.93	0.4±0.15	16.11±1.41	0.4±0.02

Outdoor warm phase

Site	Week	R2	χ^2	Vegetative Detritus	Wood smoke	Ship Emissions	Soil	Mobile sources	SOA**	Other WIOM**	Sulfate
G1	1	0.88	4.5	0±0.09	0.23±0.11	0.45±0.05	6±1	10.95±0.74	1.91±0.16	0.75±0.59	6.18±0.04
	2	0.95	2.02	0±0.09	0.05±0.1	0.37±0.04	5.7±1.02	13.33±0.75	2.43±0.14	0±0.53	6.37±0.05
	3	0.95	3.15	0±0.08	0.18±0.1	0.26±0.03	11.37±1.73	12.06±3.71	1.66±0.15	0±1.8	5.08±0.06
	4	0.95	2.76	0±0.1	0.02±0.1	0.37±0.05	4.67±0.94	14.26±4.24	2.45±0.14	0±2	5.87±0.04
	5	0.78	8.92	0±0.08	0.21±0.11	0.38±0.05	3.81±0.7	8.85±0.6	1.51±0.18	1.94±0.43	6.83±0.07
	6	0.74	10.71	0±0.08	0.22±0.11	0.17±0.03	4.99±0.83	8.91±0.61	1.73±0.17	0.66±0.43	4.41±0.05
G2	1	0.72	9.97	0.05±0.09	0.26±0.12	0.33±0.05	7.53±1.14	3.39±4.52	1.55±0.16	8.64±2.16	5.51±0.13
	2	0.91	2.91	0±0.07	0.46±0.14	0.26±0.03	2.9±0.56	6.93±0.58	0.86±0.19	2.19±0.4	2.97±0.04
	3	0.97	1.09	0±0.11	1.1±0.33	0.47±0.06	5.64±1.06	14.42±1.04	1.37±0.41	0.42±0.67	6.03±0.14
	4	0.98	0.96	0±0.11	0.1±0.11	0.18±0.03	5.22±1.06	17.19±4.95	2.8±0.16	2.57±2.38	3.15±0.04
	5	0.8	8.36	0±0.09	0.15±0.1	0.1±0.02	1.51±0.57	11.96±5.12	0.92±0.15	5.43±2.46	1.58±0.04
	6	0.89	5.12	0.09±0.1	0.2±0.11	0.33±0.04	3.5±0.78	10.72±5.09	1.98±0.15	4.37±2.41	3.91±0.05
G3	1	0.94	1.82	0±0.09	0.09±0.1	0.15±0.02	1.91±0.51	4.78±4.22	1.19±0.17	6.14±2	3.86±0.1
	2	0.9	2.35	0±0.1	0.15±0.1	0.13±0.02	0.89±0.51	10.8±0.89	1.46±0.17	2.96±0.65	4.37±0.07
	3	0.94	1.76	0±0.1	0.14±0.1	0.14±0.02	0±0.49	9.72±4.97	2.64±0.17	4.37±2.35	6.19±0.08
	4	0.91	2.37	0±0.08	0.2±0.11	0.22±0.03	1.3±0.43	7.09±0.61	0.42±0.17	2.2±0.4	9.4±0.03
	5	0.87	2.96	0.12±0.09	0.18±0.1	0.2±0.03	0.75±0.46	1.78±4.54	3.24±0.17	4.64±2.18	3.98±0.04
	6	0.92	1.94	0±0.09	0.39±0.14	0.21±0.03	0.3±0.48	2.84±4.67	1.64±0.21	6.96±2.2	4.82±0.04

Outdoor cold phase

Site	Week	R2	χ^2	Vegetative Detritus	Wood smoke	Ship Emissions	Soil	Mobile sources	SOA**	Other WIOM**	Sulfate
G1	1	0.98	0.54	0.02±0.08	0.15±0.11	0.11±0.02	0±0.32	6.64±3.06	2.77±0.37	0.61±1.5	2.79±0.04
	2	0.96	1.64	0±0.09	0.25±0.12	0.11±0.02	0±0.4	11.78±0.69	1.14±0.2	1.15±0.49	1.84±0.03
	3	0.88	2.66	0±0.1	0.72±0.19	0.06±0.01	0.05±0.48	10.43±0.96	0.48±0.25	4.58±0.81	0.72±0.03
	4	0.92	2.5	0±0.11	0.19±0.12	0.09±0.02	5.78±0.95	10.81±0.84	1.09±0.17	0.93±0.63	1.07±0.04
	5	0.95	1.46	0±0.13	0.83±0.23	0.1±0.02	2.45±0.74	16±1.25	0.39±0.3	2.53±0.84	1.22±0.03
	6	0.98	0.97	0.09±0.1	0.65±0.18	0.1±0.02	0.05±0.47	13±0.84	0.77±0.24	0±0.55	2.48±0.05
G2	1	0.98	1.2	0±0.1	1.27±0.29	0.11±0.02	0±0.55	18.45±5.16	0±0.36	1.05±2.5	1.18±0.03
	2	0.97	0.97	0.05±0.09	0.82±0.21	0.01±0.01	0±1.71	11.86±0.76	0±0.26	4.6±0.77	0.5±0.03
	3	0.9	4.48	0.41±0.11	0.51±0.17	0.04±0.01	0±0.47	11.57±0.68	0.08±0.22	2.7±0.5	1.18±0.03
	4	0.98	0.93	0±0.09	1.59±0.31	0.21±0.03	0±0.55	17.69±5.22	0.25±0.39	6.4±2.5	4.53±0.09
	5	0.93	3.26	0±0.09	0.3±0.12	0.12±0.02	0±0.47	15.02±4.49	0.66±0.16	1.98±2.16	1.62±0.03
	6	0.9	3.09	0±0.08	0.24±0.11	0.08±0.01	2.88±0.55	5.86±3.44	0.25±0.15	6.1±1.68	1.65±0.03
G3	1	0.92	1.96	3.28±0.53	0.14±0.1	0.1±0.02	2.76±0.87	0	1.55±0.16	15.27±3.05	2.19±0.03
	2	0.94	2.18	0±0.13	0.46±0.17	0.15±0.02	1.32±0.63	10.85±5.56	2.65±0.24	10.13±2.63	3.35±0.03
	3	0.84	6.46	0±0.09	0.19±0.1	0.12±0.02	2±0.51	7.81±3.94	0.63±0.15	16.92±1.86	1.26±0.02
	4	0.88	4	0.08±0.09	0.29±0.11	0.05±0.01	1.74±0.47	5.91±3.95	0.82±0.17	16.16±1.89	0.63±0.02
	5	0.92	2.07	1.71±0.29	0.81±0.21	0.05±0.01	1.51±0.55	1.36±4.54	0.42±0.27	13.27±2.16	0.76±0.02

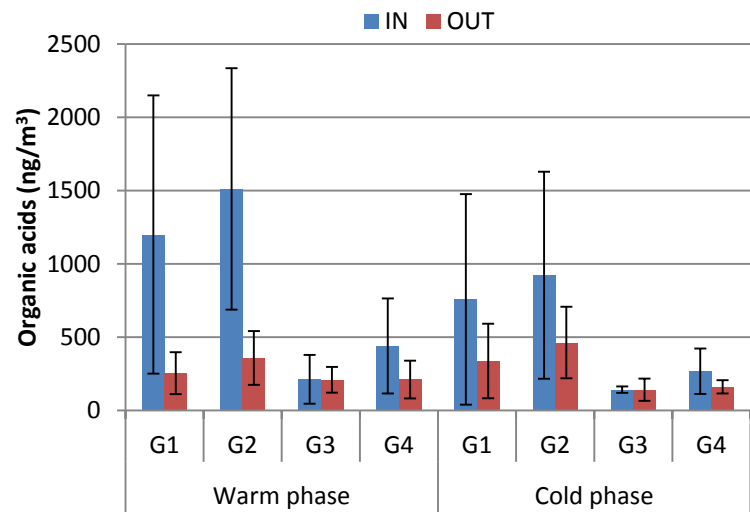
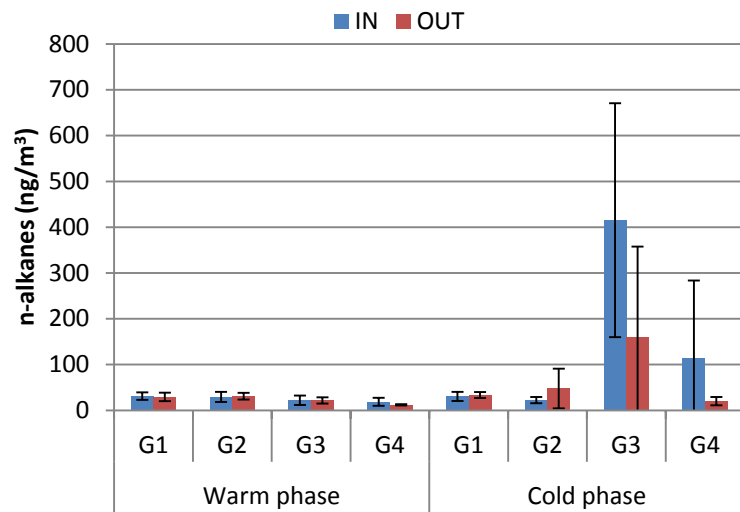
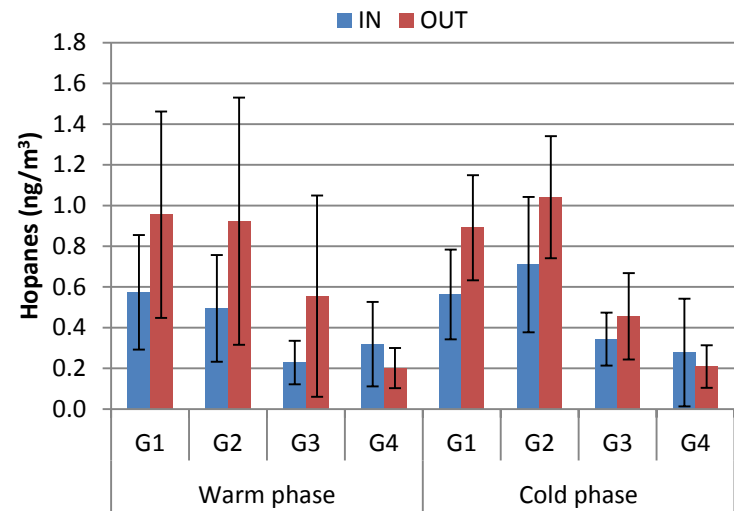
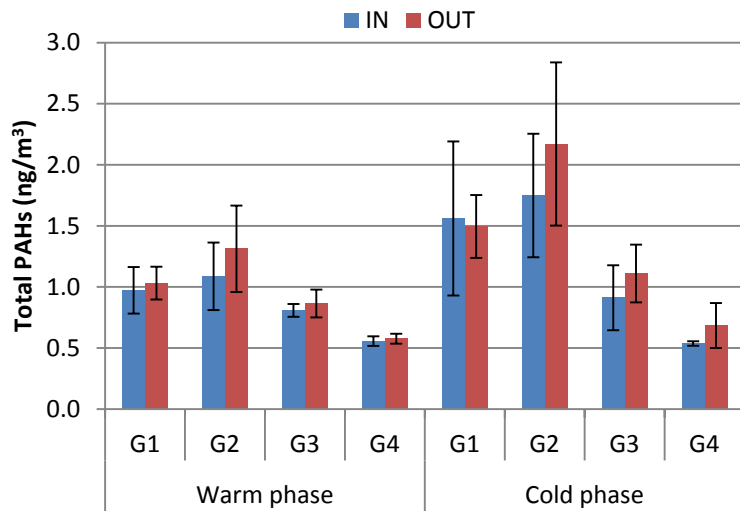
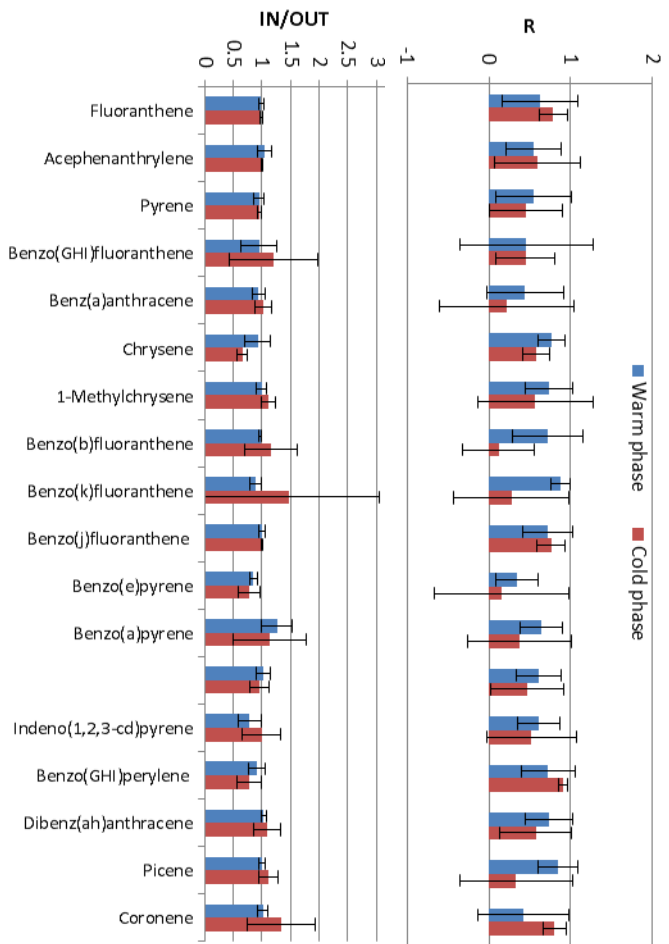
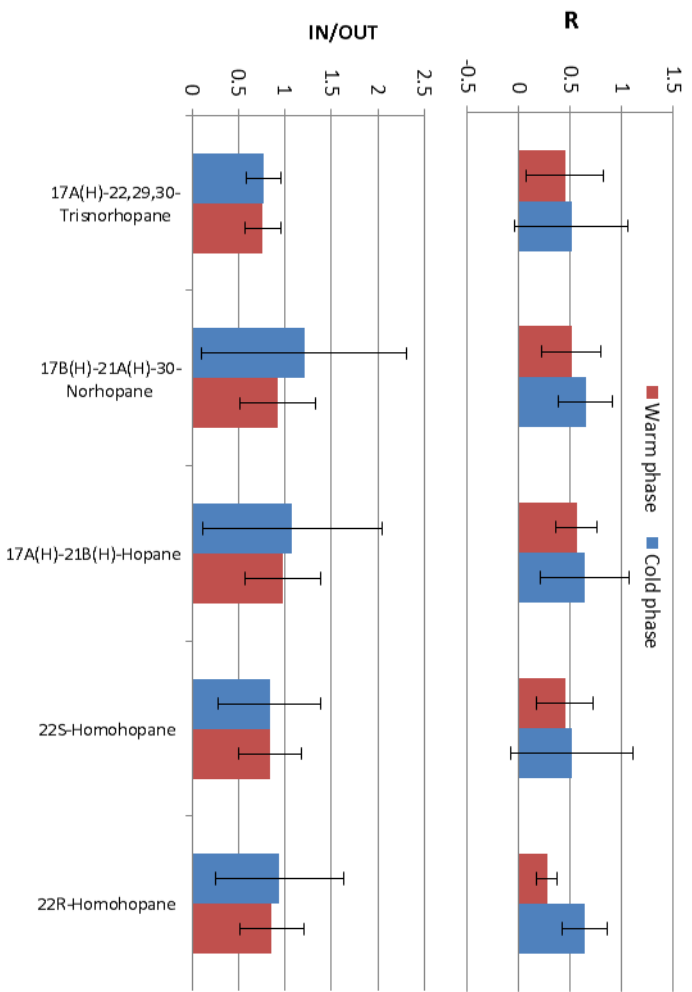


Figure 3.1. Average concentration of a) PAHs, b) hopanes, c) n-alkanes and d) organic acids at the indoor and outdoor sampling sites during the warm and cold phases. Error bars correspond to one standard deviation.

(a) PAH



(b) hopanes



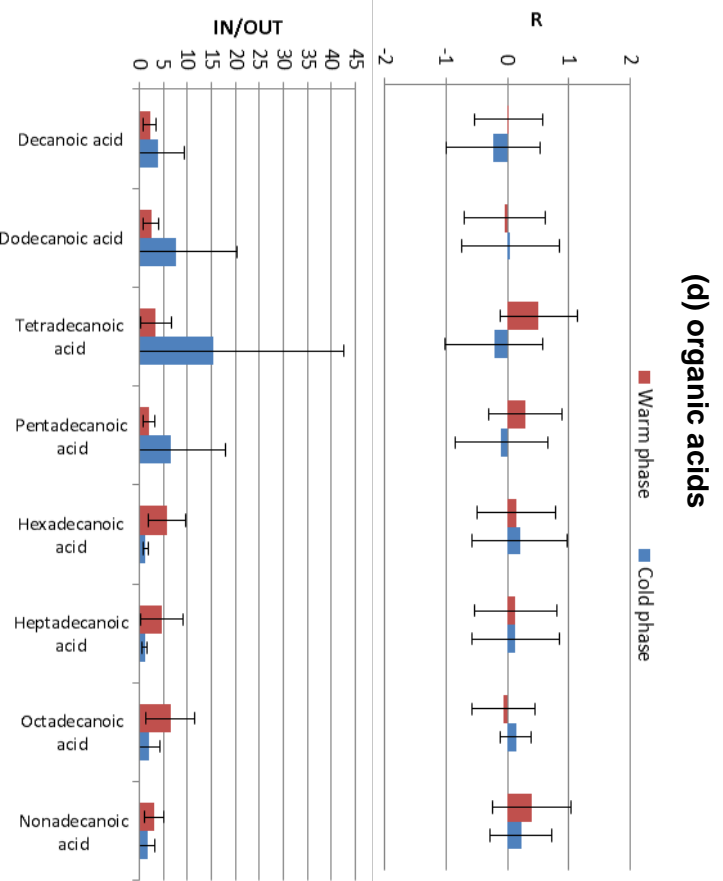
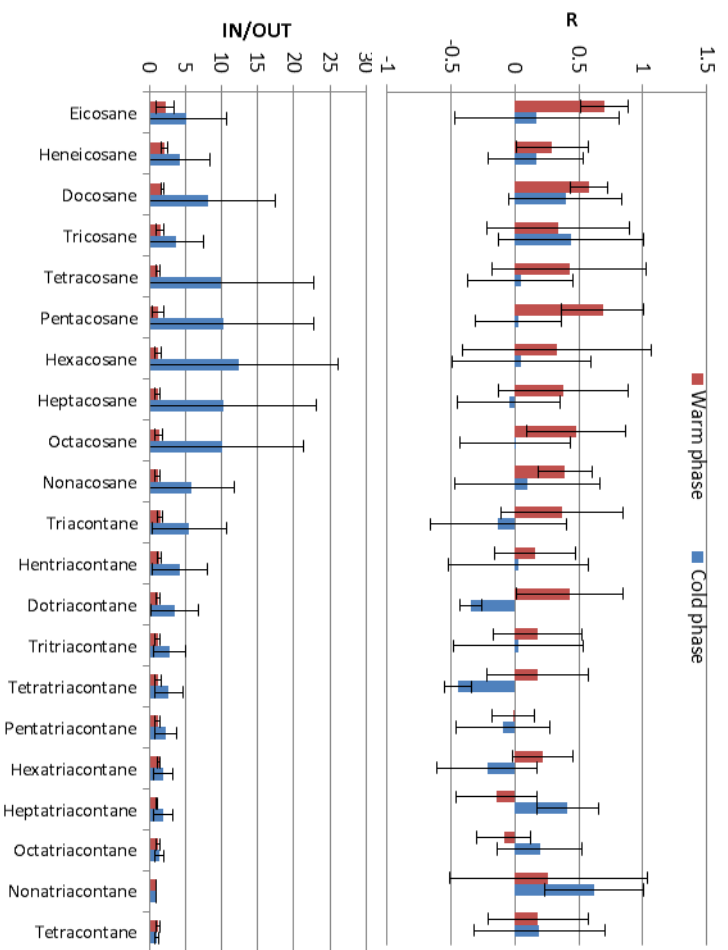


Figure 3.2. Average indoor-to-outdoor ratios and Pearson correlation coefficients between indoor and outdoor concentrations of (a) PAHs, (b) hopanes, (c) n-alkanes and (d) organic acids during the warm and cold phases. Values are averaged across the sampling sites and error bars correspond to one standard deviation.

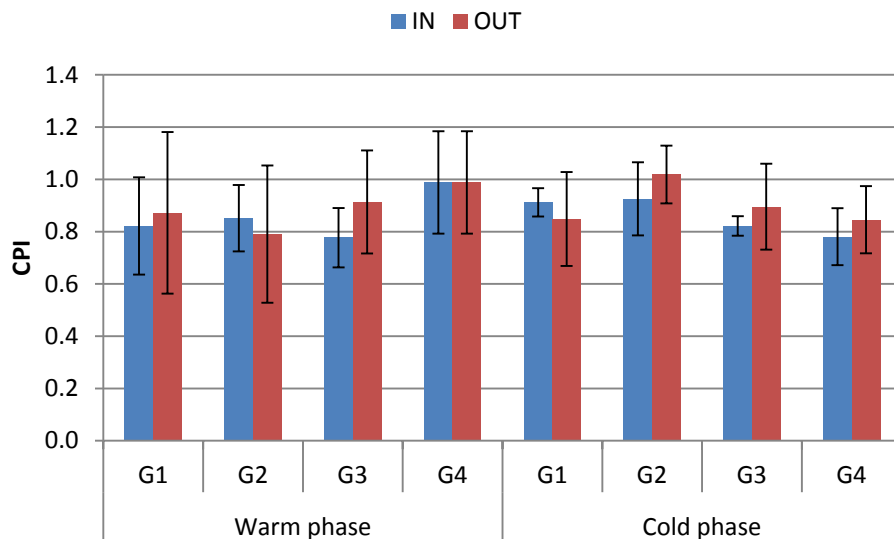


Figure 3.3. Average carbon preference index (CPI) of n-alkanes (C₁₉-C₄₀) at the indoor and outdoor sampling sites during the warm and cold phases. Error bars correspond to one standard deviation.

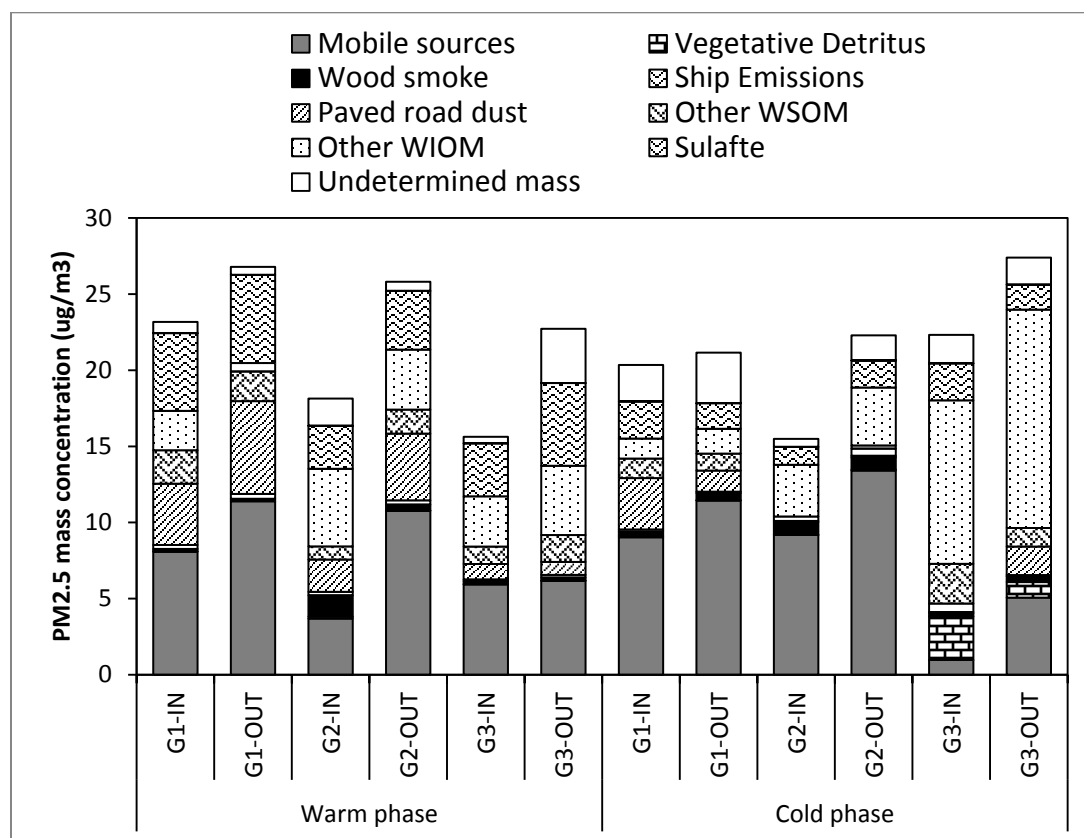


Figure 3.4. Contribution of different sources to fine PM mass at the sampling sites during the warm and cold phases. Samples affected by adsorption artifacts are not shown in the plot.

References

- Agrawal, H., Malloy, Q.G.J., Welch, W.A., Wayne Miller, J., Cocker III, D.R., 2008. In-use gaseous and particulate matter emissions from a modern ocean going container vessel. *Atmospheric Environment* 42, 5504-5510.
- Arhami, M., Minguillón, M.C., Polidori, A., Schauer, J.J., Delfino, R.J., Sioutas, C., 2010. Organic compound characterization and source apportionment of indoor and outdoor quasi-ultrafine PM in retirement homes of the Los Angeles basin. *Indoor Air* 20, 17-30.
- Arhami, M., Sillanpää, M., Hu, S., Olson, M.R., Schauer, J.J., Sioutas, C., 2009. Size-segregated inorganic and organic components of PM in the communities of the Los Angeles harbor. *Aerosol Science and Technology* 43, 145-160.
- Destailats, H., Lunden, M.M., Singer, B.C., Coleman, B.K., Hodgson, A.T., Weschler, C.J., Nazaroff, W.W., 2006. Indoor secondary pollutants from household product emissions in the presence of ozone: a bench-scale chamber study. *Environmental Science & Technology* 40, 4421-4428.
- Fine, P.M., Cass, G.R., Simoneit, B.R.T., 1999. Characterization of fine particle emissions from burning church candles. *Environmental Science & Technology* 33, 2352–2362.
- Fine, P.M., Cass, G.R., Simoneit, B.R.T., 2004. Chemical characterization of fine particle emissions from the wood stove combustion of prevalent United States tree species. *Environmental Engineering Science* 21, 705-721.
- Herner, J.D., Green, P.G., Kleeman, M.J., 2006. Measuring the trace elemental composition of size-resolved airborne particles. *Environmental science & technology* 40, 1925-1933.
- Hughes, L.S., Allen, J.O., Salmon, L.G., Mayo, P.R., Johnson, R.J., Cass, G.R., 2002. Evolution of nitrogen species air pollutants along trajectories crossing the Los Angeles area. *Environmental science & technology* 36, 3928-3935.
- Jenkins, P.L., Phillips, T.J., Mulberg, E.J., Hui, S.P., 1992. Activity patterns of Californians: Use of and proximity to indoor pollutant sources. *Atmospheric Environment. Part A. General Topics* 26, 2141-2148.
- Kam, W., Liacos, J.W., Schauer, J.J., Delfino, R.J., Sioutas, C., 2012. Size-segregated composition of particulate matter (PM) in major roadways and surface streets. *Atmospheric Environment* 55, 90-97.
- Kleeman, M.J., Robert, M.A., Riddle, S.G., Fine, P.M., Hays, M.D., Schauer, J.J. and Hannigan, M.P., 2008. Size distribution of trace organic species emitted from biomass combustion and meat charbroiling. *Atmospheric Environment* 42, 6152–6154.
- Liacos, J.W., Kam, W., Delfino, R.J., Schauer, J.J., Sioutas, C., 2012. Characterization of organic, metal and trace element PM_{2.5} species and derivation of freeway-based emission rates in Los Angeles, CA. *Science of the Total Environment* 435, 159-166.
- Lough, G.C., Christensen, C.G., Schauer, J.J., Tortorelli, J., Mani, E., Lawson, D.R., Clark, N.N., Gabele, P.A., 2007. Development of Molecular Marker Source Profiles for Emissions from On-Road Gasoline and Diesel Vehicle Fleets. *Journal of the Air & Waste Management Association* 57, 1190-1199.
- Nicolaidis, N., 1974. Skin lipids: Their biochemical uniqueness. *Science of the Total Environment* 186 19–26.
- Polidori, A., Arhami, M., Delfino, R.J., Allen, R., Sioutas, C., 2007. Indoor-outdoor relationships, trends and carbonaceous content of fine particulate matter in retirement

- communities of the Los Angeles basin. *Journal of Air and Waste Management Association* 57, 366-379.
- Polidori, A., Cheung, K.L., Arhami, M., Delfino, R.J., Sioutas, C., 2009. Relationships between size-fractionated indoor and outdoor trace elements at four retirement communities in southern California. *Atmospheric Chemistry and Physics* 9, 4521-4536.
- Robinson, A.L., Subramanian, R., Donahue, N.M., Bernardo-Bricker, A. and Rogge, W.F., 2006. Source apportionment of molecular markers and organic aerosol. 3. Food cooking emissions. *Environmental Science & Technology* 40, 7820–7827.
- Rodhe, H., 1999. Human impact on the atmospheric sulfur balance. *Tellus A Dyn. Meteorol. Oceanogr* 51, 110-122.
- Rogge, W.F., Hildemann, L.M., Mazurek, M.A., Cass, G.R., Simoneit, B.R.T., 1993. Sources of fine organic aerosol. 4. Particulate abrasion products from leaf surfaces of urban plants. *Environmental Science & Technology* 27, 2700-2711.
- Rogge, W.F., Hildemann, L.M., Mazurek, M.A., Cass, G.R., Simoneit, B.R.T., 1997. Sources of fine organic aerosol. 8. Boilers burning No. 2 distillate fuel oil. *Environmental science & technology* 31, 2731-2737.
- Sannigrahi, P., Sullivan, A.P., Weber, R.J., Ingall, E.D., 2006. Characterization of water-soluble organic carbon in urban atmospheric aerosols using solid-state ¹³C NMR spectroscopy. *Environmental science & technology* 40, 666-672.
- Schauer, J.J., 1998. Source contributions to atmospheric organic compound concentrations: emission measurements and model predictions., *Environmental Engineering Science*. California Institute of Technology, Pasadena, p. 400.
- Schauer, J.J., Kleeman, M.J., Cass, G.R. and Simoneit, B.R.T., 1999. Measurement of emissions from air pollution sources. 1. C-1 through C-29 organic compounds from meat charbroiling. *Environmental Science & Technology* 33, 1566–1577.
- Schauer, J.J., Rogge, W.F., Hildemann, L.M., Mazurek, M.A., Cass, G.R., Simoneit, B.R.T., 1996. Source apportionment of airborne particulate matter using organic compounds as tracers. *Atmospheric Environment* 30, 3837-3855.
- Sheesley, R.J., Schauer, J.J., Zheng, M., Wang, B., 2007. Sensitivity of molecular marker-based CMB models to biomass burning source profiles. *Atmospheric Environment* 41, 9050-9063.
- Simoneit, B.R.T., 1986. Characterization of organic-constituents in aerosols in relation to their origin and transports: a review. *International journal of environmental analytical chemistry* 23, 207–237.
- Stone, E.A., Snyder, D.C., Sheesley, R.J., Sullivan, A.P., Weber, R.J., Schauer, J.J., 2008. Source apportionment of fine organic aerosol in Mexico City during the MILAGRO experiment 2006. *Atmospheric Chemistry and Physics* 8, 1249-1259.
- Turpin, B.J., Lim, H.-J., 2001. Species contributions to PM_{2.5} mass concentrations: Revisiting common assumptions for estimating organic mass. *Aerosol Science & Technology* 35, 602-610.
- Watson, J.G., 1984. Overview of receptor model principles. *Journal of Air Pollution Control Association* 34, 619-623.
- Weber, R.J., Sullivan, A.P., Peltier, R.E., Russell, A., Yan, B., Zheng, M., De Gouw, J., Warneke, C., Brock, C., Holloway, J.S., 2007. A study of secondary organic aerosol formation in the anthropogenic-influenced southeastern United States. *Journal of Geophysical Research* 112.

- Weschler, C.J., Nazaroff, W.W., 2008. Semivolatile organic compounds in indoor environments. *Atmospheric Environment* 42, 9018-9040.
- Zhang, Y., Schauer, J.J., Shafer, M.M., Hannigan, M.P., Dutton, S.J., 2008. Source apportionment of in vitro reactive oxygen species bioassay activity from atmospheric particulate matter. *Environmental science & technology* 42, 7502-7509.

4. CHAPTER FOUR: TASK 3

Task 3. To conduct an epidemiologic analysis of the relations between gene expression and exposure to particle mass, components, and source tracers of PM_{0.25} and PM_{0.25-2.5} from Tasks 1 and 2 as well as to PM mass and metal content in PM_{2.5-10}. Gene expression data for 35 genes selected *a priori* were available from NIH, NIEHS-funded work. This includes genes involved in oxidative stress, antioxidant defense, xenobiotic metabolism, inflammation, coagulation, and endoplasmic reticulum stress. (Dr. Ralph Delfino and colleagues, UCI)

4.0 Introduction

We conducted a cohort panel study of acute cardiovascular outcomes with home-based ambient air pollution monitoring in the Los Angeles air basin from July 2005 through February 2006 and July 2006 through February 2007. Given the urban study location, our initial interest was on the effects of traffic-related ultrafine particles since they have been shown to be enriched in chemical components that have a pro-oxidant effect on cells (Ayres et al. 2008, Verma et al. 2009). Exposure data using accumulation-mode PM samples from Tasks 1-2 for this analysis were combined with exposure data already available for the quasi-ultrafine fraction and other air pollutant data we have collected for comparison (e.g., criteria gases, EC and OC). In this manner, the present study extends the CHAPS investigation using gene expression data (Figures 1.1 and 1.2).

Using a hypothesis-driven approach based on existing human studies, and the *in vitro* and *in vivo* experiments cited, we selected ten biological pathways relevant to air pollution exposure responses and examined changes in candidate gene expression (see section 1.1, Gene Expression) in our cohort panel of elderly subjects with CAD (Delfino et al. 2008, 2009, 2010). Biopathways included: coagulation, Klf2-mediated immune response, NF-κB signaling, acute phase response, Nrf2-mediated oxidative stress response, endoplasmic reticulum stress (UPR), glutathione metabolism, phase I and phase II metabolism, endogenous reactive oxygen species (ROS) production, and cytokine signaling (Figure 4.1, Table 4.1). Evaluating gene expression changes along these pathways in an urban cohort panel can provide coherence with studies of potential mechanistic pathways through which air pollutants may cause adverse cardiovascular outcomes.

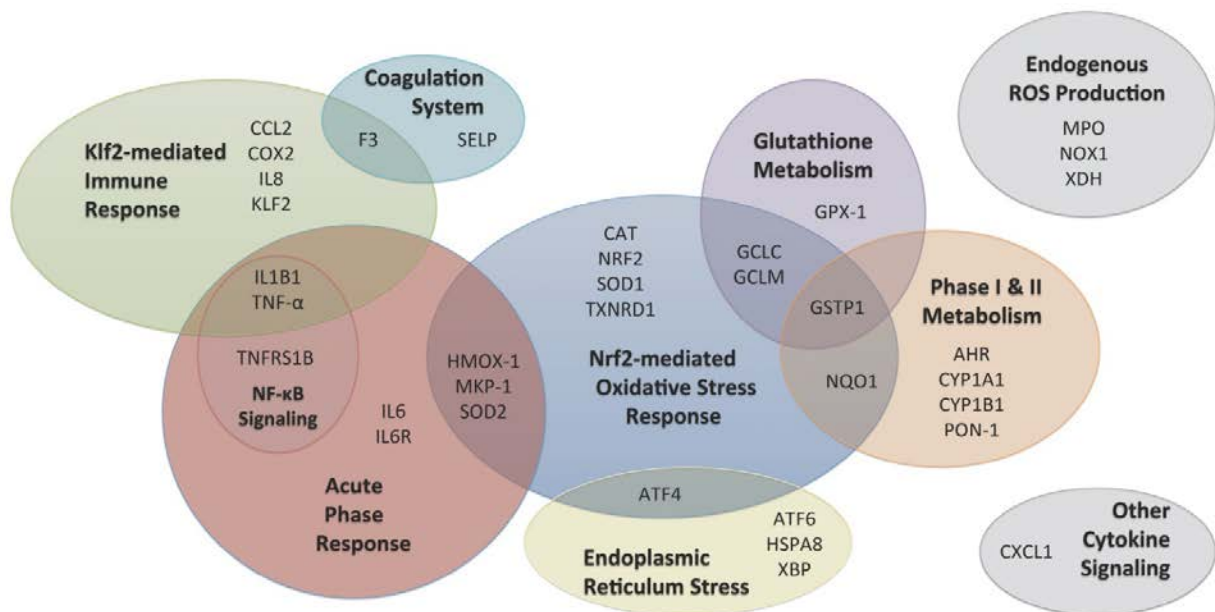


Figure 4.1. Candidate Genes grouped by biopathway. Gene abbreviations and NCBI identification numbers are listed in Table 4.1. Adapted from Wittkopp et al.

Table 4.1. Candidate Gene Names and NCBI identification numbers.

Symbol	Gene Name	Synonyms	NCBI Gene ID number
AHR	Aryl hydrocarbon receptor	bHLHe76	196
ATF4	CREB activating transcription factor 4	CREB-2, TAXREB67	468
ATF6	CREB activating transcription factor 6	ATF6A	22926
CAT	Catalase	-	847
CCL2	Chemokine (C-C motif) ligand 2	GDCF-2, HC11, MCAF, MCP-1, MCP1, MGC9434, SMC-CF	6347
CXCL1	Chemokine (C-X-C motif) ligand 1	GROa, MGSA-a, NAP-3, SCYB1	2919
CYP1A1	Cytochrome P450, subfamily A1	CP11, P1-450, P450-C, P450DX	1543
CYP1B1	Cytochrome P450, subfamily B1	CP1B	1545
DUSP1	Dual specificity phosphatase 1	CL100, HVH1, MKP-1	1843
F3	Tissue factor (Thromboplastin, coagulation factor III)	CD142	2152
GCLC	Glutamate-cysteine ligase, catalytic subunit	GCS	2729
GCLM	Glutamate-cysteine ligase, modifier subunit		30
GPX1	Glutathione peroxidase 1		2876
GSTP1	Glutathione S-transferase pi	GSTP	2950
HMOX1	Heme oxygenase (decycling) 1	bK286B10, HO-1	3162
HSPA8	Heat shock 70kda protein 8	HSC70, HSC71, HSP73	3312
IL1B	Interleukin-1beta	IL-1B, IL1-BETA, IL1F2	3553
IL6	Interleukin 6	BSF2, HGF, HSF, IL-6	3569
IL6R	Interleukin 6 receptor	CD126	3570
IL8	Interleukin 8	3-10C, AMCF-I, b-ENAP, CXCL8, GCP-1, GCP1, IL-8, K60, LECT, LUCT, LYNAP, MDNCF, MONAP, NAF, NAP-1, NAP1, SCYB8, TSG-1	3576
KLF2	Kruppel-like factor 2	LKLF	10365
MPO	Myeloperoxidase		4353
NFE2L2	Nuclear factor (erythroid-derived 2)-like 2	NRF2	4780
NOX1	NADPH oxidase 1	GP91-2, MOX1, NOH-1, NOH1	27035
NQO1	NAD(P)H dehydrogenase, quinone 1	DHQU, DTD, QR1	1728
PON1	Paraoxonase 1	ESA	5444
PTGS2	Prostaglandin-endoperoxide synthase 2	COX2	5743
SELP	Selectin P (antigen CD62)	CD62, CD62P, GMP140, PADGEM, PSEL	6403
SOD1	Superoxide dismutase 1 [Cu-Zn]	IPOA	6647
SOD2	Superoxide dismutase 2 [Mn], mitochondrial		6648
TNF	Tumor necrosis factor	DIF, TNF-alpha, TNFSF2	7142
TNFRSF1B	Tumor necrosis factor receptor superfamily, member 1B	CD120b, p75, TNF-R-II, TNF-R75, TNFBR, TNFR80	7133
TXNRD1	Thioredoxin reductase 1	GRIM-12, Trxr1, TXNR	7296
XBP1	X-box binding protein 1		7494
XDH	Xanthine dehydrogenase	XO, XOR	7498

4.1 Methods

4.1.1 Gene Expression Profiling

We used RNA from weekly whole blood samples to analyze 35 candidate genes and 5 housekeeping genes. In general, whole blood is an excellent sampling system for use in evaluating short-term (hours to days or weeks) environmental impacts on systemic sites because it reflects changes in a subject's internal and external environment (Dumeaux et al. 2010). In the present study evaluating up to 18 subjects in a single day, it was not feasible to perform additional fractionation procedures to isolate different cell types because *ex vivo* changes leading to alterations in gene expression profiles would have occurred because of sample handling and prolonged transportation (Debey et al. 2004, 2006; Rainen et al. 2002). Furthermore, whole blood carries a plurality of gene expression from other cell types, including granulocytes (neutrophils, eosinophils and basophils), which are important in the cascade of events that occur in response to pollutant-induced stress. Nevertheless, week-to-week changes in the relative distribution of cell types might change expression levels (see pilot assessment of adjustment factors below).

Therefore, we used the PaxGene Blood RNA System (BD Diagnostics, Franklin Lakes, NJ) that permits standardized collection of whole blood by stabilizing the RNA profile immediately after blood withdrawal (Debey et al. 2006; Rainen et al. 2002; Wang et al. 2004). The PaxGene system includes a stabilizing additive in a blood collection Vacutainer® tube to avoid processing-induced changes in gene expression and RNA degradation and a standardized processing reagent set for purification of intracellular RNA from whole blood. Samples were collected each Friday, at the same time of day for each subject to control for temporal and circadian variability. Tubes were inverted five times to mix with the stabilizing additive, immediately frozen, transported to the laboratory and stored at -80 °C until tested.

Total RNA was isolated by using a robotic workstation for automated RNA purification (QIAcube™) in combination with the PAXgene Blood RNA Kit and according to the manufacturer's handbook (Qiagen, Valencia, CA). Isolated RNA was quantified on a NanodropND-1000 Spectrophotometer and analyzed for integrity on an Agilent 2100 Bioanalyzer. Aliquots of RNA were then reverse transcribed into first-strand cDNA (ThermoScript RT-PCR kit, Invitrogen, CA) for subsequent polymerase chain reaction (PCR) gene expression analysis.

Candidate genes (Figure 4.1, Table 4.1) were selected based on biological function and reported pollutant exposure effects. Pathway information is derived from Ingenuity Pathway™ Software Analysis, the PANTHER classification system (<http://www.pantherdb.org>) and NCBI databases (<http://www.ncbi.nlm.nih.gov>). Gene expression levels were determined using end-point competitive polymerase chain reaction (PCR), with internal standards (the competitors) and sample cDNA co-amplified in the same reaction (Elvidge et al. 2005). The products were resolved with linear Matrix-Assisted Laser Desorption/Ionization Mass Spectrometry (MassARRAY™ Quantitative Gene Expression) and concentrations of the target transcripts were calculated from the ratio of the PCR products. All samples from a given subject were assayed on the same plate. Signal acquisition, allele assignment, peak area integration, data processing and analysis were carried out using the MassARRAY™ platform and software (Sequenom, San Diego, CA). Services were contracted with Immune Sciences Lab (David H. Murdock Research Institute, Kannapolis, NC).

Transcript copy numbers were determined based on the EC₅₀ calculated by non-linear regression analysis of the cDNA and competitor allele frequencies. Normalization of copy numbers was based on a multiplexed set of well-characterized reference transcripts ("housekeeping genes") in order to control for experimental variance. Copy numbers were normalized using the geNorm algorithm described by Vandesompele et al. (2002). We calculated the expression stability for a reference (housekeeping) gene as the average pairwise variation with other tested reference genes. We determined the most stable

reference genes (*ACTB*, *B2M*, and *GAPDH*) by stepwise exclusion of genes with the highest instability. Gene expression normalization factors for each sample were generated from the geometric mean of reference genes. All calculations were carried out using the qBase^{PLUS} data-analysis and integrated geNORM software (BiogazelleTM).

Pilot Assessment of Potential Adjustments for Cell Distributions:

We realize that gene expression profiling from complex tissues such as whole blood presents a challenge related to the variety of heterogeneous cell types, including dilution effects whereby a particular gene may only be expressed in a small subset of cells (Fan and Hegde 2005; Wurmbach et al. 2002). For instance, changes in inflammatory cell populations may change expression levels. Our aim though is not to assess expression levels in particular cell types, but to instead characterize overall expression levels in peripheral blood.

Our pilot approach to overcoming potential limitations was to consider the possibility that we could adjust regression results by repeated measures in every blood sample of the normalized gene expression levels of five cell type-specific surface molecules.

We evaluated the distribution of gene expression for five cell surface markers (in addition to the 35 candidate genes selected) and found, as expected, data were log normally distributed. After removal of outliers over 3 SD above the mean and natural log transformation, data distributions were sufficiently normal.

We then tested the relations between gene expression for five cell surface markers against leukocyte counts as follows:

Cell Specific Marker	Cell Type Percentage of Total leukocyte count
CD19	Lymphocyte percentage (actually B-cells)
CD3G	Lymphocyte percentage (actually T-cells)
RPS24	Lymphocyte percentage
CD19 + CD3G + RPS24	Lymphocyte percentage
SELL	Neutrophil percentage
CD14	Monocyte percentage

This was done for the 43 CHAPS subjects using their average gene expression data (around 360 total repeated measures) in relation to baseline leukocyte counts (43 samples only, i.e., no repeated measures). This was also done for paired samples from a study of 10 subjects with asthma with blood samples taken before and after exercise (NIH NIEHS K23-RR021624, C. Schwindt). In all models, relations were nonsignificant, suggesting that cell surface markers are not sufficiently representative of cell distribution.

As a result, we tested exposure-response models without adjustment for gene expression for cell surface markers. Despite this result, we are confident that the approach of using whole blood gene expression is valid, particularly since the statistical analysis focused on the repeated measures of exposures and outcomes where each subject served as his or her own control over time. Compared with the inherent biological variability in leukocyte differentials (different cell types) between people, leukocyte differentials within subject are anticipated to be relatively stable (Ross et al. 1988). An important determinant of within-subject variability is time of day due to circadian variation (Fan and Hegde 2005), which we have controlled by design in that blood was drawn on the same day of the week (Friday) and around the same hour each Friday afternoon.

4.1.2 Air pollutant exposures

Measured air pollutant exposures:

Four retirement communities were selected for the recruitment of subjects and monitoring of air pollution to enhance the accuracy of measurements to reflect subject exposures. This was accomplished by using outdoor community air monitoring in a fully equipped trailer provided by CARB. It was parked on the property of each retirement community site and away from main roadways. A parallel set of indoor data were collected on instruments placed in the main community areas of each retirement community. All exposure data were obtained for each week preceding gene expression outcome measurements in the three of the four communities that were located in the San Gabriel Valley. Other supplemental analyses of genetic polymorphisms that evaluated effect modification of relations between air pollution exposures and protein expression (e.g., soluble platelet selectin) utilized exposure and outcome data from all four communities (Chapter 5).

The exposure measurements include the following:

- 1) 24-h mean mass concentrations ($\mu\text{g}/\text{m}^3$) of primarily condensation mode (quasi-ultrafine) particles, $<0.25 \mu\text{m}$ in diameter ($\text{PM}_{0.25}$), accumulation mode particles, $0.25\text{-}2.5 \mu\text{m}$ in diameter ($\text{PM}_{0.25\text{-}2.5}$), and coarse mode particles, $2.5\text{-}10 \mu\text{m}$ in diameter ($\text{PM}_{2.5\text{-}10}$). Particles were collected on Teflon filters with impactor samplers operated at 9 L/min (Personal Cascade Impactor Sampler, SKC, Inc., Eighty Four, PA) (Misra et al. 2002; Singh et al. 2003).
- 2) Continuous total particle number concentration (particles/ cm^3) (Condensation Particle Counter model 3785, TSI Inc, Shoreview, MN).
- 3) Hourly $\text{PM}_{2.5}$ elemental carbon (EC) and organic carbon (OC) using the semi-continuous OC_EC analyzer (Model 3F, Sunset Laboratory Inc., Tigard, OR) (Arhami et al. 2006; Baea et al. 2004);
- 4) Hourly black carbon (BC) collected with an Aethelometer (Magee Scientific, Berkeley, CA).
- 5) Organic compounds analyzed by GC-MS to provide selected tracers of key PM sources (e.g., hopanes for vehicular emissions, n-alkanoic acids for photochemically-generated SOA, and levoglucosan for biomass smoke). These were measured from $\text{PM}_{0.25}$ filters (previous work) and $\text{PM}_{0.25\text{-}2.5}$ filters (see Chapter Two, Task 1);
- 6) Detailed inorganic profiles (50 elements) in the filter-collected PM were determined at the Wisconsin State Laboratory of Hygiene in Drs. Schauer's and Shafer's clean laboratory using Magnetic-Sector Inductively Coupled Plasma-Mass Spectroscopy (SF-ICP-MS) (Schauer et al. 2006). This included concentrations of many trace metals, including: Fe, V, Zn, Cr, Ni, Cu, Pb and Mn extracted from five-day composites of $\text{PM}_{0.25}$, $\text{PM}_{0.25\text{-}2.5}$ and $\text{PM}_{2.5\text{-}10}$ from indoor and outdoor filter samples;
- 7) Water soluble organic carbon (WSOC) measured by extracting sections of both $\text{PM}_{0.25}$ and $\text{PM}_{0.25\text{-}2.5}$ Teflon filters in high purity water, filtering, and then conducting analyses using a Sievers (GE Instruments) Total Organic Carbon (TOC) Analyzer (Zhang et al. 2008). WSOC will serve as a marker of SOA.
- 8) Particle oxidative potential from aqueous extracts of the five-day filter composites of $\text{PM}_{0.25}$ and $\text{PM}_{0.25\text{-}2.5}$ using an *in vitro* assay of reactive oxygen species (ROS) (see Chapter Two, Task 1).
- 9) Hourly pollutant gases (O_3 , NO_2 , NO_x , and CO) using federal reference methods.
- 10) Meteorological data were collected at the air sampling trailer and at the indoor monitoring location.

We used the Sioutas™ Personal Cascade Impactor Sampler (SKC, Inc., Eighty Four, PA), to measure daily size-fractionated PM mass concentrations for the analysis of 24-hr outcomes (Misra et al. 2002; Singh et al. 2003). The analysis included particles 0-0.25 µm in diameter (PM_{0.25}), accumulation mode particles, 0.25-2.5 µm in diameter (PM_{0.25-2.5}), and coarse mode particles, 2.5-10 µm in diameter (PM_{2.5-10}). PM_{0.25} is considered “quasi-ultrafine” because the traditional cutpoint for the ultrafine mode is around 0.1 to 0.2 µm. Filter samples of PM_{0.25}, PM_{0.25-2.5} and PM_{2.5-10} were collected for 24-hr periods over five days each week prior to the blood draw whereas the hourly samples of EC, OC, BC, particle number, pollutant gases and weather were collected continuously. Indoor and outdoor quasi-ultrafine, accumulation and coarse particle mass concentrations were determined by weighing the Teflon substrates using standard methods. Subsequent to weighing, weekly composite samples were prepared from five daily filters for each size mode, and analyzed for composition (see Chapters Two and Three, Tasks 1 and 2, respectively). The contributions of PM sources to PM_{0.25} and PM_{0.25-2.5} samples were quantified using source apportionment techniques as described above (see Chapter Three, Task 2).

Some samplers were run in duplicate (BC, all gases) and there were almost no missing data. Missing indoor PM mass data ranges from 13-29 out of 240 monitored days whereas missing indoor particle number, EC and OC data ranges from 37-43 out of 336 days. Missing outdoor PM mass data ranges from 14-23 out of 240 monitored days whereas missing particle number, EC and OC ranges from 33-58 out of 336 days. Because we require at least 75% of hours or days be non-missing in exposure averaging times (e.g., 3 days out of a 4-day average) this results in fewer missing data.

We estimated the mass of total organic carbon (OC) attributed to secondary OC (SOC, a surrogate of photochemically-derived OC) and the mass of OC attributed to primary OC (OC_{pri}, attributable to primary combustion sources, mostly traffic in the study regions). These estimates were based on the EC tracer method that uses EC as a tracer of primary combustion generated OC, and are described elsewhere (Polidori et al. 2007; Cabada et al. 2004; Lim et al. 2003; Turpin et al. 1995). OC_{pri} and EC are assumed to be emitted from the same combustion sources. Data points primarily during rush hour traffic are characterized by high CO and NO peaks and are thus used to identify times dominated by primary sources with less formation of secondary aerosols. The primary OC/EC ratio that characterizes each month of study was determined by regressing the OC and EC data we collected during these periods. Deming linear least-squares regression (Cornbleet and Gochman 1979) was used since the uncertainties in OC and EC were assumed equal. OC_{pri} and SOC were estimated by the following expressions:

$$OC_{pri} = a \times EC + b$$

$$SOC = OC - OC_{pri}$$

where $a = (OC/EC)_{pri}$, which is the characteristic primary OC/EC ratio for the study area, and $b =$ non-combustion primary OC. Usually, the SOC values estimated by this method vary with season and sampling location and are higher during afternoon hours in the warm seasons with photochemical smog episodes.

We also estimated indoor PM exposures of outdoor origin using the following methods that were also used in Delfino et al. 2008. We found in that study that associations were stronger for indoor exposures to PM of outdoor origin than uncharacterized indoor exposures. We concluded that outdoor home measurements are sufficient to capture the cardiovascular health impacts of outdoor air pollutants even though people spend most of their time indoors.

First, air exchange rates and infiltration factors (F_{inf}) at each site were determined. The average AERs calculated during CHAPS at the four retirement communities ranged from 0.21 to 0.40 hr⁻¹ (see Arhami et al. 2009 for more details). Estimated F_{inf} and measured

particle concentrations were then used in a single compartment mass balance model to assess the contributions of indoor and outdoor sources to measured indoor EC, OC_{pri}, SOC, and PN (Polidori et al. 2007). Indoor exposures to PM of outdoor origin are relevant to personal PM exposures given that people generally spend most of their time indoors. The combined indoor and outdoor exposure data we use here are those data where we were able to estimate indoor concentrations of outdoor origin (PN, EC, OC_{pri}, and SOC) from data from our work with Constantinos Sioutas and colleagues at the University of Southern California (Polidori et al. 2007).

A single compartment mass balance model (Meng et al. 2005; Polidori et al. 2007; Wallace 1996) was used to assess the mean contributions of indoor and outdoor sources to measured indoor OC, EC, PM_{2.5} and PN concentrations. Under the assumption of perfect instantaneous mixing and that the factors affecting the indoor concentrations were constant or changed slowly with time, the steady state indoor concentration of any particulate species can be described by the following equation:

$$C_{in} = \frac{P(AER)C_{out}}{AER+k} + \frac{Q_i/V}{AER+k} = F_{inf}C_{out} + C_{ig} = C_{og} + C_{ig}$$

where, C_{in} is the indoor concentration of the species of interest ($\mu\text{g}/\text{m}^3$), C_{out} is the corresponding outdoor concentration ($\mu\text{g}/\text{m}^3$), F_{inf} is the corresponding infiltration factor (dimensionless), C_{ig} is the indoor-generated concentration for the same species found indoors and C_{og} is the outdoor-generated concentration for the same species found indoors. Typically, in the mass balance model C_{ig} is expressed by $Q_i/V(a+k)$, where Q_i is the indoor source strength ($\mu\text{g}/\text{h}$), and V is the house volume (m^3).

The infiltration factor (F_{inf} , defined as the equilibrium fraction of ambient particles that penetrate indoors and remain suspended) is a key determinant of the indoor concentrations of particulate species. F_{inf} is described by the following eq:

$$F_{inf} = P(AER)/(AER+k)$$

where, P is the penetration coefficient (dimensionless). F_{inf} for particles varies with particle composition, particle size and volatility, surface to volume ratio of the indoor sampling location and indoor air-speed. F_{inf} is typically highest for non-volatile species such as EC (Lunden et al. 2003; Sarnat et al. 2006). F_{inf} for OC, EC, and PN were estimated from the corresponding indoor/outdoor concentration ratios. In particular, hourly indoor/outdoor ratios (I/O) for each particulate species were determined at times when no indoor particle sources, such as cooking or cleaning, were likely to be present (i.e. only I/O ratios ≤ 1 were considered). Daily F_{inf} estimates were then obtained by averaging these segregated hourly I/O ratios. Mean F_{inf} for each group and phase of the study were also determined by averaging the corresponding daily values. To verify these results the same analysis of the I/O concentration ratios was then repeated by using only nighttime data (from 00:00 to 06:00 am), for at this time resident activities causing indoor particle generation were expected to be minimal.

The indoor-outdoor air exchange rates (AER; h^{-1}) at each community site were estimated from indoor CO measurements collected during periods affected by a dominant indoor source. We considered in our calculations only time-periods when the CO concentration peaked at values significantly higher than the background CO level and that was followed by a non-source period (mostly observed in the morning and probably associated with cooking activities). Assuming an exponential decay of particles, that AER and outdoor concentrations are constant during the decay period, and that indoor concentrations are well mixed, then:

$$C_t = e^{-(AER+k)t} C_0 \quad \text{or} \\ \ln C_t = -(AER+k)t + \ln C_0$$

where, C_t is the indoor CO concentration after time t (after the decay period), C_0 is the initial peak CO concentration (right after CO emission) and k is the indoor loss rate for particles or gases (h^{-1}) (Abt et al 2000). Since k is rather negligible for CO, it was possible to estimate the AERs for the sites directly from the above-mentioned eq (2) by regressing $\ln C_t$ over $\ln C_0$.

4.1.3 Analysis

We first evaluated the distributions of the Biogazelle normalized gene expression concentrations (all genes were non-normally distributed) after applying the natural logarithm. If the distribution was sufficiently normal then the log-transformed gene expression data for that individual gene was retained for analysis. Otherwise, for the genes that were not log-normally distributed (*AHR*, *CCL2*, *F3*, *GCLC*, *IL6*, *IL6R*, *IL8*, *NQO1*, *SELP*, *TNF*, *TNFRSF1B*), we applied an autoscale standardization method developed specifically for these cases (Willems et al. 2008). This required centering the log-transformed gene expression data relative to the subject-specific mean and scaling the data by the ratio of the individual to the group standard deviations. This transformation normalized the distributions for the purposes of model fitting and parameter estimation. For the autoscaled genes the fold-change estimates presented here are interpreted relative to changes in the predictor of interest scaled by the ratio of the individual to the group standard deviation of the outcome.

We developed predictive models of expression levels for each gene as a function of the exposure concentration. Each model was fitted and validated using around 360 person-observations per gene on average in 43 subjects. We evaluated all available exposure measurements to gain a clearer understanding of the importance of the temporality of associations, and PM components (e.g., organic carbon fractions, PAH and metals), size fractions (e.g., UFP), and sources (e.g., primary traffic emissions). These main explanatory variables are continuous-scaled.

To analyze the within-subject relation of gene expression to air pollution exposures we used the general linear mixed effects model (Diggle et al. 2000). It estimates both fixed and random effects and accounts for longitudinal repeated measurements taken on each subject (up to 12). Random effects for each subject (random intercepts) reflect the basic principle that measurements taken for the same individual are likely to be more similar to each other than to measurements taken on different individuals. We estimated random intercepts by subject, nested within season and community, to account for correlated within-individual repeated measures.

Specifically, a general mixed model for a gene of interest may be described as follows. Let the index i indicate the retirement community ($i = 1,2,3$), j indicate season (phase) within year 1 and 2 ($j = 1,2,3,4$) nested within community, k indicate subject ($k=1,\dots,43$) within community, and m indicate the repeated gene expression measurement ($m = 1,\dots,12$). Then a given gene measurement, $Y_{i,j,k,m}$ was related to the following two types of variables:

- 1) a vector of time dependent air pollutant exposure levels, $X_{i,j,k,m}$ representing time periods preceding each gene measurement. Interaction terms may be included by multiplying elements of this vector to form additional components (e.g., genotypes); and
- 2) a vector of time-independent subject characteristics ($Z_{i,j,k}$), specifically genetic variation in selected genes.

The basic model can then be written as:

$$Y_{i,j,k,m} = a_{i,j,k} + \alpha Z_{i,j,k,m} + \beta x_{i,j,k,m} + \varepsilon_{i,j,k,m} \quad (1)$$

where $a_{i,j,k}$ is the random subject intercept, and $\varepsilon_{i,j,k,m}$ denotes random within-person error in the gene expression measurement assumed (initially) to be an independent normally distributed random variable. Model estimation used restricted maximum likelihood to estimate variance components (Lindstrom and Bates, 1988). The best fitting covariance structure was autoregressive of order 1, as determined by the Akaike's information criterion. Here the primary interest is on the parameter β , which relates the air pollution concentration to gene expression.

Pollutant concentrations were averaged for 1 to 7 days preceding blood draws. Exposures were mean-centered by season and community, as in our previous analyses (Delfino et al. 2010). This was done to adjust for between-subject and between-phase exposure effects because exposures were measured in two separate seasonal phases and at four retirement communities (Sheppard et al. 2005). This assured that our results reflected relations of gene expression to within-subject, within-phase mean centered exposure. Temperature effects were adjusted *a priori* for the same averaging time as the air pollutant. We tested raw as compared with smoothed penalized spline terms of temperature adjusting for potential nonlinear temperature associations. Spline terms did not improve the model fit over raw temperature and were not retained. Regression models were not adjusted for individual time-invariant characteristics because the mixed models estimate within-subject associations with variation in air pollution levels. Differences between subjects in time invariant characteristics (e.g., gender, race/ethnicity) are partly accounted for by the random subject intercepts. Infections could alter transcription levels along inflammatory and other pathways of importance to the gene expression results. Therefore, person-weeks when subjects reported any infections were excluded from analyses (N = 11 person-weeks, 3% of total). Results were expressed for interquartile range (IQR) increases in air pollutant levels to standardize comparisons between the pollutants.

An evaluation of many models such as the present analysis can produce false positives or type I errors due to multiple comparisons. We quantified the extent of this by using a permutation analysis to simulate the distribution of the Wald statistic for each estimate of association under the strong null hypothesis that there is no relationship between gene expression level and air pollutant level. Gene expression level outcomes were permuted 26,500 times for each and every exposure, within each individual subject. We then re-ran our mixed effects model and compared our observed Wald statistic to the critical value corresponding to a family-wise level .05 test resulting from the simulated distribution after accounting for all comparisons. This computationally intensive method was employed rather than the more conservative Bonferroni adjustment because air pollutant exposures are correlated, and as such, the resulting tests are also likely to be correlated. Although the permutation correction approach does partially account for the observed correlation among tests, it is likely to produce a conservative inference because it bounds the family-wise type I error relative to the maximum observed statistic across all comparisons. This method demonstrated that our p -values did not hold up to this somewhat conservative adjustment, as expected. This is may be attributable to the limited number of subjects and large number of models. We performed this simulation for a two gene subset (*IL1B* and *NFE2L2*) and present one, *NFE2L2*, as an example in the appendix (Figure S1 and Table S1). The observed regression estimates presented in this report are adjusted with the permutation correction and it should be understood that these p -values are likely to be non-significant when adjusting the family-wise type I error rate at level .05. Therefore, we consider the observed p -values more as a measure of potential effects for future hypothesis generation.

4.2 Results

Population and Exposures

Baseline subject characteristics are shown in Table 4.2. Subjects were elderly (about 85 years of age, on average) and primarily white reflecting the racial makeup of the retirement communities that volunteered to participate. In this population of subjects with

CAD the high prevalence of congestive heart failure, hypertension, hypercholesterolemia, and use of cardiovascular medications was as expected.

Table 4.3 shows descriptive statistics of outdoor air pollutant exposures measured at the three retirement communities used in the gene expression analysis and indoor air pollution data are described in Table 4.4. Tables 4.5 and 4.6 show results for all 4 communities (this exposure data were used in Chapter 5 for the analysis of soluble platelet selectin). In addition, Chapter 3 (Task 2, and our previous publications (Arhami et al. 2009, 2010; Polidori et al. 2007) provide more detailed analysis of indoor vs. outdoor exposures and differences across the four retirement communities.

Correlations between outdoor air pollutants are shown in Tables 4.7 and 4.8, and they are similar for indoor exposures (not shown). Briefly, the correlation matrix for air pollutants measured continuously showed that traffic-related (primary) air pollutants (EC, BC, OC_{pri}, NO_x and CO) were strongly correlated with each other but were weakly correlated with the photochemically-related secondary pollutants (O₃ and SOC). The correlation matrix for air pollutant particle components measured from the 5-day PM composites in each size fraction shows that correlations between other components were strongest within the same size fraction. As previously observed by us (Delfino et al. 2010a), PM_{0.25} hopanes and PM_{0.25} PAH had a Spearman correlation coefficient of 0.77. This supports the likelihood that PAH is largely attributable to traffic sources in the Los Angeles study area. Because of strong correlations between the primary air pollutants, our regression models test one pollutant at a time.

Table 4.2. Characteristics of Subjects in the Gene Expression Analyses (N=43).

Characteristic	Value
Age (years Mean ± SD)	84.7 ± 5.83
Female	53.5%
Race	
Hispanic	2.3%
White	97.7%
Cardiovascular History	
Confirmation of CAD	
Myocardial Infarction	44.2%
Coronary artery bypass graft or angioplasty	32.6%
Positive angiogram or stress test	16.3%
Clinical diagnosis	7.0%
Congestive heart failure	27.9%
Hypertension (by history)	76.7%
Hypercholesterolemia (by history)	67.4%
Medications	
ACE inhibitors and Angiotensin II receptor antagonists	41.9%
HMG-CoA reductase inhibitors (statins)	51.2%

Table 4.3. Descriptive statistics of outdoor air pollutant exposures in three retirement communities of the Los Angeles Air Basin.

Exposure ^a	Mean (SD)	Median	IQR	Min/Max
PM _{0.25} Mass (µg/m ³)	9.89 (3.97)	9.25	6.27	3.31/ 19.3
PM _{0.25} Macrophage ROS (µg Zymosan equivalents/m ³)	41.4 (38.5)	21.3	56.2	2.59/ 147
PM _{0.25} Organic Components				
WSOC (µg/m ³) ^b	0.50 (0.22)	0.49	0.28	0.08/ 1.01
PAH total (ng/m ³)	1.13 (0.48)	0.97	0.46	0.55/ 2.70
PAH LMW (ng/m ³)	0.41 (0.15)	0.36	0.16	0.21/ 0.74
PAH MMW (ng/m ³)	0.37 (0.18)	0.34	0.18	0.11/ 0.96
PAH HMW (ng/m ³)	0.35 (0.20)	0.30	0.27	0.13/ 1.01
Hopanes (ng/m ³)	0.33 (0.31)	0.25	0.44	0.06/ 1.57
Organic Acids (µg/m ³)	0.26 (0.22)	0.19	0.35	0.06/ 0.96
PM _{0.25-2.5} Mass (µg/m ³)				
PM _{0.25-2.5} Macrophage ROS (µg Zymosan equivalents/m ³)	84.9 (55.8)	84	97.8	9.03/ 203
PM _{0.25-2.5} Organic Components				
WSOC (µg/m ³) ^b	0.50 (0.29)	0.48	0.36	0.16/ 1.37
PAH total (ng/m ³)	0.53 (0.17)	0.47	0.26	0.36/ 1.01
PAH LMW (ng/m ³)	0.17 (0.03)	0.15	0.03	0.14/ 0.30
PAH MMW (ng/m ³)	0.14 (0.09)	0.09	0.10	0.08/ 0.39
PAH HMW (ng/m ³)	0.22 (0.06)	0.21	0.07	0.13/ 0.41
Hopanes (ng/m ³)	0.49 (0.29)	0.39	0.25	0.16/ 1.45
Organic Acids (ng/m ³)	48.8 (38.5)	40.7	41.6	9.74/ 150
PM _{2.5} components				
Elemental carbon (µg/m ³)	1.63 (0.60)	1.58	0.82	0.36/ 3.34
Organic carbon (µg/m ³)	6.81 (2.80)	6.09	3.57	2.46/ 13.8
Black carbon (µg/m ³)	1.88 (0.76)	1.76	0.91	0.50/ 4.51
Primary organic carbon (µg/m ³)	4.37 (2.11)	3.62	2.39	1.41/ 10.6
Secondary organic carbon (µg/m ³)	2.76 (1.41)	2.61	1.82	0.27/ 7.65
Particle number (particle no./cm ³)	14,686 (5,910)	13,331	6,729	2,019/ 30,180
Gases				
NO ₂ (ppb)	31.8 (9.58)	31.3	13.2	9.91/ 58.1
NO _x (ppb)	56.5 (30.3)	50.0	35.3	11.8/ 183
CO (ppm)	0.63 (0.27)	0.57	0.38	0.21/ 1.68
O ₃ (ppb)	24.9 (11.4)	23.5	15.2	3.83/ 60.7
Temperature (°C)	19.6 (5.43)	19.6	8.92	8.42/ 31.4

IQR: interquartile range; WSOC: water soluble organic carbon; PAH: polycyclic aromatic hydrocarbons; LMW: low molecular weight (2-3 ring); MMW: medium molecular weight (4 ring); HMW: high molecular weight (>4 ring). ROS: reactive oxygen species.

^a These data refer to the three communities where gene expression analyses were performed. PMROS and organic component measurements are from extracts of 5-day composites of particle filters. PM mass, PM_{2.5} components and gas exposure data are from daily average measurements.

^b WSOC (in µg C/m³) was multiplied by 1.8 to yield mass of organic components in µg/m³ according to Turpin and Lim (2001).

Table 4.4. Descriptive statistics of indoor air pollutant exposures in three retirement communities of the Los Angeles Air Basin.

Exposure ^a	Mean (SD)	Median	IQR	Min/Max
PM _{0.25} Mass (µg/m ³)	10.6 (11.8)	8.46	3.86	3.92/ 69.9
PM _{0.25} Macrophage ROS (µg Zymosan equivalents/m ³)	33.6 (34.2)	22.0	40.7	2.13/ 156
PM _{0.25} Organic Components				
WSOC (µg/m ³) ^b	0.56 (0.31)	0.54	0.46	0.09/ 1.25
PAH total (ng/m ³)	1.00 (0.44)	0.86	0.54	0.33/ 2.20
PAH LMW (ng/m ³)	0.34 (0.10)	0.34	0.13	0.12/ 0.55
PAH MMW (ng/m ³)	0.32 (0.16)	0.30	0.16	0.09/ 0.69
PAH HMW (ng/m ³)	0.35 (0.23)	0.27	0.26	0.10/ 0.99
Hopanes (ng/m ³)	0.23 (0.16)	0.19	0.26	0.05/ 0.56
Organic Acids (µg/m ³)	0.80 (0.81)	0.49	1.23	0.06/ 2.77
PM _{0.25-2.5} Mass (µg/m ³)				
PM _{0.25-2.5} Macrophage ROS (µg Zymosan equivalents/m ³)	56.8 (39.3)	52.4	70.7	3.16/ 152
PM _{0.25-2.5} Organic Components				
WSOC (µg/m ³) ^b	0.44 (0.28)	0.42	0.34	0.02/ 1.53
PAH total (ng/m ³)	0.48 (0.18)	0.42	0.13	0.35/ 1.15
PAH LMW (ng/m ³)	0.16 (0.03)	0.15	0.02	0.14/ 0.27
PAH MMW (ng/m ³)	0.12 (0.06)	0.09	0.02	0.08/ 0.32
PAH HMW (ng/m ³)	0.21 (0.10)	0.18	0.09	0.13/ 0.66
Hopanes (ng/m ³)	0.26 (0.13)	0.26	0.18	0.10/ 0.62
Organic Acids (ng/m ³)	42.8 (38.0)	29.6	35.6	8.29/ 184
PM _{2.5} components				
Elemental carbon (µg/m ³)	1.36 (0.47)	1.31	0.73	0.40/ 2.54
Organic carbon (µg/m ³)	6.16 (2.33)	5.63	2.64	2.47/ 12.6
Primary organic carbon (µg/m ³)	3.33 (2.30)	2.58	1.63	0.60/ 10.9
Secondary organic carbon (µg/m ³)	2.20 (1.26)	1.85	1.63	0.10/ 6.36
Particle number (particle no./cm ³)	11,361 (7,793)	10,618	9,795	815/ 35,946
Gases				
NO ₂ (ppb)	28.1 (10.0)	28.5	15.6	5.86/ 52.0
NO _x (ppb)	55.0 (32.2)	47.2	38.2	10.2/ 196
CO (ppm)	0.71 (0.29)	0.65	0.33	0.23/ 1.91
Temperature (°C)	24.1 (1.49)	23.9	1.9	18.5/ 28.8

IQR: interquartile range; WSOC: water soluble organic carbon; PAH: polycyclic aromatic hydrocarbons; LMW: low molecular weight (2-3 ring); MMW: medium molecular weight (4 ring); HMW: high molecular weight (>4 ring). ROS: reactive oxygen species.

^a These data refer to the three communities where gene expression analyses were performed. PM ROS and organic component measurements are from extracts of 5-day composites of particle filters. PM mass, PM_{2.5} components and gas exposure data are from daily average measurements.

^b WSOC (in µg C/m³) was multiplied by 1.8 to yield mass of organic components in µg/m³ according to Turpin and Lim (2001).

Table 4.5. Descriptive statistics of outdoor air pollutant exposures in 4 retirement communities of the Los Angeles Air Basin.

Exposure ^a	Mean (SD)	Median	IQR	Min/Max
PM _{0.25} Mass (µg/m ³)	9.11 (3.95)	8.46	7.37	3.31/19.34
PM _{0.25} Macrophage ROS (µg Zymosan equivalents/m ³)	36.3 (34.9)	20.1	35.4	2.6/147.2
PM _{0.25} Organic Components				
WSOC (µg/m ³) ^b	0.45 (0.23)	0.47	0.37	0.06/1.01
PAH total (ng/m ³)	0.96 (0.50)	0.90	0.56	0.40/2.70
PAH LMW (ng/m ³)	0.36 (0.15)	0.34	0.19	0.17/0.74
PAH MMW (ng/m ³)	0.30 (0.19)	0.28	0.24	0.08/0.96
PAH HMW (ng/m ³)	0.30 (0.20)	0.23	0.21	0.11/1.01
Hopanes (ng/m ³)	0.26 (0.30)	0.08	0.35	0.06/1.57
Organic Acids (µg/m ³)	0.24 (0.20)	0.17	0.29	0.06/0.96
PM _{0.25-2.5} Mass (µg/m ³)	11.0 (5.36)	9.83	8.36	2.28/28.1
PM _{0.25-2.5} Macrophage ROS (µg Zymosan equivalents/m ³)	75.0 (53.1)	64.6	86.4	7.1/203.0
PM _{0.25-2.5} Organic Components				
WSOC (µg/m ³) ^b	0.46 (0.27)	0.40	0.30	0.09/1.37
PAH total (ng/m ³)	0.49 (0.16)	0.43	0.16	0.33/1.01
PAH LMW (ng/m ³)	0.16 (0.03)	0.15	0.03	0.13/0.30
PAH MMW (ng/m ³)	0.13 (0.08)	0.09	0.06	0.08/0.39
PAH HMW (ng/m ³)	0.20 (0.07)	0.20	0.10	0.12/0.41
Hopanes (ng/m ³)	0.40 (0.29)	0.34	0.32	0.10/1.45
Organic Acids (ng/m ³)	41.6 (37.2)	28.2	42.6	9.74/150
PM _{2.5} components				
Elemental carbon (µg/m ³)	1.52 (0.62)	1.47	0.90	0.32/3.34
Organic carbon (µg/m ³)	7.78 (3.68)	6.92	5.20	2.46/18.7
Black carbon (µg/m ³)	1.67 (0.79)	1.60	1.02	0.29/4.51
Primary organic carbon (µg/m ³)	5.34 (2.92)	4.27	4.37	1.41/12.5
Secondary organic carbon (µg/m ³)	2.90 (1.54)	2.64	2.14	0.27/7.65
Particle number (particle no./cm ³)	12,817 (5,889)	11,900	6,351	2,019/30,180
Gases				
NO ₂ (ppb)	27.5 (11.6)	28.0	17.4	2.91/58.1
NO _x (ppb)	46.6 (31.4)	41.2	42.3	3.2/184
CO (ppm)	0.53 (0.30)	0.47	0.42	0.01/1.68
O ₃ (ppb)	27.1 (11.5)	25.7	17.4	3.8/60.7
Temperature (°C)	18.7 (5.89)	18.4	8.79	3.25/31.4

IQR: interquartile range; WSOC: water soluble organic carbon; PAH: polycyclic aromatic hydrocarbons; LMW: low molecular weight (2-3 ring); MMW: medium molecular weight (4 ring); HMW:

high molecular weight (>4 ring). ROS: reactive oxygen species.

^a PM ROS and organic component measurements are from extracts of 5-day composites of particle filters. PM mass, PM_{2.5} components and gas exposure data are from daily average measurements.

^b WSOC (in µg C/m³) was multiplied by 1.8 to yield mass of organic components in µg/m³ according to Turpin and Lim (2001).

Table 4.6. Descriptive statistics of indoor air pollutant exposures in 4 retirement communities of the Los Angeles Air Basin.

Exposure ^a	Mean (SD)	Median	IQR	Min/Max
PM _{0.25} Mass (µg/m ³)	9.5 (10.3)	7.11	4.84	3.92/69.9
PM _{0.25} Macrophage ROS (µg Zymosan equivalents/m ³)	29.6 (31)	19.7	28.4	2.13/156
PM _{0.25} Organic Components				
WSOC (µg/m ³) ^b	0.48 (0.30)	0.39	0.47	0.03/ 1.25
PAH total (ng/m ³)	0.85 (0.46)	0.76	0.62	0.33/ 2.20
PAH LMW (ng/m ³)	0.30 (0.11)	0.28	0.16	0.12/ 0.55
PAH MMW (ng/m ³)	0.26 (0.17)	0.23	0.25	0.09/ 0.69
PAH HMW (ng/m ³)	0.29 (0.22)	0.20	0.26	0.10/ 0.99
Hopanes (ng/m ³)	0.18 (0.16)	0.07	0.24	0.05/ 0.56
Organic Acids (µg/m ³)	0.68 (0.74)	0.37	1.05	0.06/ 2.77
PM _{0.25-2.5} Mass (µg/m ³)	6.00 (3.20)	4.96	4.61	1.07/ 14.3
PM _{0.25-2.5} Macrophage ROS (µg Zymosan equivalents/m ³)	48.7 (38.1)	41.7	51.4	1.57/ 152
PM _{0.25-2.5} Organic Components				
WSOC (µg/m ³) ^b	0.38 (0.27)	0.31	0.33	0.02/ 1.53
PAH total (ng/m ³)	0.46 (0.16)	0.39	0.10	0.34/ 1.15
PAH LMW (ng/m ³)	0.16 (0.03)	0.15	0.02	0.14/ 0.27
PAH MMW (ng/m ³)	0.11 (0.06)	0.09	0.01	0.08/ 0.32
PAH HMW (ng/m ³)	0.19 (0.09)	0.16	0.07	0.12/ 0.66
Hopanes (ng/m ³)	0.26 (0.15)	0.22	0.19	0.10/ 0.74
Organic Acids (ng/m ³)	36.4 (35.2)	24.1	29.0	8.03/ 184
PM _{2.5} components				
Elemental carbon (µg/m ³)	1.31 (0.44)	1.29	0.6	0.40/ 2.54
Elemental carbon of OO (µg/m ³)	1.08 (0.38)	1.01	0.54	0.29/ 2.54
Organic carbon (µg/m ³)	7.56 (3.58)	6.42	5.11	2.47/ 17.2
Primary organic carbon of OO (µg/m ³)	4.51 (3.25)	3.13	5.28	0.60/ 12.5
Secondary organic carbon of OO (µg/m ³)	2.47 (1.69)	2.05	1.84	0.10/ 10.9
Particle number (particle no./cm ³)	9,434 (7,279)	6,051	8,321	814/ 35,946
Gases				
NO ₂ (ppb)	24.2 (11.2)	22.9	19.0	5.86/ 51.9
NO _x (ppb)	45.8 (32.3)	35.9	38.8	7.99/ 196
CO (ppm)	0.67 (0.27)	0.62	0.29	0.23/ 1.91
Temperature (°C)	24.3 (1.57)	24.1	2.04	18.5/ 29.3

IQR: interquartile range; WSOC: water soluble organic carbon; PAH: polycyclic aromatic hydrocarbons; LMW: low molecular weight (2-3 ring); MMW: medium molecular weight (4 ring); HMW: high molecular weight (>4 ring). ROS: reactive oxygen species. OO: outdoor origin.

^a PM ROS and organic component measurements are from extracts of 5-day composites of particle filters. PM mass, PM_{2.5} components and gas exposure data are from daily average measurements.

^b WSOC (in $\mu\text{g C/m}^3$) was multiplied by 1.8 to yield mass of organic components in $\mu\text{g/m}^3$ according to Turpin and Lim (2001).

Table 4.7. Spearman correlation matrix for air pollutants measured daily.

	Elemental Carbon	Organic Carbon	Black Carbon	Primary Organic Carbon	Secondary Organic Carbon	Particle Number	NO _x	Carbon Monoxide	Ozone
Elemental Carbon	1								
Organic Carbon	0.61	1							
Black Carbon	0.89	0.63	1						
Primary Organic Carbon	0.97	0.65	0.88	1					
Secondary Organic Carbon	-0.03	0.72	0.07	0.00	1				
Particle Number	0.50	0.27	0.40	0.47	-0.08	1			
NO _x	0.82	0.46	0.86	0.79	-0.09	0.63	1		
Carbon Monoxide	0.78	0.59	0.79	0.75	0.11	0.45	0.82	1	
Ozone	-0.39	-0.05	-0.38	-0.36	0.26	-0.38	-0.53	-0.29	1

Table 4.8. Spearman correlation matrix for PM air pollutants measured weekly.

		PM _{0.25} exposure variables									PM _{0.25-2.5} exposure variables								
		Particle mass	Oxidative potential	WSOC	PAH	PAH LMW	PAH MMW	PAH HMW	Hopanes	Organic Acids	Particle mass	Oxidative potential	WSOC	PAH	PAH LMW	PAH MMW	PAH HMW	Hopanes	Organic Acids
PM _{0.25} exposure variables	Particle mass	1																	
	Oxidative potential ^a	0.42	1																
	WSOC	0.41	0.29	1															
	PAH	0.37	0.25	0.29	1														
	PAH LMW	0.50	0.46	0.35	0.86	1													
	PAH MMW	0.37	0.19	0.23	0.97	0.80	1												
	PAH HMW	0.27	0.03	0.27	0.91	0.65	0.89	1											
	Hopanes	0.22	-0.00	0.37	0.77	0.64	0.73	0.78	1										
	Organic Acids	-0.13	-0.11	0.08	0.20	0.05	0.14	0.40	0.32	1									
PM _{0.25-2.5} exposure variables	Particle mass	0.26	0.16	0.57	0.25	0.32	0.21	0.24	0.42	0.22	1								
	Oxidative potential	0.19	0.12	0.58	0.03	0.18	-0.03	-0.02	0.24	0.19	0.81	1							
	WSOC	0.15	0.25	0.50	0.08	0.27	0.06	-0.04	0.15	-0.04	0.70	0.73	1						
	PAH	0.08	0.04	0.32	0.56	0.36	0.57	0.66	0.52	0.17	0.22	-0.12	-0.05	1					
	PAH LMW	-0.02	0.03	0.27	0.16	0.06	0.17	0.27	0.30	0.18	0.24	-0.01	-0.10	0.74	1				
	PAH MMW	-0.10	-0.09	0.13	0.31	0.12	0.33	0.44	0.40	0.22	0.12	-0.21	-0.15	0.85	0.83	1			
	PAH HMW	0.10	0.11	0.29	0.63	0.48	0.61	0.67	0.57	0.15	0.21	-0.11	-0.06	0.93	0.62	0.72	1		
	Hopanes	0.20	0.10	0.45	0.73	0.59	0.68	0.72	0.58	0.17	0.41	0.18	0.32	0.68	0.31	0.46	0.65	1	
	Organic Acids	-0.05	0.23	0.18	0.39	0.34	0.37	0.38	0.25	0.14	0.47	0.29	0.45	0.37	0.22	0.29	0.37	0.54	1

^a Macrophage ROS production from the 5-day PM extracts.

Regression Models: Gene Expression and Air Pollution

We found that expression levels of five genes were too low for quantification (*CYP1A1*, *PON1*, *SOD1*, *NOX1*, and *XDH*). Therefore, we analyzed the expression levels for the remaining 30 genes from 43 subjects. The overall repeated measures sample size was 360 person-observations per gene on average. Findings from the linear mixed-effects models showed that daily outdoor traffic-related air pollutants were associated with the expression of genes in several key *a priori*-selected pathways including Nrf2-mediated oxidative stress response, inflammation, and platelet activation (Figure 4.2). Many of the 95% CIs for the fold change estimates included 1.0 (i.e., *p*-values were not < 0.05). Nevertheless, associations were consistent with respect to their magnitude and direction (positive) across each of the genes within the pathways. In particular, we found positive associations of primary pollutants (EC, BC, OC_{pri}, and NO_x) with the Nrf2 gene (*NFE2L2*) as well as the Nrf2-mediated or linked genes (*HMOX1*, *NQO1*, and *SOD2*). The largest association of these air pollutants with *NFE2L2* was for the 7-day average of OC_{pri} (per IQR increase there was a 2.51 fold-change, 95% confidence interval [CI]: 1.18-5.53). Traffic-related air pollutants were also positively associated, and often significantly so, with increased expression of *IL1B*, *SELP*, and *CYP1B1* whose transcription is not directly Nrf2-mediated. The largest associations found for *SELP* and *CYP1B1* were again with OC_{pri}. Per IQR increase in 5-day OC_{pri} there was a 1.53 fold-change in *SELP* (95% CI: 1-2.35), and a 1.96 fold-change in *CYP1B1* (95% CI: 1.01-3.80).

Figure 4.3 shows relations of gene expression fold-change estimates with PM outdoor concentrations from the 5-day size-fractionated PM composite samples (from Tasks 1-2), including total mass concentrations, chemical components, and the oxidative potential of particle extracts. Findings for PAH from particle extracts in Figure 4.3 are consistent with findings for the other markers of exposure to products of fossil fuel combustion (EC, BC, and primary OC) (Figure 4.2). Generally we found that PAH was positively associated with gene expression levels of *CYP1B1*, *HMOX1*, *IL1B*, *NQO1*, *NFE2L2*, *SELP*, and *SOD2*. There did not appear to be substantial differences in association by PAH molecular weight (low, medium and high). The fold change for an IQR increase were not particularly large with the strongest of these associations between *IL1B* expression and exposure to PM_{0.25} PAH showing a 1.33 fold change in *IL1B* (95% CI: 1.08-1.64) per IQR increase in PM_{0.25} high molecular weight PAH. Accumulation mode high molecular weight PAH was significantly and positively associated with *NQO1* (1.18 fold-change, 95% CI: 1.06-1.31, per IQR increase) and *NFE2L2* (1.34 fold-change increase, 95% CI: 1.01-1.77, per IQR increase). Although non-significant, accumulation mode high molecular weight PAH was also positively associated with *CYP1B1*, *HMOX1*, and *SELP*.

Figure 4.3 also shows that PM_{0.25} *in vitro* ROS was associated with increases in *NFE2L2* gene expression (1.15 fold-change per IQR increase in PM_{0.25} ROS, 95% CI: 0.98 – 1.34). *NQO1* and *CYP1B1* were also positively associated with PM_{0.25} *in vitro* ROS, whereas PM_{0.25-2.5} ROS was only associated with *CYP1B1*. PM from biomass burning was significantly associated with *HMOX1* (not shown), and was positively, but not significantly, associated with expression of several other genes in pathways including Klf2-mediated immune response (*KLF2* and *IL1B*), endoplasmic reticulum stress (*ATF6* and *XBP1*), endogenous ROS production (*MPO*) and other genes that like *HMOX1* are also involved in Nrf2-mediated oxidative stress response (*ATF4* and *GCLM*). Secondary air pollutant exposures were not associated with gene expression, including size-fractionated particle components (SOA estimated from WSOC, and organic acids), PM_{2.5} SOC, and O₃ (Table 4.9). Other air pollutants measured (metals, total OC and CO) were not associated with the expression of the target genes (not shown). We also found no trends in association with any pollutants suggesting the down regulation of genes.

Models including the indoor exposures were largely consistent with associations found for outdoor exposures discussed above, but with generally wider confidence intervals (Figures 4.4 and 4.5). For the traffic-related exposures, there was consistency between

models for associations with indoor primary OC of outdoor origin and with outdoor primary OC as well as with indoor and outdoor NO_x (Figure 4.4). There was less consistency for associations with indoor EC of outdoor origin and with outdoor EC. Indoor EC of outdoor origin was not more strongly positively associated with gene expression than total indoor EC and both were largely nonsignificant.

Figure 4.5 shows relations of gene expression fold-change estimates with PM exposures from the 5-day size-fractionated PM composite samples. Again, findings of positive associations of gene expression (*NFE2L2*, *SELP*, *SOD2*, *IL1B*, *NQO1* and *CYP1B1*) with PM_{0.25} PAH and PM_{0.25} *in vitro* ROS from indoor particle extracts are consistent with findings for outdoor models of the same exposures and are consistent with findings for other markers of indoor exposure to products of fossil fuel combustion (EC and primary OC of outdoor origin and NO_x). However, most 95% confidence intervals contained zero. As with outdoor exposures, indoor secondary air pollutant exposures were generally not associated with gene expression, including size-fractionated particle components (SOA and organic acids), PM_{2.5} SOC, and O₃ (not shown). As with outdoor measurements, other indoor air pollutants measured (metals, total OC and CO) were also generally not associated with the expression of the target genes (not shown).

Finally, none of the air pollutant exposures were associated with expression of the following 15 genes: *AHR*, *CCL2*, *CXCL1*, *DUSP1*, *F3*, *GCLC*, *GPX-1*, *GSTP1*, *HSPA8*, *IL6*, *IL6R*, *IL8*, *PTGS2*, *TNF*, *TNFRS1B*. These genes were in all of the studied pathways (Figure 4.1, Table 4.1) except endogenous ROS production (MPO).

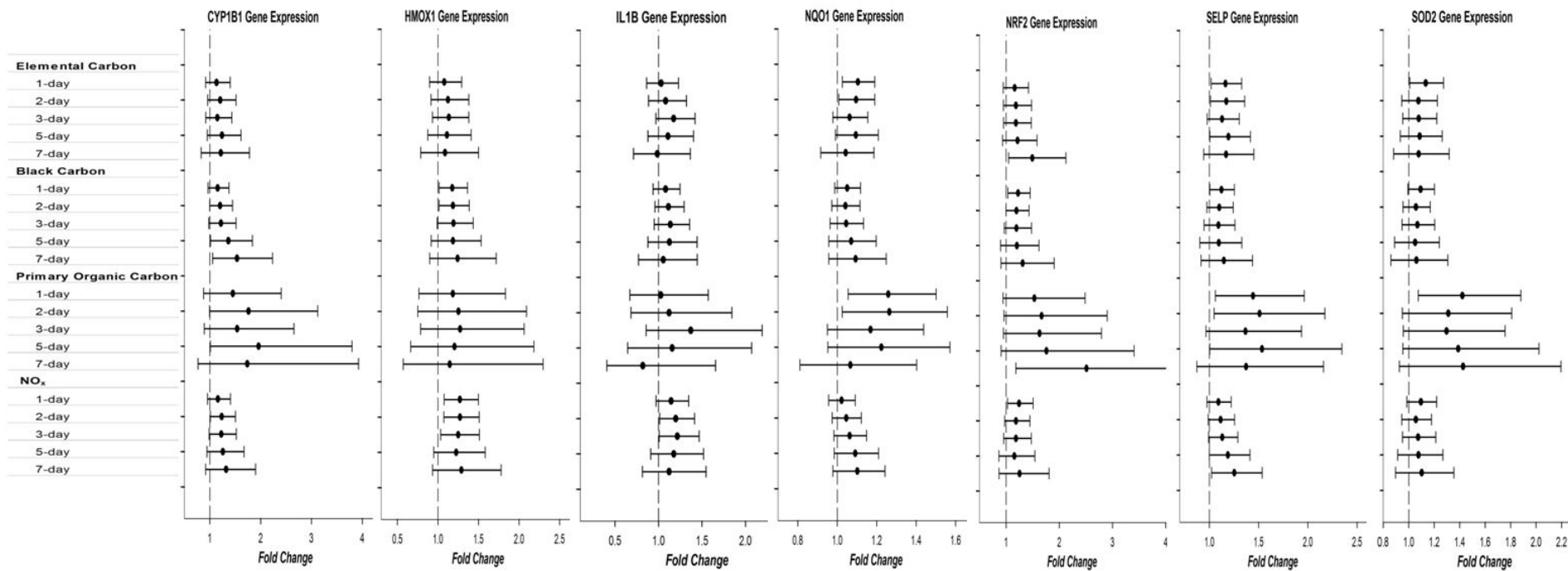


Figure 4.2. Fold-Change and 95% confidence interval for qPCR expression level of *CYP1B1* (A), *HMOX1* (B), *IL1B* (C), *NQO1* (D), *NFE2L2* (E), *SELP* (F), and *SOD2* (G) in association with outdoor traffic-related air pollutants measured hourly (elemental carbon, black carbon, primary organic carbon, and NO_x).

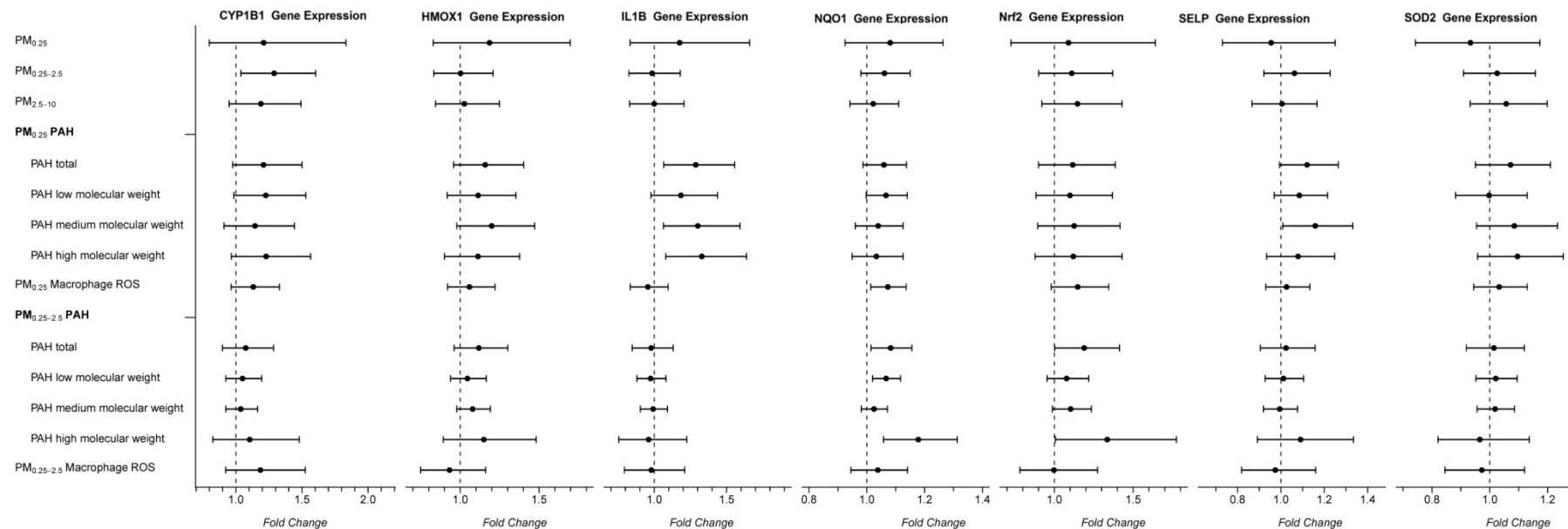


Figure 4.3. Fold-Change and 95% confidence interval for qPCR expression level of *CYP1B1*, *HMOX1*, *IL1B*, *NQO1*, *NFE2L2*, *SELP*, and *SOD2* in association with outdoor particulate matter size fractions, polycyclic aromatic hydrocarbons and oxidative potential (measured as macrophage ROS production *in vitro*).

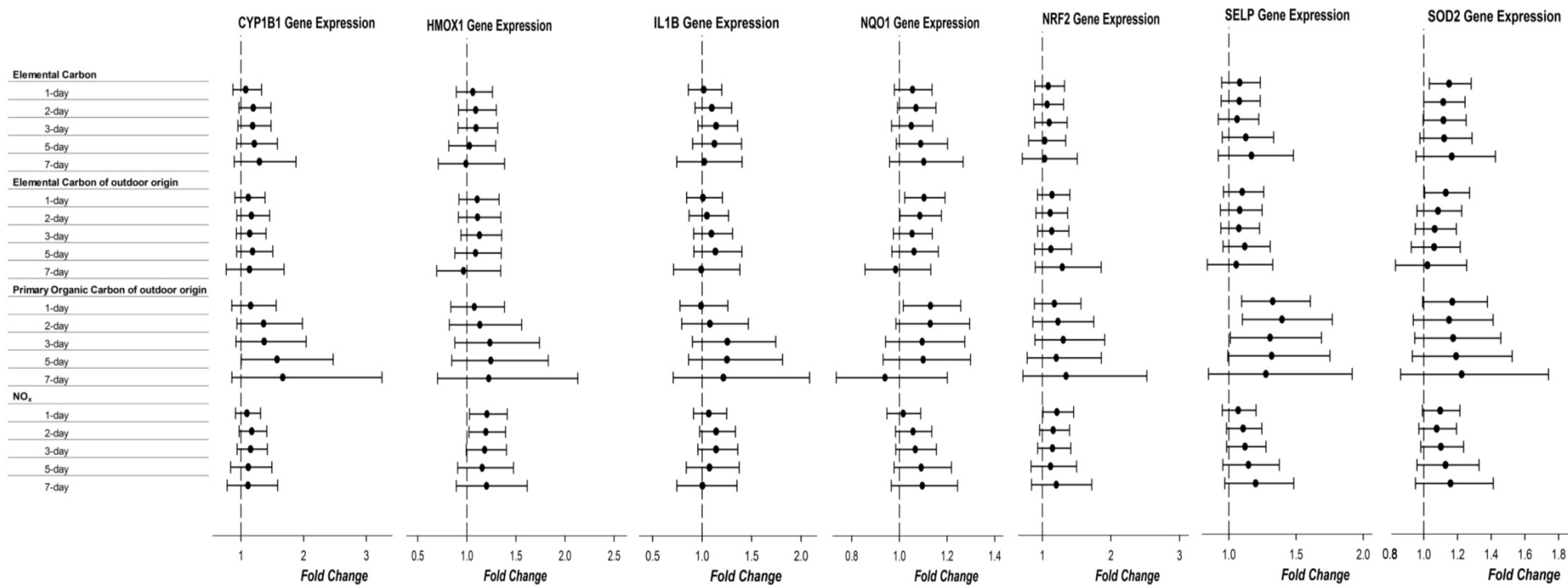


Figure 4.4. Fold-Change and 95% confidence interval for qPCR expression level of *CYP1B1*, *HMOX1*, *IL1B*, *NQO1*, *NFE2L2*, *SELP*, and *SOD2* in association with indoor traffic-related air pollutants measured hourly (elemental carbon, elemental carbon of outdoor origin, primary organic carbon of outdoor origin, and NO_x).

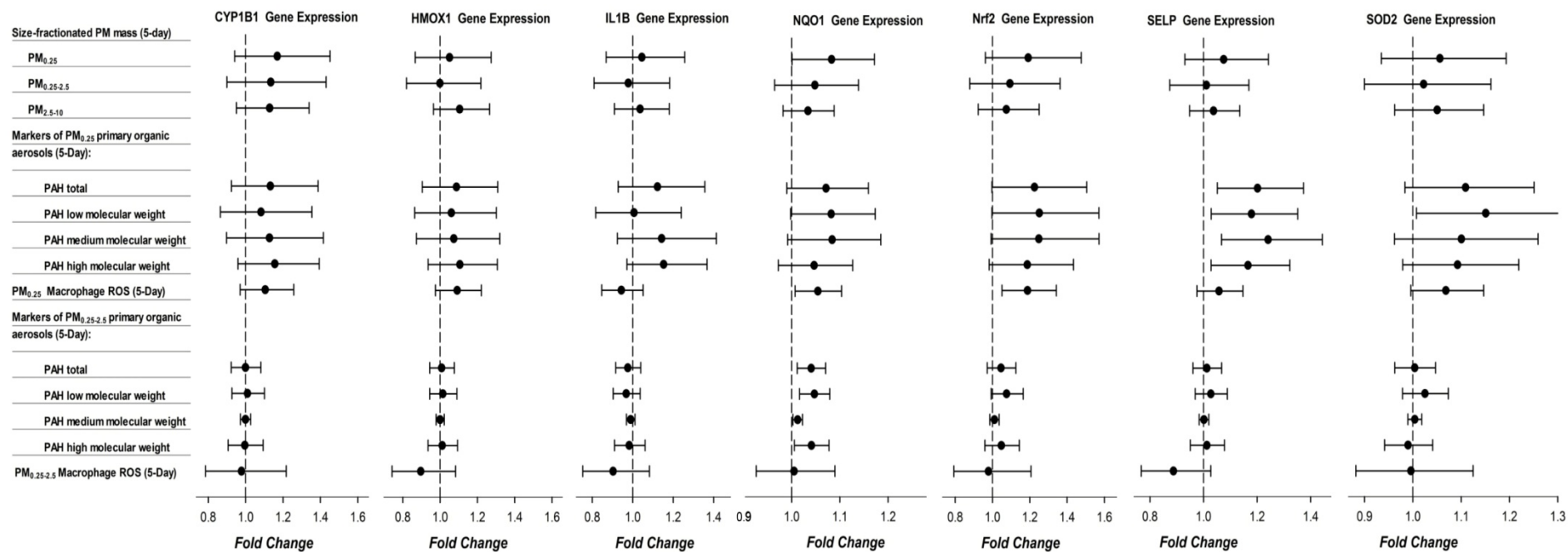


Figure 4.5. Fold-Change and 95% confidence interval for qPCR expression level of *CYP1B1*, *HMOX1*, *IL1B*, *NQO1*, *NFE2L2*, *SELP*, and *SOD2* in association with indoor particulate matter size fractions, polycyclic aromatic hydrocarbons and oxidative potential (measured as macrophage ROS production *in vitro*).

Table 4.9. Gene expression model estimates for markers of outdoor secondary organic aerosols. Fold change in gene expression (95% CI).^a

Air Pollutant	CYP1B1	HMOX1	IL1B	NQO1	NRF2	SELP	SOD2
O₃							
1-day average	0.70 (0.63, 1.03)	0.67 (0.49, 0.93)	0.64 (0.47, 0.88)	0.93 (0.8, 1.07)	0.77 (0.53, 1.10)	0.74 (0.58, 0.94)	0.89 (0.72, 1.09)
2-day average	0.58 (0.37, 0.92)	0.53 (0.35, 0.81)	0.51 (0.34, 0.77)	0.95 (0.79, 1.14)	0.77 (0.48, 1.23)	0.73 (0.54, 0.98)	0.91 (0.70, 1.18)
3-day average	0.69 (0.43, 1.09)	0.60 (0.40, 0.92)	0.51 (0.34, 0.77)	0.99 (0.84, 1.18)	0.83 (0.51, 1.33)	0.77 (0.58, 1.02)	0.85 (0.65, 1.11)
5-day average	0.89 (0.55, 1.43)	0.70 (0.46, 1.07)	0.63 (0.42, 0.95)	1.09 (0.93, 1.29)	0.95 (0.59, 1.54)	0.80 (0.60, 1.05)	0.80 (0.61, 1.05)
7-day average	1.16 (0.72, 1.88)	0.77 (0.50, 1.17)	0.75 (0.50, 1.11)	1.17 (0.99, 1.38)	0.86 (0.53, 1.39)	0.81 (0.61, 1.08)	0.79 (0.60, 1.03)
PM_{2.5} Secondary Organic Carbon							
1-day average	0.96 (0.79, 1.18)	0.93 (0.79, 1.10)	0.99 (0.84, 1.16)	1.02 (0.95, 1.09)	0.98 (0.81, 1.18)	0.93 (0.83, 1.04)	1.02 (0.92, 1.14)
2-day average	0.93 (0.73, 1.17)	0.92 (0.76, 1.12)	0.97 (0.81, 1.18)	1.00 (0.92, 1.09)	0.98 (0.79, 1.22)	0.91 (0.79, 1.04)	1.04 (0.92, 1.19)
3-day average	0.93 (0.72, 1.18)	0.91 (0.74, 1.11)	0.92 (0.75, 1.11)	0.99 (0.91, 1.08)	0.97 (0.77, 1.22)	0.91 (0.79, 1.05)	1.04 (0.91, 1.18)
5-day average	1.01 (0.77, 1.34)	0.95 (0.76, 1.20)	0.96 (0.77, 1.19)	0.97 (0.88, 1.07)	0.99 (0.76, 1.29)	0.92 (0.79, 1.08)	1.05 (0.90, 1.22)
7-day average	1.12 (0.78, 1.60)	0.96 (0.70, 1.30)	0.89 (0.66, 1.20)	1.01 (0.89, 1.14)	0.98 (0.70, 1.39)	1.00 (0.82, 1.23)	1.10 (0.91, 1.34)
Organic PM_{0.25} Components (5-Day)							
Water soluble organic carbon	1.05 (0.83, 1.33)	0.97 (0.80, 1.19)	1.02 (0.84, 1.24)	1.00 (0.92, 1.09)	0.89 (0.71, 1.12)	0.82 (0.71, 0.95)	0.93 (0.82, 1.06)
Organic Acids	1.09 (0.89, 1.33)	1.00 (0.84, 1.18)	0.99 (0.84, 1.17)	1.02 (0.94, 1.10)	0.99 (0.82, 1.20)	0.94 (0.82, 1.07)	0.99 (0.89, 1.10)
Macrophage ROS	1.13 (0.96, 1.33)	1.06 (0.92, 1.22)	0.96 (0.83, 1.10)	1.07 (1.01, 1.14)	1.15 (0.98, 1.34)	1.03 (0.93, 1.13)	1.03 (0.94, 1.13)
Organic PM_{0.25-2.5} Components (5-Day)							
Water soluble organic carbon	1.07 (0.94, 1.21)	0.94 (0.84, 1.05)	0.97 (0.87, 1.08)	1.03 (0.98, 1.08)	1.03 (0.90, 1.17)	1.02 (0.93, 1.12)	0.97 (0.90, 1.04)
Organic Acids	1.09 (0.95, 1.25)	0.98 (0.87, 1.10)	1.02 (0.91, 1.15)	1.01 (0.96, 1.07)	1.02 (0.89, 1.16)	1.01 (0.92, 1.10)	0.97 (0.90, 1.05)
Macrophage ROS	1.19 (0.92, 1.53)	0.93 (0.75, 1.16)	0.98 (0.79, 1.21)	1.04 (0.94, 1.14)	1.00 (0.78, 1.27)	0.97 (0.82, 1.16)	0.97 (0.84, 1.12)

^a Estimates in bold were significant at two-side p -values < 0.05.

Given the results, we were interested in assessing the significance of the inference that genes whose transcription is mediated by Nrf2 were differentially expressed relative to those that are not. To accomplish this we performed a *post hoc* pathway analysis based on the Gene Set Analysis methods proposed by Efron and Tibshirani (Efron and Tibshirani, 2007). This method involved permuting the pathway designation (indicating if a gene is Nrf2-mediated or not) of the Z_{obs} from our models, where Z equals regression coefficient divided by standard error. We used the maxmean statistic for the observed data and for each permutation. The maxmean is the larger of the absolute values of the average positive Z or the average negative Z . This statistic minimizes the effect of up- and down-regulation of a gene's averaging to insignificant pathway results. This was done 5000 times to generate a distribution of maxmean statistics under the null hypothesis that the associations with pollutants are equivalent for genes mediated by Nrf2 (*AHR*, *ATF4*, *CAT*, *CYP1B1*, *DUSP1*, *GCLC*, *GCLM*, *GSTP1*, *HMOX1*, *NQO1*, *NFE2L2*, *SOD2*, *TXNRD1*) and those that are not (17 remaining measurable genes). We included *AHR* and *CYP1B1* among the Nrf2-mediated genes on the basis of the established cross-talk between aryl hydrocarbon receptor xenobiotic response element and Nrf2 antioxidant response element pathways (Shin et al, 2007). All 30 measurable genes were included in this analysis. We then compared the observed maxmean for the Nrf2-mediated genes (0.786105) with the permuted distribution to evaluate the overall significance of the associations of the group of genes in the pathway. The p-value for the differential effect of the Nrf2 pathway was non-significant at 0.28, which is likely a reflection of our limited sample size.

4.3 Discussion

We followed a cohort panel of elderly subjects with CAD living in the Los Angeles air basin and found positive associations between candidate gene expression levels from whole blood with exposure to traffic-related air pollution exposures. This included 15 of the 30 candidate genes selected based on the literature that had quantifiable gene expression levels (five others did not). Results revealed numerous positive associations of air pollution exposure with gene expression among genes that are part of the Nrf2-mediated oxidative stress response pathway. Although many associations were not statistically significant, they were consistent in the direction (positive) and often the magnitude of the estimated effects across markers of traffic-related air pollution and across pollutant averaging times. Overall, findings support our hypothesis that traffic-related air pollutant exposures would be associated with the expression of genes in pathways that are relevant to the adverse effects of pro-oxidant air pollutant exposures. The present hypothesis-driven analysis produced informative epidemiological results that support the experimental data (*in vivo* and *in vitro* toxicological studies). Findings also support the need for further studies employing the present panel-study approach but with a larger sample size and more genes in the biopathways of interest. Our group is currently doing just that in an NIH, NIEHS-funded study of over 100 elderly Californian subjects (R01 ES-012243, years 06-10).

Our novel findings for the Nrf2 gene (*NFE2L2*) are important. The Nrf2 transcription factor regulates Phase II and other antioxidant genes by binding to antioxidant response elements (ARE) of their promoter regions. An *in vitro* study by Zhu et al (2005) showed that in cardiac fibroblasts Nrf2 expression was critical for total enzymatic activity of both SOD and NQO1. Further *in vitro* evidence revealed that Nrf2 protein expression was increased with diesel exhaust particles (Li et al. 2004). Huang et al. 2011 found that urban fine and ultrafine PM induced expression of both oxidative stress response pathway genes mediated by Nrf2 as well as genes in the xenobiotic metabolism signaling pathway. Araujo et al. (2008) used a mouse model to demonstrate that ultrafine PM exposure increased *NFE2L2*, *SOD2*, *CAT*, *NQO1* and *ATF4* gene expression.

The positive associations of *NFE2L2* expression with PAHs that we found are consistent with expectations based upon experimental data. PAHs are most clearly markers of traffic-related air pollution in the region of the present study. PAHs are known to activate the aryl hydrocarbon receptor (*AHR*) that when bound leads to *AHR* interaction with the

xenobiotic response elements (XRE) in the promoter regions of genes coding for phase I and phase II metabolic enzymes. This first initiates the metabolism of PAH to pro-oxidant compounds (importantly to quinones) by phase I oxygenases (e.g., cytochrome P450s), and then detoxification by phase II conjugating enzymes. In this manner, Nrf2-ARE pathways are triggered by PAH metabolites. On the other hand, Shin et al 2007 showed that Nrf2 binds to a functional ARE in the promoter region of AHR in mouse embryonic fibroblasts. Thus, *NFE2L2* expression can activate AHR-XRE that were previously considered to be separate response pathways from Nrf2-ARE pathways. This recent evidence suggests that there is crosstalk between the xenobiotic and antioxidant response pathways. Indirect support for this mechanism is evident in the increased *NFE2L2* expression along with increases in gene expression of downstream genes in both Nrf2-ARE and AHR-XRE pathways found in this study. Our novel findings here are in agreement with the existing experimental literature that describes Nrf2 as a master regulator of antioxidant response (Zhu et al 2005).

We previously published results from the present cohort panel showing significant and large increases in ambulatory blood pressure with exposure to PM markers of traffic-related air pollutants (Delfino et al. 2010). We also showed that the same air pollutants were associated with ambulatory electrocardiographic evidence of cardiac ischemia (ST segment depression ≥ 1 mm) (Delfino et al. 2011a) and ventricular arrhythmia (Bartell et al. 2013). The involvement of the Nrf2 pathway in the associations we observed between gene expression and air pollution exposure supports the view that oxidative stress is a potential mode of action by which exposure to traffic-related air pollutants increases the risk of adverse cardiovascular responses we have observed as well as the many other air pollution studies that are consistent with our findings in CHAPS (Brook et al. 2010).

An isolated finding was the association of biomass burning PM with increased expression of several other genes that were not associated with traffic-related air pollution. It is unclear whether this set of findings represents an underlying effect of biomass smoke exposure and further work is needed. However, our positive associations of *HMOX1* and *MPO* with biomass smoke suggest that oxidative stress is also involved in the consistent associations of adverse respiratory outcomes with smoke from biomass burning (Naeher et al. 2007).

Other key findings are the positive associations of *IL1B* and *SELP* with traffic-related air pollutant exposure. In the present panel we previously found positive associations between air pollution exposure and the circulating protein marker of platelet activation (soluble platelet selectin) that is encoded by *SELP*. This finding is of clinical importance in that subjects with higher air pollution exposures had increased potential for a thrombotic event (Delfino et al. 2009). Platelet selectin has an established role in vascular disease progression (Woollard and Chin-Dusting 2007). IL-1 β contributes to atherosclerosis progression by mediating vascular injury responses (Galea et al. 1996). Given this evidence in the literature it is reasonable to infer that the air pollutant-related increases in the expression of *IL1B* and *SELP* genes that we found herein may represent endothelial dysfunction or damage that could trigger heightened coagulation and/or plaque progression. Induction of these genes may occur via non-oxidative stress mechanisms because they do not rely on the Nrf2-mediated oxidative stress response and neither gene showed a clear association with PM oxidative potential.

Our study has several limitations. First is the limited number of subjects (N=43), who all were very elderly on average and all had CAD. This limits the generalizability of results to the larger general population. Nevertheless, the use of many repeated measures for each individual (≤ 12) allowed us study within-individual associations while limiting between-subject confounding and this likely enabled us to detect trends in expression at low fold-change levels. However, our results did not retain significance with an adjustment for multiple comparisons, as our study is likely underpowered for the number of models we analyzed. A larger sample size may have increased the precision of the estimates since

many 95% CIs for the fold change estimates included 1. Nevertheless, there was overall consistency in the direction of the associations for each gene and exposure group (namely primary air pollutants). This included multiple positive associations of similar magnitude (despite some being nonsignificant) and consistent findings for models using different averaging times. This provides support for an overall relationship between a given gene and air pollutant. Although the multiple relationships tested increases the likelihood of multiple testing bias, if our findings resulted from chance we would not expect to see trends within pollutant classes or grouping of results by hypothesized biological pathways. Furthermore, we developed *a priori* hypotheses regarding specific candidate gene expression changes. Therefore, as previously reviewed, our inferences regarding the results are supported by biological plausibility and experimental evidence. However, air pollutants were not associated with quantifiable gene expression levels of 15 of the 30 genes studied (*AHR*, *CCL2*, *CXCL1*, *DUSP1*, *F3*, *GCLC*, *GPX-1*, *GSTP1*, *HSPA8*, *IL6*, *IL6R*, *IL8*, *PTGS2*, *TNF*, *TNFRS1B*). These genes were in all of the studied pathways (Figure 4.1) except endogenous ROS production. It is possible that some of these genes reflect downstream or upstream effects and thus, on the day of blood draw were at basal expression levels. Recall that many of the experimental studies used to select our candidate genes, examined other cell types, including endothelial and epithelial cells, and macrophages, or blood cells in isolation, namely monocytes. Therefore, whole blood may not be the optimum biospecimen to reveal effects of pollutants on expression of these genes. However, the lack of association for these genes does not signify that these gene products are unimportant in air pollution-associated health outcomes, as there may be more substantial regulatory effects at the level of protein activation, rather than gene expression.

Another limitation in the exposure measurement methods used to assess subject exposures is that although measurements were made in the subject's retirement community, subjects could have different personal exposures within their own residence or while traveling outside of the community.

Between-subject differences in time invariant factors (e.g., gender) are unlikely to confound associations as we modeled random intercepts in mixed models to account for time-invariant subject differences. Nevertheless, some of the observed associations could have resulted from unmeasured confounding from temporal factors such as time-varying factors that could differ between individuals (e.g. diet). Many of the factors affecting variability in blood cell gene expression identified by Dumeaux et al. (2010) were either not relevant or controlled for in our study. Other unmeasured factors include the complex systems that underlie the biological responses leading to gene expression, including feedback pathways and compensatory mechanisms such as the balance between pro-oxidant and antioxidant enzyme responses (Delfino et al. 2011b). These could have affected the dose-response relationships between pollutants and gene expressions outcomes. Finally, given the elderly largely white population with CAD studied we cannot generalize our results to younger, more racially diverse, and healthier populations. Geographic variation in air pollutant composition also limits our ability to generalize results beyond this southern California region. Nevertheless, the sources of air pollution in the present study, primarily traffic, are common to most urban communities.

Finally, the study is limited by the fact that gene expression data was derived from a complex tissue (whole blood) that carries a variety of heterogeneous cell types that may be distributed differently from week to week and there may be dilution effects whereby a particular gene may only be expressed in a small subset of cells (Wurmbach et al. 2002; Fan and Hegde 2005). Changes in inflammatory cell populations are also expected to change expression levels. The pilot study testing the use of cell surface markers as a surrogate of cell differentials was unsuccessful, suggestion that future studies collect repeated complete blood cell counts with differentials along with preserved RNA. Nevertheless, our aim though was not to assess expression levels in particular cell types, but to instead to characterize overall expression levels in peripheral blood.

4.4 Summary and Conclusions

To our knowledge, this is the first cohort panel study to report the association of gene expression with exposure to air pollution exposures in an urban home environment. We found increased expression of genes in key biological pathways in association with increased exposure to traffic-related air pollution exposures in a Los Angeles cohort of elderly subjects with CAD. These associations are coherent with experimental reports of various potential mechanisms and with published reports showing associations between traffic-related air pollution exposure and adverse cardiovascular outcomes, including hospital admissions and mortality (Brook et al. 2010).

We confirmed our hypothesis that expression levels of key genes would be more strongly associated with markers of primary (combustion-related) organic aerosols than with secondary (photochemically-related) organic aerosols. Also, although there did not appear to be any clear difference in associations by particle size when using total mass concentrations, there were generally stronger associations for $PM_{0.25}$ PAH and/or ROS than for $PM_{0.25-2.5}$ PAH and ROS. This supports the use of size-fractionated particle composition data in epidemiologic studies, which have historically been heavily reliant on PM mass data, in part due to the availability of data from government air monitoring stations. The potential importance of ultrafine or quasi-ultrafine PM to human health is once again demonstrated in this study.

Most importantly, the role of Nrf2 in the adverse health effects of air pollution is supported by the present panel study results (both gene expression and effect modification by the -617 A risk allele). The inferred causality of our findings for *NFE2L2* gene expression is supported by experimental data as discussed above. Overall, our results suggest that *NFE2L2* gene expression may link effects of traffic-related air pollution on phase I and phase II enzyme genes via pathway crosstalk at the promoter transcription level.

The results of the present study need to be confirmed by additional research in other more diverse populations. Experimental designs are also needed to clearly characterize the causal role of the Nrf2-mediated oxidative stress response pathway in cardiovascular responses to traffic-related air pollutant exposure.

References

- Abt E, Suh HH, Catalano P, Koutrakis P. 2000. Relative contribution of outdoor and indoor particle sources to indoor concentrations, *Environ Sci Technol*, 34:3579–3587.
- Araujo JA, Barajas B, Kleinman M, et al. Ambient particulate pollutants in the ultrafine range promote early atherosclerosis and systemic oxidative stress. *Circ Res* 2008;102(5):589-96.
- Arhami M, Kuhn T, Fine PM, Delfino RJ, Sioutas C. 2006. Effects of sampling artifacts and operating parameters on the performance of a semi-continuous particulate EC/OC monitor. *Environ Sci Technol* 40:945-53.
- Arhami M, Polidori A, Delfino RJ, Tjoa T, Sioutas C. 2009. Associations between personal, indoor, and residential outdoor pollutant concentrations: Implications for exposure assessment to size fractionated PM. *J Air Waste Manage Assoc*, 59:392–404.
- Baea M-S, Schauer JJ, DeMinter JT, Turner JR, Smith D, Cary RA. 2004. Validation of a semi-continuous instrument for elemental carbon and organic carbon using a thermal-optical method. *Atmospheric Environment*, 38:2885–2893.
- Bartell S, Tjoa T, Longhurst J, et al. Particulate air pollution, ambulatory heart rate variability and arrhythmia in elderly subjects with coronary artery disease. *Environ Health Perspect* in press.
- Brook RD, Rajagopalan S, Pope CA, 3rd, et al. Particulate matter air pollution and cardiovascular disease: An update to the scientific statement from the American Heart Association. *Circulation* 2010;121(21):2331-78.
- Cabada J.C; Pandis S.N.; Subramanian R.; Robinson A.L.; Polidori A.; Turpin B. 2004. Estimating the Secondary Organic Aerosol Contribution to PM_{2.5} Using the EC Tracer Method. *Aerosol Sci. Technol* 38:140-155.
- Cornbleet, P.J.; Gochman, N. 1979. Incorrect Least-Squares Regression Coefficients in Method-Comparison Analysis; *Clin. Chem* 25:432-438.
- Debey S, Schoenbeck U, Hellmich M, Gathof BS, Pillai R, Zander T, Schultze JL. 2004. Comparison of different isolation techniques prior gene expression profiling of blood derived cells: impact on physiological responses, on overall expression and the role of different cell types. *Pharmacogenomics J* 4:193-207.
- Debey S, Zander T, Brors B, Popov A, Eils R, Schultze JL. 2006. A highly standardized, robust, and cost-effective method for genome-wide transcriptome analysis of peripheral blood applicable to large-scale clinical trials. *Genomics*, 87:653-660.
- Delfino RJ, Gillen DL, Tjoa T, et al. Electrocardiographic ST-segment depression and exposure to traffic-related aerosols in elderly subjects with coronary artery disease. *Environ Health Perspect* 2011a;119(2):196-202.
- Delfino RJ, Staimer N, Tjoa T, et al. Air pollution exposures and circulating biomarkers of effect in a susceptible population: clues to potential causal component mixtures and mechanisms. *Environ Health Perspect* 2009;117(8):1232-8.
- Delfino RJ, Staimer N, Tjoa T, et al. Association of biomarkers of systemic inflammation with organic components and source tracers in quasi-ultrafine particles. *Environ Health Perspect* 2010;118(6):756-62.
- Delfino RJ, Staimer N, Tjoa T, et al. Circulating biomarkers of inflammation, antioxidant activity, and platelet activation are associated with primary combustion aerosols in subjects with coronary artery disease. *Environ Health Perspect* 2008;116(7):898-906.

- Delfino RJ, Tjoa T, Gillen DL, et al. Traffic-related air pollution and blood pressure in elderly subjects with coronary artery disease. *Epidemiology* 2010;21(3):396-404.
- Delfino RJ, Staimer N, Vaziri ND. Air pollution and circulating biomarkers of oxidative stress. *Air Qual Atmos Health*, 2011b;4:37-52.
- Diggle PJ, Heagerty P, Liang K-Y, Zeger SL. Analysis of Longitudinal Data, 2nd edition. Oxford: Oxford U. Press, 2002.
- Dumeaux V, Olsen KS, Nuel G, et al. Deciphering normal blood gene expression variation--The NOWAC postgenome study. *PLoS genetics* 2010;6(3):e1000873.
- Efron B, Tibshirani R: On Testing the Significance of Sets of Genes. *The Annals of Applied Statistics* 2007, 1:107-129.
- Elvidge GP, Price TS, Glennly L, et al. Development and evaluation of real competitive PCR for high-throughput quantitative applications. *Anal Biochem* 2005;339(2):231-41.
- Fan H, Hegde PS. 2005. The transcriptome in blood: challenges and solutions for robust expression profiling. *Current Molecular Medicine* 5:3-10.
- Galea J, Armstrong J, Gadsdon P, et al. Interleukin-1 beta in coronary arteries of patients with ischemic heart disease. *Arterioscler Thromb Vasc Biol* 1996;16(8):1000-6.
- Huang YC, Karoly ED, Dailey LA, et al. Comparison of gene expression profiles induced by coarse, fine, and ultrafine particulate matter. *Journal of toxicology and environmental health Part A* 2011;74:296-312.
- Li N, Alam J, Venkatesan MI, et al. Nrf2 is a key transcription factor that regulates antioxidant defense in macrophages and epithelial cells: protecting against the proinflammatory and oxidizing effects of diesel exhaust chemicals. *J Immunol* 2004;173(5):3467-81.
- Lim, H.J.; Turpin, B.J.; Russell, L.M.; Bates, T.S. 2003. Organic and Elemental Carbon Measurements during ACE-Asia Suggest a Longer Atmospheric Lifetime for Elemental Carbon; *Environ. Sci. Technol* 37:3055-3061.
- Lindstrom MJ, Bates DM. 1988. Newton-Raphson and EM algorithms for linear mixed-effects models for repeated-measures data. *J Am Stat Assoc* 83:1014-1022.
- Lunden, M.M.; Revzan, K.L.; Fischer, M.L.; Thatcher, T.L.; Littlejohn, D, et al. 2003. The transformation of outdoor ammonium nitrate aerosols in the indoor environment. *Atmos. Environ* 37:5633-5644.
- Meng QY, Turpin BJ, Polidori A, Lee JH, Weisel C, Morandi M, et al. 2005. PM_{2.5} of ambient origin: estimates and exposure errors relevant to PM epidemiology. *Environ Sci Technol* 39:5105-112.
- Misra C, Singh M, Shen S, Sioutas C, Hall PA. 2002. Development and evaluation of a personal cascade impactor sampler (PCIS). *J. Aerosol Sci.* 33, 1027-1047.
- Naeher LP, Brauer M, Lipsett M, et al. Woodsmoke health effects: a review. *Inhal Toxicol* 2007;19(1):67-106.
- Polidori A, Arhami M, Delfino RJ, Allen R, Sioutas C. 2007. Indoor-outdoor relationships, trends and carbonaceous content of fine particulate matter in retirement communities of the Los Angeles basin. *J Air Waste Manage Assoc* 57:366-379.
- Rainen L, Oelmueller U, Jurgensen S, et al. Stabilization of mRNA expression in whole blood samples. *Clin Chem* 2002;48(11):1883-90.
- Ross DW, Ayscue LH, Watson J, Bentley SA. Stability of hematologic parameters in healthy subjects. Intraindividual versus interindividual variation. *Am J Clin Pathol.* 1988 Sep;90(3):262-7.

- Sarnat, S.E.; Coull, B.A.; Ruiz, P.A.; Koutrakis, P.; Suh, H.H. 2006. The Influences of Ambient Particle Composition and Size on Particle Infiltration in Los Angeles, CA, Residences, *J. Air & Waste Manage. Assoc* 56:186-196.
- Schauer JJ, Lough GC, Shafer MM, Christensen WF, Arndt MF, DeMinter JT, Park JS. 2006. Characterization of metals emitted from motor vehicles. *Res Rep Health Eff Inst.* 133:1-76
- Sheppard L, Slaughter JC, Schildcrout J, et al. Exposure and measurement contributions to estimates of acute air pollution effects. *J Expo Anal Environ Epidemiol* 2005;15(4):366-76.
- Shin S, Wakabayashi N, Misra V, Biswal S, Lee GH, Agoston ES, Yamamoto M, Kensler TW: NRF2 modulates aryl hydrocarbon receptor signaling: influence on adipogenesis. *Mol Cell Biol* 2007, 27:7188-7197.
- Singh M, Misra C, Sioutas C. 2003. Field evaluation of a personal cascade impactor sampler (PCIS). *Atmos Environ* 37:4781-4793.
- Turpin, B.J. and Lim, H.J. (2001) Species contributions to PM_{2.5} mass concentrations: revisiting common assumptions for estimating organic mass, *Aerosol Sci. Technol.*, 35, 602–610.
- Turpin, B.J.; Huntzicker, J.J. 1995. Identification of Secondary Organic Aerosol Episodes and Quantitation of Primary and Secondary Organic Aerosol Concentrations during SCAQS; *Atmos. Environ* 29:3527-3544.
- Vandesompele J, De Preter K, Pattyn F, et al. Accurate normalization of real-time quantitative RT-PCR data by geometric averaging of multiple internal control genes. *Genome biology* 2002;3(7):RESEARCH0034.
- Wallace L. 1996 . Indoor particles: a review. *J. Air Waste Manag. Assoc* 46: 98, 126.
- Wang J, Robinson, JF, Khan HM, Carter DE, McKinney J, Miskie BA, Hegele RA. 2004. Optimizing RNA extraction yield from whole blood for microarray gene expression analysis. *Clin Biochem* 37:741-744.
- Willems E, Leyns L, Vandesompele J. Standardization of real-time PCR gene expression data from independent biological replicates. *Anal Biochem* 2008;379(1):127-9.
- Woollard KJ, Chin-Dusting J. Therapeutic targeting of p-selectin in atherosclerosis. *Inflammation & allergy drug targets* 2007;6(1):69-74.
- Wurmbach E, Gonzalez-Maeso J, Yuen T, Ebersole BJ, Mastaitis JW, Mobbs CV, Sealfon SC. 2002. Validated genomic approach to study differentially expressed genes in complex tissues. *Neurochem Res* 27:1027-33.
- Zhang, Y., Schauer, J.J., Shafer, M.M., Hannigan, M.P. and Dutton, S.J. (2008) Source apportionment of in vitro reactive oxygen species bioassay activity from atmospheric particulate matter, *Environ. Sci. Technol.*, 42, 7502–7509.
- Zhu H, Itoh K, Yamamoto M, et al. Role of Nrf2 signaling in regulation of antioxidants and phase 2 enzymes in cardiac fibroblasts: protection against reactive oxygen and nitrogen species-induced cell injury. *FEBS Lett* 2005;579(14):3029-36.

5. CHAPTER 5. SUPPLEMENTAL ANALYSES: GENE-ENVIRONMENT INTERACTIONS

Introduction:

Although not originally proposed, it was considered highly relevant to evaluate gene expression models for the modifying effects of potentially important genetic variants of selected genes. This was relevant to the original project goals since finding evidence that a genetically susceptible subset of the population has different gene expression responses to air pollution can provide biological plausibility to the overall findings. Specifically, there is an emerging literature on how known functional genetic variants affect gene expression in human populations (e.g., Göring et al. 2007). These studies are primarily genome-wide studies of between-subject differences in expression quantitative trait loci. We had the opportunity to assess whether known functional genetic variants affect gene expression and how variants might modify the effects of air pollutants on gene expression. Where relevant, we also analyzed modifying effects of genetic polymorphisms on protein expression using available biomarker data in CHAPS. The following briefly summarizes methods and results for these supplemental analyses for each gene. Another analysis involved mitochondrial genetics that utilized the exposure data generated in the present study. This work is only cited under Presentations and Publications produced (Wittkopp et al. 2013).

SELP:

Background: Epidemiological and toxicological studies support an adverse effect of air pollution exposure on cardiovascular outcomes, and proposed mechanisms include increased thrombosis and coagulation. Previously, we showed higher air pollution exposure is associated with increased plasma levels of soluble platelet selectin (sP-selectin) (Delfino et al. 2009) and increased expression of the platelet selectin gene (SELP) (Wittkopp et al. in preparation) as described above; both findings indicate a probable increase in platelet activation and thus thrombosis from air pollutant exposures. A functional polymorphism (rs6136) in the gene that codes for sP-selectin (SELP) is of interest in its potential to modify these associations. This polymorphism (Thr715Pro) results in proline at position 715 in the protein, instead of the wildtype threonine. Carter et al. (2003) found that subjects with the Pro715 allele polymorphism have been shown to have lower circulating levels of sP-selectin and they could thus have decreased risk for venous thromboembolism compared to those homozygous for the Thr715 allele). Another way of saying this is that the Thr715 allele is believed to increase risk of thrombosis. Pro715 may thus be protective for myocardial infarction, however, Carter et al 2003 did not find any association with myocardial infarction history of stenosis $\geq 50\%$ in the coronary arteries. Another large study found no associations with risk of CAD or ischemic stroke (Volcik et al. 2006). We hypothesized that carriers of the Pro allele would have weaker associations of gene expression and related protein levels with air pollution exposure versus non-carriers.

Methods: As previously described (Delfino et al. 2009), we measured plasma sP-selectin levels weekly for all 60 subjects using an ELISA assay. The SELP Thr715Pro genotypes were determined using restriction fragment length polymorphism analysis as described by Carter et al. (2003). Whole blood gene expression levels were measured using quantitative polymerase chain reactions, for a subset of 40 subjects as described above (3 subjects had insufficient DNA for analysis). Air pollutant exposures measured at subject residences were as described above. T-tests were used to assess between-group differences in outcomes. Linear mixed effects models were used to analyze effect modification of air pollution exposure-response relations by the polymorphism. This was accomplished with an interaction term between each air pollutant and the SELP genotype, to determine if variation at position 715 of the genotype was an effect modifier of the relationship between gene expression and air pollutant exposure.

Results: We determined that out of 63 subjects in CHAPS overall, 12 subjects were carriers of the protective, Pro715 allele, and they had lower sP-selectin levels versus Thr715 homozygotes (34.78 ng/mL vs 42.03 ng/mL, $p < 0.001$ by t-test). Pro715 allele carriers in the gene expression analysis (N=9) also had 39% lower SELP expression versus Thr715 homozygotes ($p < 0.005$). However, in mixed effects regression models including a product term between the SELP genotype and air pollutant exposure, there was no significant interaction between carrier status and air pollutant exposures (p -value = 0.1 or greater), except for an increase in SELP expression with $PM_{0.25-2.5}$ mass in Pro715 carriers, which is the opposite of what was expected (Figures 5.1-5.3).

Conclusions: While it appears that both SELP gene expression and protein expression increase in association with air pollution exposure and these levels are lower in Pro715 carriers, we found no effect modification of exposure-response relationships by genotype except for a counterintuitive finding for $PM_{0.25-2.5}$ mass. Recent data suggest that lower plasma sP-selectin in 715Pro carriers results from decreased N-glycosylation and subsequent sequestration in the Golgi apparatus (Subramanian et. al. 2012). To our knowledge, there are no research data indicating that N-glycosylation changes as a result of air pollution exposure. We conclude that differences in the soluble protein levels due to the presence of this polymorphism are not altered as a result of changes in air pollution exposure.

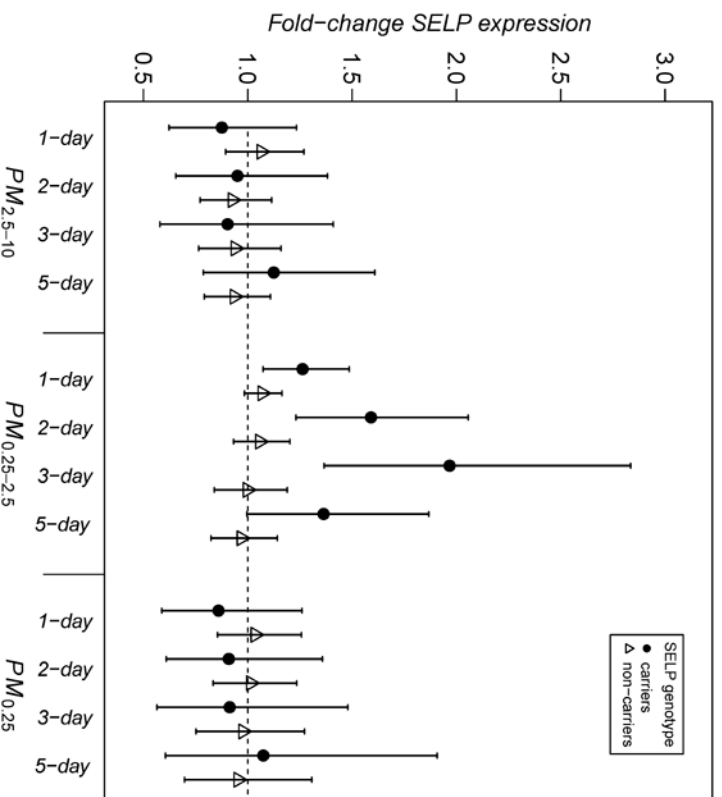


Figure 5.1. Relations between SELP gene expression and PM mass size fraction: effect modification by the SELP Pro715 allele genotype.
 UFP: $PM_{0.25}$; Acc: $PM_{0.25-2.5}$; Coarse: $PM_{2.5-10}$.

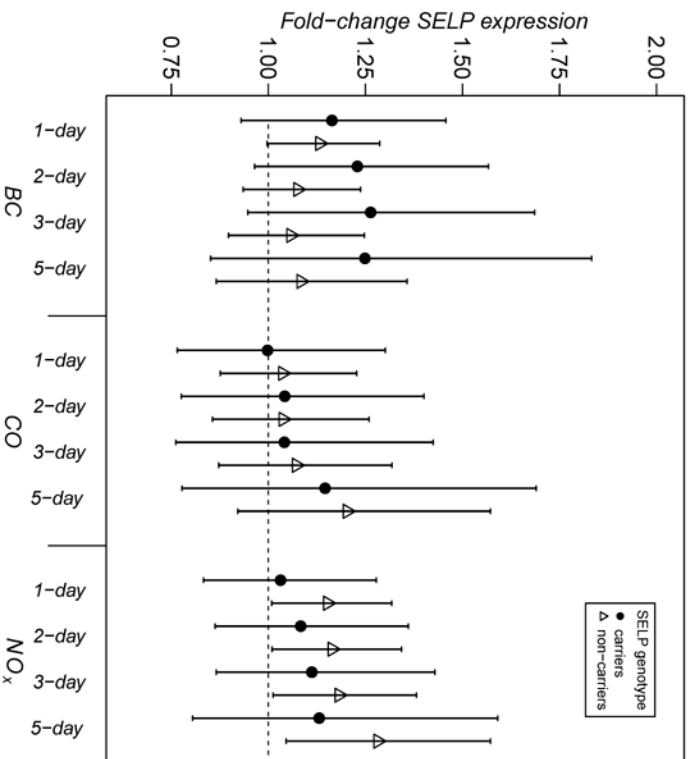


Figure 5.2. Relations between SELP gene expression and traffic-related air pollutants (BC, CO and NO_x): effect modification by the SELP Pro715 allele genotype.

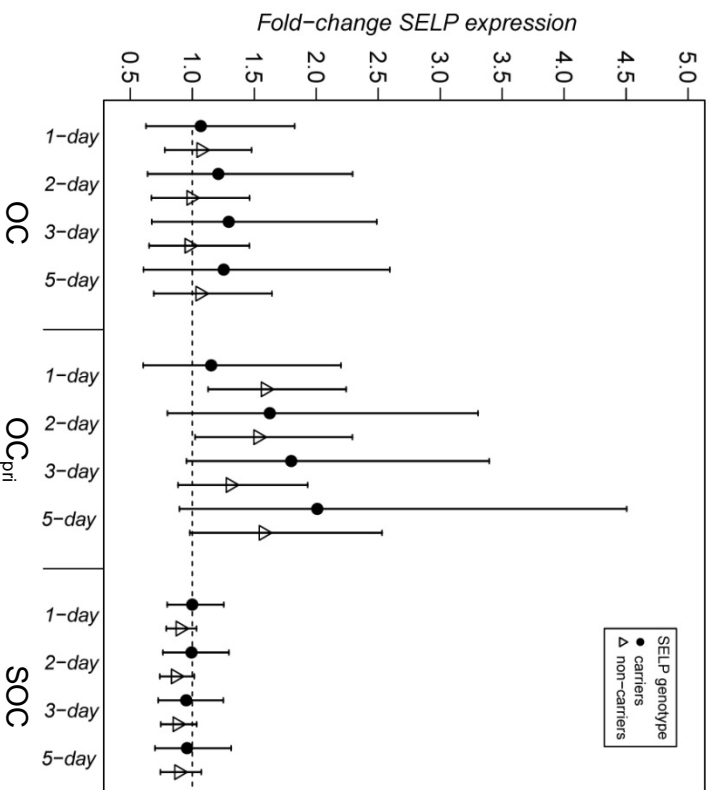


Figure 5.3. Relations between SELP gene expression and exposure to total organic carbon (OC), primary OC (OC_{pri}), and secondary OC (SOC): effect modification by the SELP Pro715 allele genotype.

NRF2:

Background: The transcription factor called nuclear factor erythroid 2-related factor 2 (Nrf2) also known as nuclear factor (erythroid-derived 2)-like 2 (NFE2L2) is a major factor in antioxidant-response element (ARE)-dependent gene expression and thus functions to inhibit oxidative stress and inflammation. Therefore, a wide array of important genes and their protein products may be affected by polymorphisms in the Nrf2 gene. A potentially important SNP at position -617 (rs6721961) is located in the promoter region of the Nrf2 gene. Constructs containing this SNP have lower promoter activity and binding *in vitro*, i.e., a reduction in Nrf2 transcriptional activity (Marzec et al 2007). This SNP could lead to potential differences in gene induction following environmental exposures. We have already shown above that increases in expression of the Nrf2 gene are associated with exposures to traffic-related air pollution.

Methods: We performed PCR and Sanger sequencing of a portion of the Nrf2 gene. Our sequencing allowed us to determine the -617 SNP located in the promoter region of the Nrf2 gene. Whole blood gene expression levels were measured using quantitative polymerase chain reactions, for a subset of 40 subjects as described above (3 subjects had insufficient DNA for analysis). Air pollutant exposures measured at subject residences were as described above. T-tests were used to assess between-group differences in gene expression outcomes. Linear mixed effects models were used to analyze effect modification of air pollution exposure-response relations by the polymorphism. This was accomplished with an interaction term between each air pollutant and the Nrf2 genotype, to determine if variation at position -617 of the genotype was an effect modifier of the relationship between gene expression and air pollutant exposure. We tested this for Nrf2 expression itself along with genes whose transcription is Nrf2-mediated. This included: HMOX1, SOD2, NQO1, GCLC, GCLM, CAT, GSTP1, and Cyp1b1. We also tested Nrf2 gene effect modification on IL1B1 and SELP gene expression, which showed significant associations with air pollutant exposures in our gene expression analysis as described above.

Results: We identified 8 carriers of the -617 A (risk) allele among those subjects for whom we have gene expression data. The distribution of alleles did not differ significantly from Hardy-Weinberg equilibrium. Surprisingly, we found subjects who were carrying the -617A risk allele to have higher average Nrf2 expression (1.9 fold higher among carriers versus non-carriers, $p = 0.002$). We can only speculate that chronically low Nrf2 due to the -617A SNP leads to a compensatory increase in basal transcription, and reduced capacity to increase transcription in times of oxidative stress (e.g., during times of high pollutant exposures).

In mixed effects regression models including a product term between the Nrf2 genotype and air pollutant exposure we found carriers as compared with non-carriers to have significantly lower Nrf2 gene expression in association with quasi-ultrafine particles (UFP, $PM_{0.25}$) (Figure 5.4). Although the differences were not significant, this was also found for $PM_{0.25}$ PAH but not accumulation mode PAH or any of the other markers of traffic-related air pollutants including EC and black carbon BC (Figure 5.5). However, carriers had higher expression in association with OC, primary organic carbon and secondary organic carbon (Figure 5.6). The reason for this difference in association is unclear. Given that Nrf2 is a transcription factor, we expect that small differences in Nrf2 level will show larger downstream effects of increased transcription of Nrf2-mediated genes. And since Nrf2 can bind its own promoter region, these effects would not be exclusive to downstream genes.

We found subjects carrying the -617 A risk allele as compared with non-carriers had significantly higher SOD2 gene expression in association with accumulation mode particles (ACC) (Figure 5.7). We found Nrf2 -617 to be an effect modifier of the relationship between SOD2 expression level and traffic-related air pollutants as well (Figure 5.8). Many interaction terms were significant at $p < 0.01$, showing -617A carriers had higher SOD2 gene expression in with exposure to traffic-related air pollutants including: $PM_{0.25}$ hopanes and

PAH, and EC, BC, and NO_x. In addition, -617A carriers had higher SOD2 gene expression associated with exposure to OC and its two fractions, including the SOC fraction that is expected to be enriched in the accumulation mode (Figure 5.9). The SOD findings indicate a possible increased inducibility of SOD2 among carriers of the Nrf2 -617A allele.

Among genes whose transcription is not regulated by Nrf2, we found TRAP associations with increased IL1B gene expression (Figure 5.10) and SELP gene expression (Figure 5.11) were greater in Nrf2 -617 risk allele carriers, although this was apparent for only a limited number of models and was generally not a significant interaction. We speculate that this may have occurred because carriers of the Nrf2-617 risk allele may have increased oxidative stress in the presence of pollutant exposure that translates directly, likely via Nrf2 transcriptional regulation, as evidenced by increased expression of antioxidant enzymes such as SOD2 (as we have observed). Although increased expression of antioxidant enzymes should decrease oxidative stress, unlike an experimental protocol the present observational findings are from a mixture of effects from different subjects and varying exposure concentration-time profiles. This increased oxidative stress may also translate indirectly, via non-Nrf2-mediated pathways, to increases in other markers of oxidative stress, inflammation, and platelet activation, such as SELP and IL1B.

Cyp1B1 had significantly decreased expression in association with TRAP and particulate matter among risk allele carriers versus non-carriers (Figures 5.12-5.14). This may indicate that Cyp1B1 gene induction in response to pollutant exposure may rely more heavily on signaling through the Nrf2-mediated pathway than the other genes we analyzed.

Models of NQO1 gene expression showed some significant interaction terms: PM_{0.25} induction of macrophage ROS and 7-day average NO_x were associated with significantly higher NQO1 expression among Nrf2 risk allele carriers versus non-carriers (not shown). Other genes that could be Nrf2-mediated based on pathway analysis (ATF4, CAT, GCLC, GCML, GSTP1, HMOX1, MKP-1, and TXNRD1) showed no clear trend of differences between Nrf2 risk allele carriers versus non-carriers (not shown). These genes may have more substantial regulation through other pathways, or their pathways may have compensatory mechanisms that make the difference in Nrf2 baseline transcription less important in responses to air pollution exposures.

Conclusions: We found important, novel findings for effect modification by the -617 A risk allele of the Nrf2 gene and its influence on Nrf2 gene expression. We expect that polymorphisms in genes of pathways important to air pollution response such as Nrf2 will have significant effects while polymorphisms in less important pathways will not. Therefore, these results support the probable importance of the Nrf2-mediated oxidative response pathway in air pollution exposure-response relationships. Results also suggest a direct effect of this SNP on the translational regulation in Nrf2-mediated genes (e.g. CYP1B1) and indirect effects on genes not regulated by Nrf2 (e.g. IL1B and SELP) that are likely due to differences in oxidative stress in the presence of the Nrf2 -617 A risk allele. Many other stratified estimates were significant for expression of many of the genes evaluated, while the interaction terms were not. Larger sample sizes may be necessary to find significant effect modification among these genes.

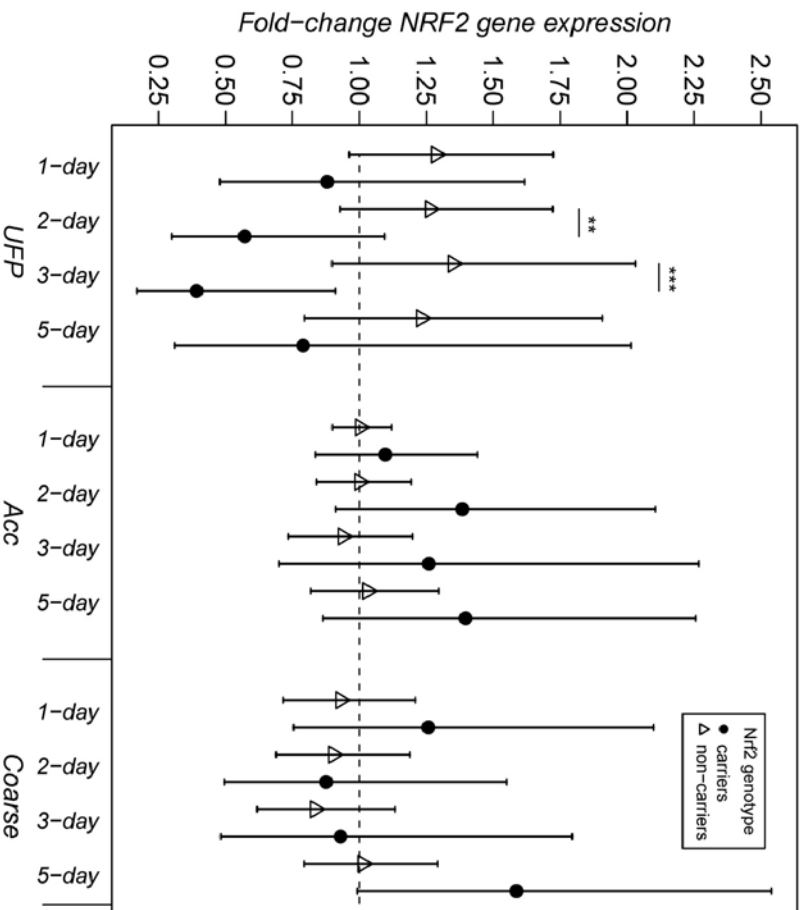


Figure 5.4. Relations between Nrf2 gene expression and PM mass size fraction: effect modification by Nrf2-617 A risk allele genotype. UFP: PM_{0.25}; Acc: PM_{0.25-2.5}; Coarse: PM_{2.5-10}.

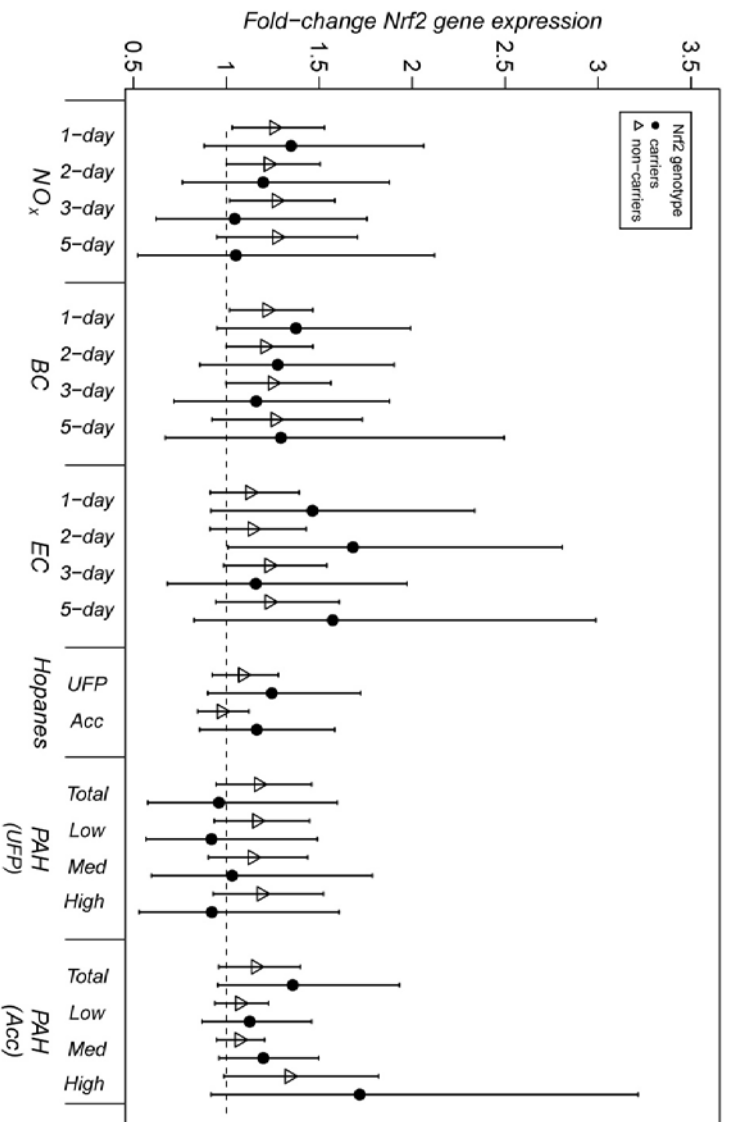


Figure 5.5. Relations between Nrf2 gene expression and traffic-related air pollutants: effect modification by Nrf2-617 A risk allele genotype. Averaging time for hopanes, and PAH are 5 days (from 5-day PM filter composites). UFP: PM_{0.25}; Acc: PM_{0.25-2.5}.

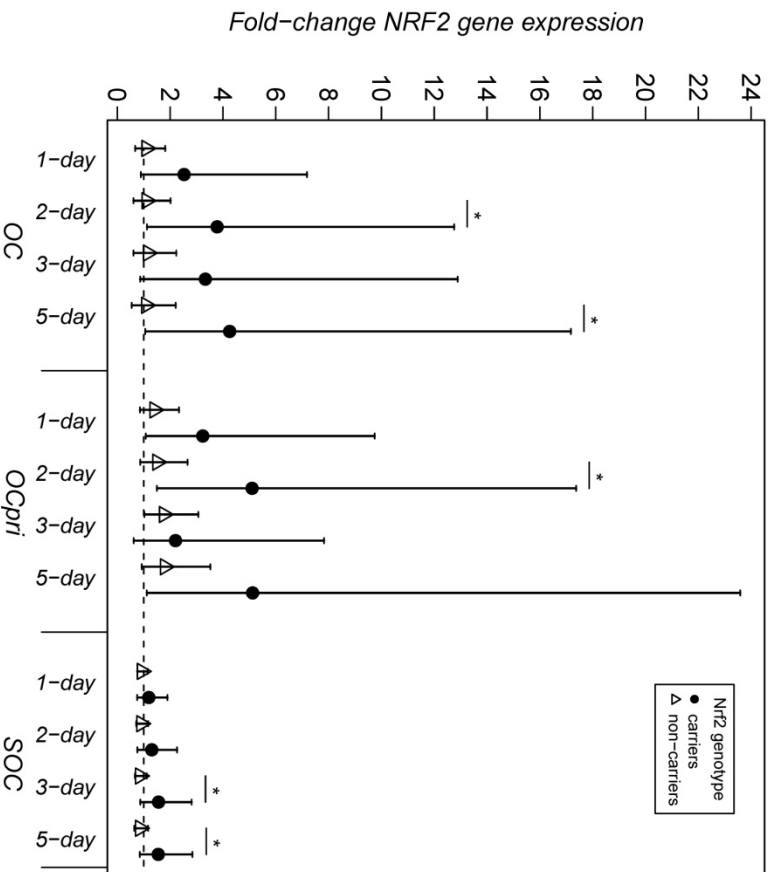


Figure 5.6. Relations between Nrf2 gene expression and exposure to total organic carbon (OC), primary OC (OCpri), and secondary OC (SOC): effect modification by Nrf2 -617 A risk allele genotype.

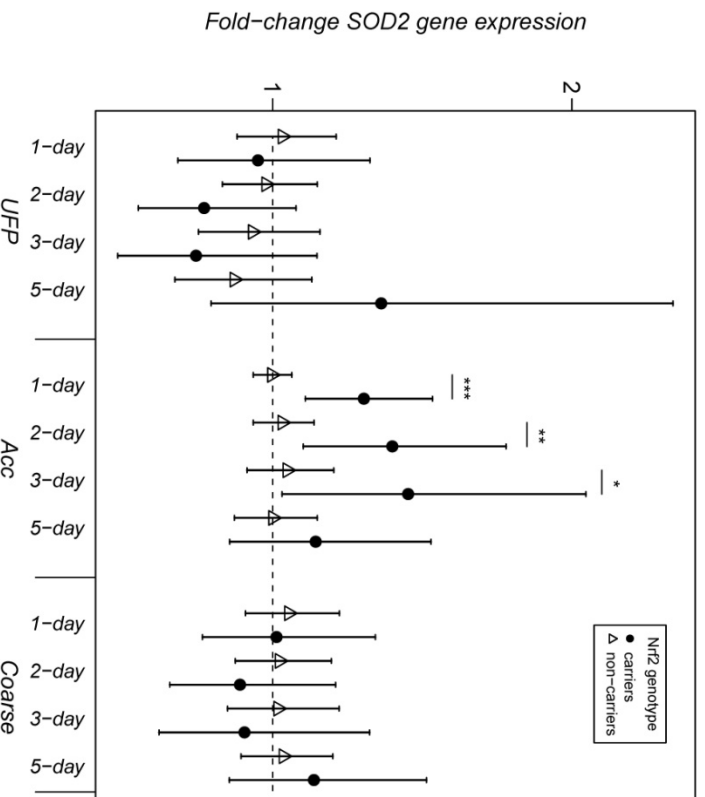


Figure 5.7. Relations between SOD2 gene expression and PM mass size fraction: effect modification by Nrf2 -617 A risk allele genotype.
 UFP: PM_{0.25}; Acc: PM_{0.25-2.5}; Coarse: PM_{2.5-10}.

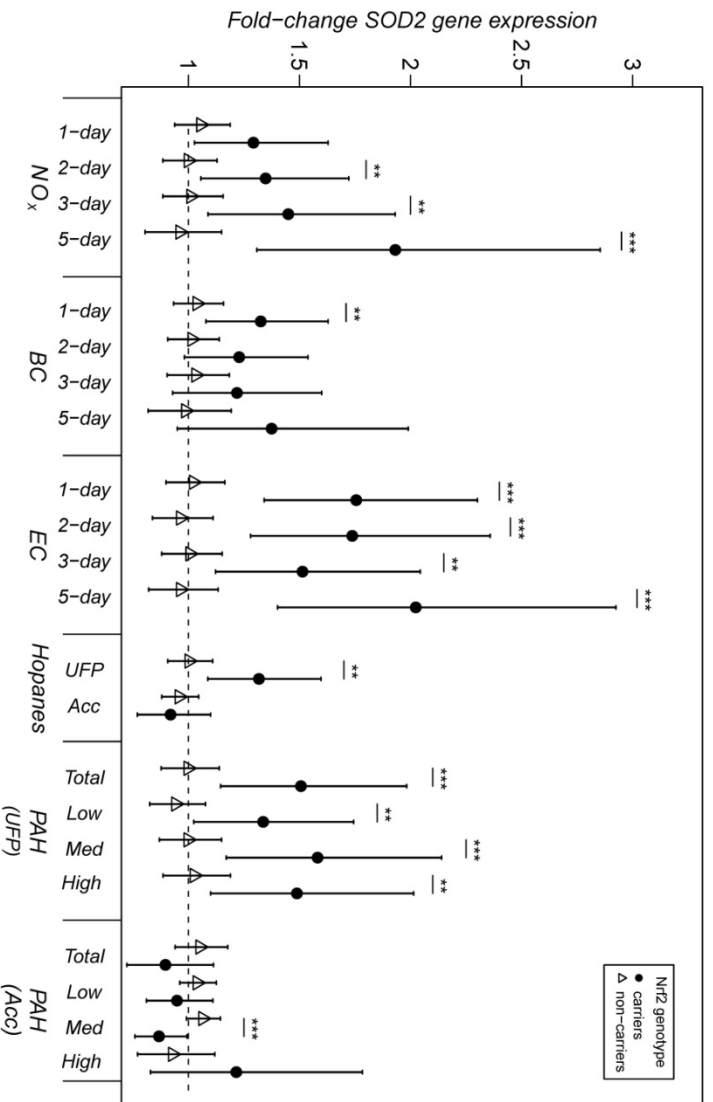


Figure 5.8. Relations between SOD2 gene expression and traffic-related air pollutants: effect modification by Nrf2-617 A risk allele genotype. Averaging time for hopanes, and PAH are 5 days (from 5-day PM filter composites). UFP: PM_{0.25}; Acc: PM_{0.25-2.5}.

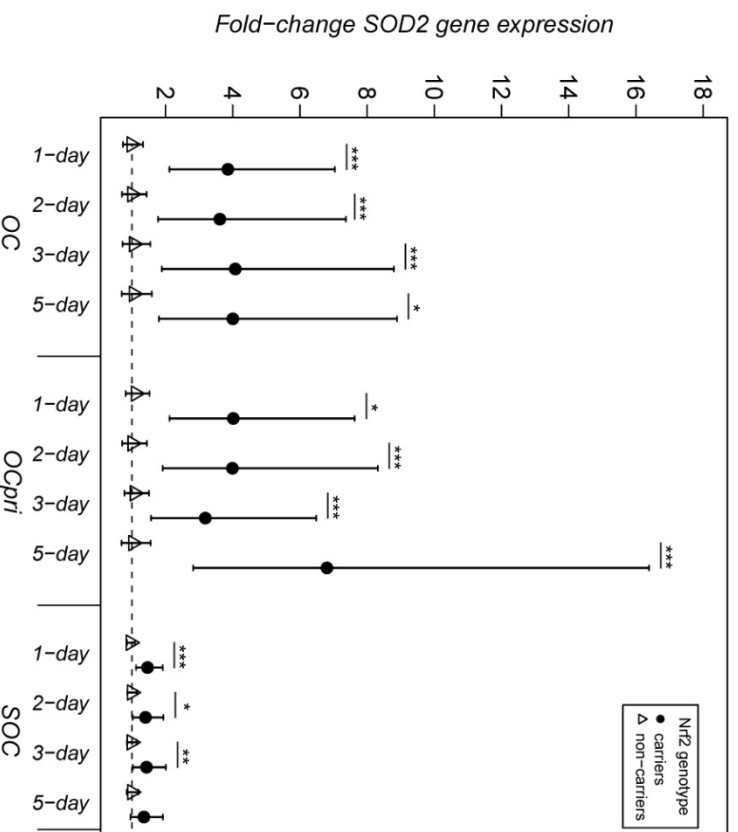


Figure 5.9. Relations between SOD2 gene expression and exposure to total organic carbon (OC), primary OC (OCpri), and secondary OC (SOC): effect modification by Nrf2-617 A risk allele genotype.

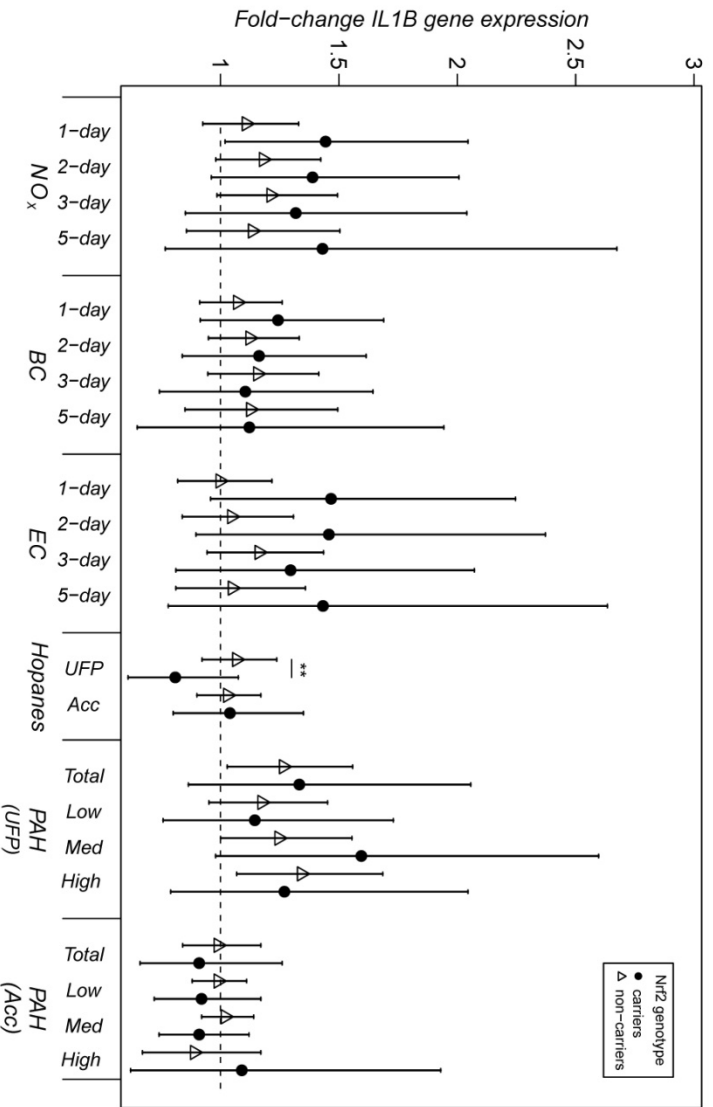


Figure 5.10. Relations between IL1B gene expression and traffic-related air pollutants: effect modification by Nrf2-617 A risk allele genotype. Averaging time for hopanes, and PAH are 5 days (from 5-day PM filter composites). UFP: PM_{0.25}; Acc: PM_{0.25-2.5}.

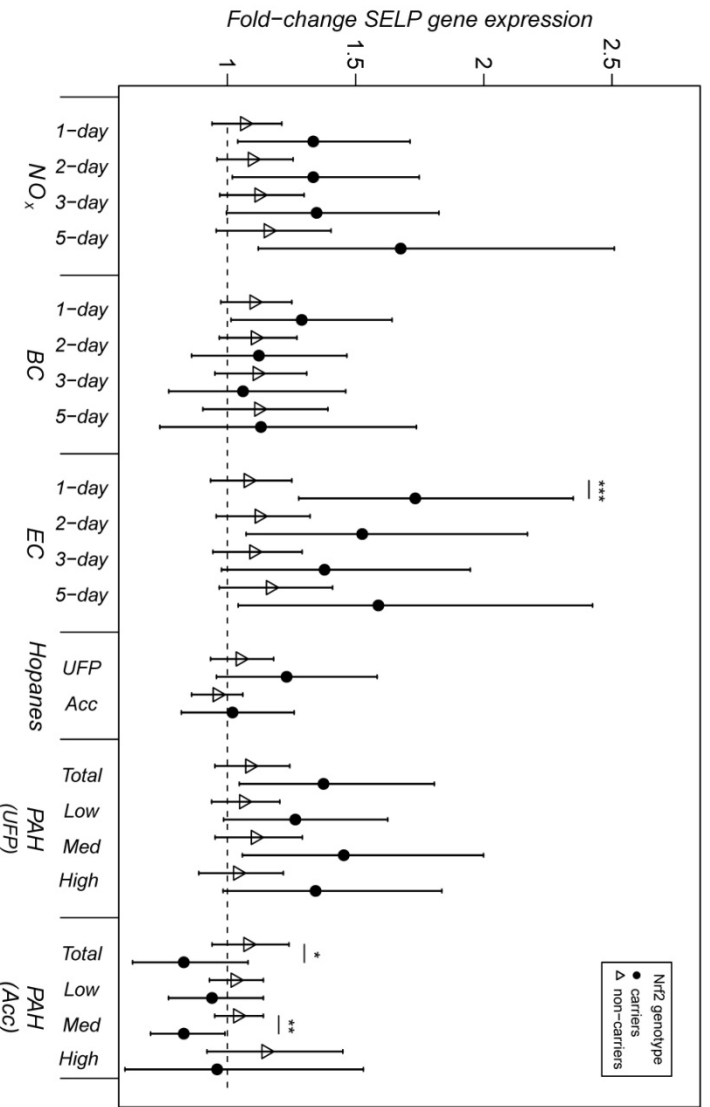


Figure 5.11. Relations between SELP gene expression and traffic-related air pollutants: effect modification by Nrf2-617 A risk allele genotype. Averaging time for hopanes, and PAH are 5 days (from 5-day PM filter composites). UFP: PM_{0.25}; Acc: PM_{0.25-2.5}.

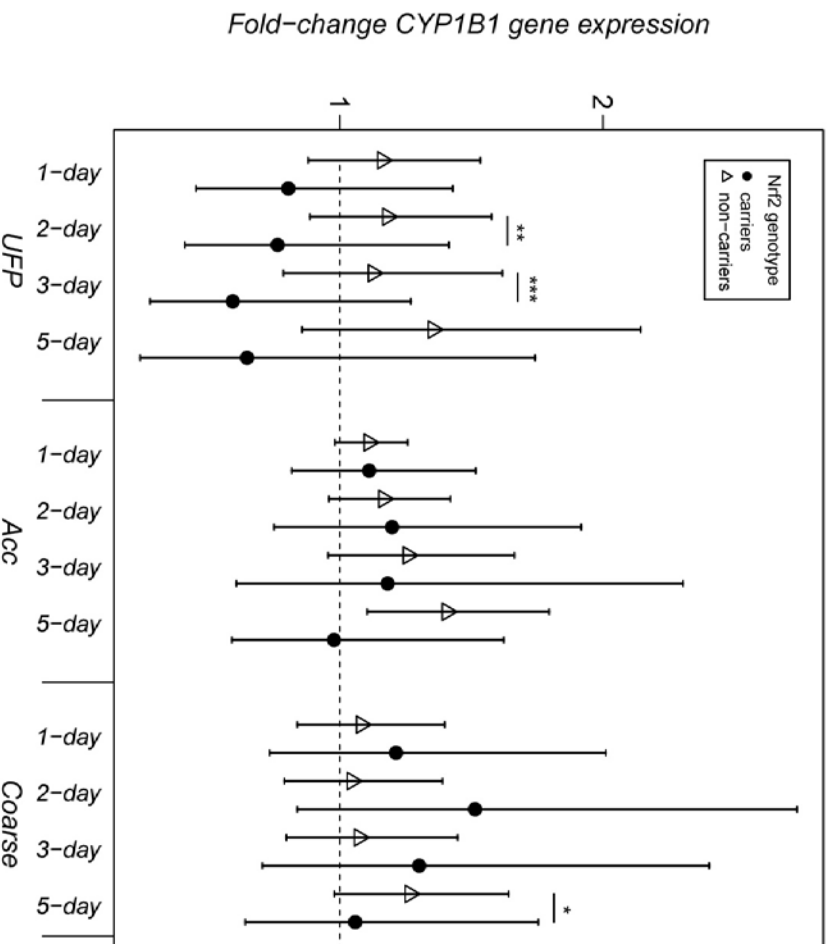


Figure 5.12. Relations between CYP1B1 gene expression and PM mass size fraction: effect modification by Nrf2-617 A risk allele genotype. UFP: PM_{0.25}; Acc: PM_{0.25-2.5}; Coarse: PM_{2.5-10}.

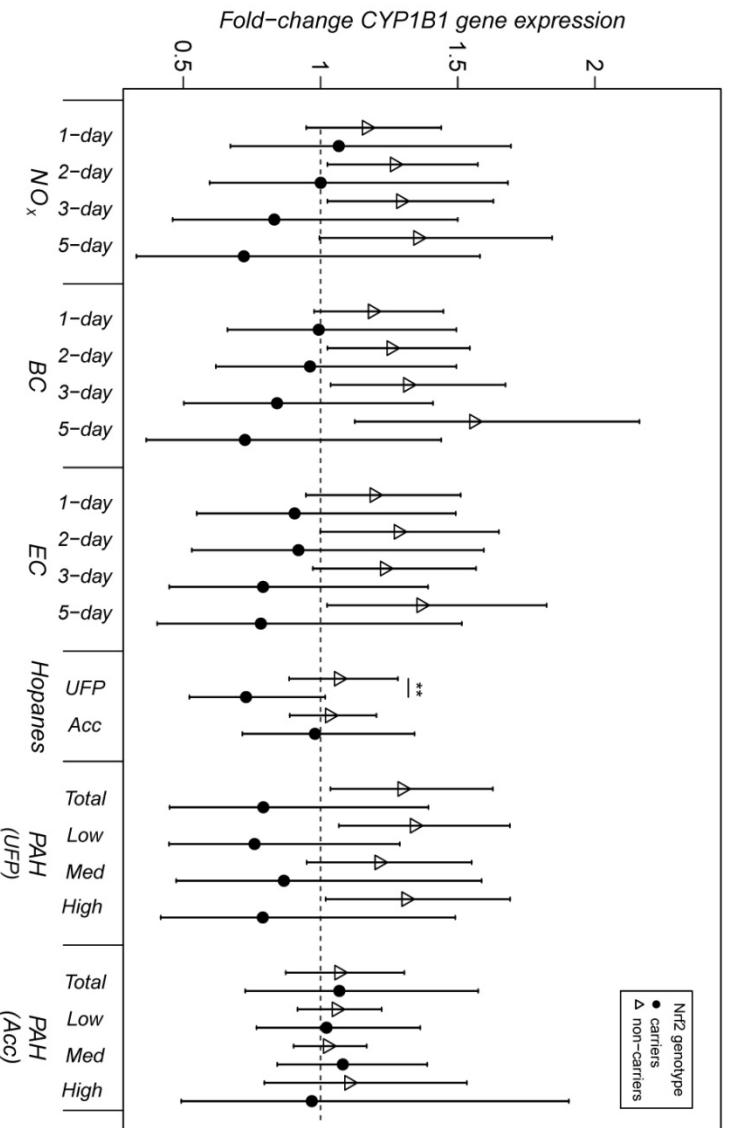


Figure 5.13. Relations between CYP1B1 gene expression and traffic-related air pollutants: effect modification by Nrf2-617 A risk allele genotype. Averaging time for hopanes, and PAH are 5 days (from 5-day PM filter composites). UFP: PM_{0.25}; Acc: PM_{0.25-2.5}.

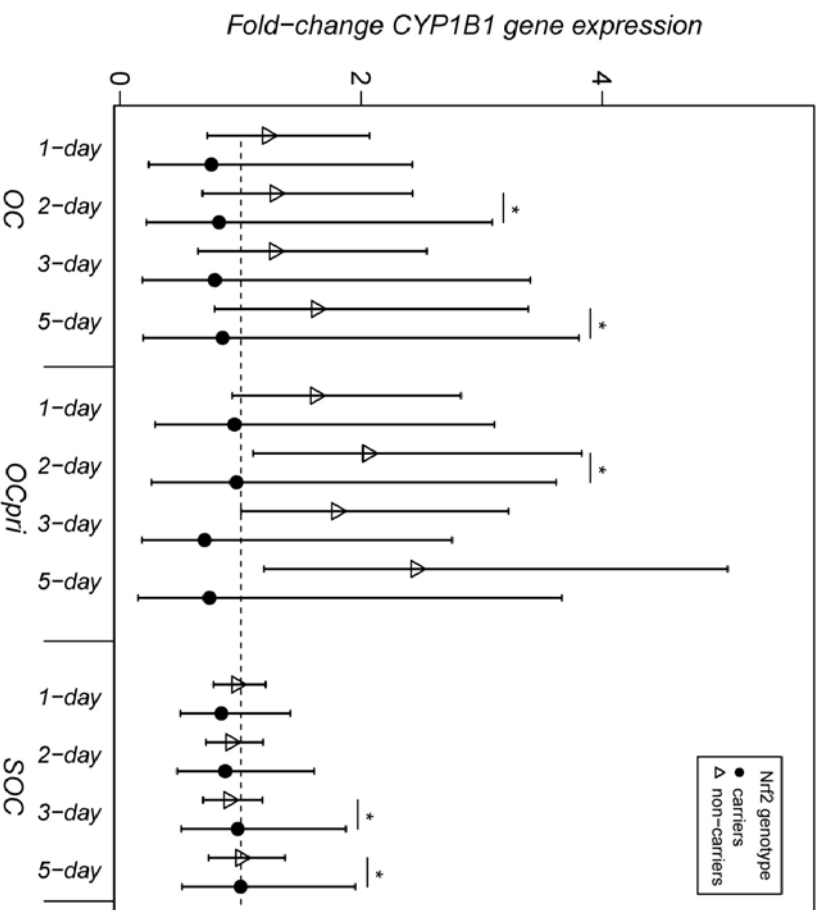


Figure 5.14. Relations between CYP1B1 gene expression and exposure to total organic carbon (OC), primary OC (OCpri), and secondary OC (SOC): effect modification by Nrf2 - 617 A risk allele genotype.

Mn-SOD (SOD2):

Background: We studied a polymorphism in an important gene that codes for a protein involved in antioxidant defense, manganese (Mn) superoxide dismutase (Mn-SOD or SOD2). SOD2 is a member of the superoxide dismutase family and functions to protect against reactive oxygen species by converting superoxide to the less reactive hydrogen peroxide. The Mn-SOD protein's active site contains manganese and functions within mitochondria. We studied the rs4880 SNP (SOD2 Ala16Val genotype) that substitutes a C>T at position 2734, resulting in a change of an amino acid in MnSOD from alanine (Ala) to valine (Val) at position 16. This results in reduced gene expression, production of an unstable mRNA, and consequent reduced import into mitochondria (Sutton et al. 2005). For this reason the SNP has been intensively studied (Crawford et al. 2012). We have determined that expression of the SOD2 gene is increased with exposure to traffic-related air pollution as described above. It is therefore of interest to identify subjects with the risk allele (Val), and investigate effect modification of the observed association between SOD2 gene expression and air pollution exposure. It is also of interest to evaluate whether this risk allele affects gene expression of other genes as well as expression of proteins that likely increase under conditions of higher oxidative stress.

Methods: To genotype our cohort we used polymerase chain reaction with restriction fragment length polymorphism analysis (adapted from Shimodo-Matsubayashi et. al. 1996). We amplified a 174 base pair region using forward primer (5'-CAGCCAGCCCTGCCGTAGACGG-3') and reverse primer (5'-GATCTGCCGGCTTGATGTGAG-3') and an annealing temperature of 64.7°C. We digested products with *Bsa* *NI* (New England Biolabs) at 60°C for 1 hour. The number of the Val

variant alleles was determined for each subject by the amount of cleaved product (0% for 2 wildtype alleles, 50% cut for heterozygotes and 100% cut for two Val alleles). A subset of 10% of subjects were repeated for validation with 100% agreement between replicates. Whole blood gene expression levels were measured using quantitative polymerase chain reactions, for a subset of 40 subjects as described above (3 subjects had insufficient DNA for analysis). Air pollutant exposures measured at subject residences were as described above. T-tests were used to assess between-gene group differences in outcomes. Linear mixed effects models were used to analyze effect modification of air pollution exposure-response relations by the polymorphism (i.e., gene-environment interaction using product terms).

Results: We found 13 non-carriers (genotype AA) and 47 carriers of the Val16 allele (29 with AV and 18 with VV). The genotypes were in Hardy-Weinberg Equilibrium in this population. We estimated the effect that carrier status had on biomarkers of inflammation using linear mixed effects models. Preliminary models showed that carriers, versus non-carriers, had increased plasma CRP (678.89 ng/mL higher than non-carriers, $p=0.0373$), MPO (11.9 mg/mL higher in carriers vs. non carriers, $p=0.0004$), TNF α (0.6603pg/mL higher in carriers, $p<0.0001$), sTNF-rII (669.6 pg/mL higher in carriers vs. non-carriers, $p<0.0001$) and sP-selectin (11.6749 ng/mL higher among carriers versus non-carriers, $p<0.0001$); and had increased erythrocyte GPx-1 activity (3.8867 U/gHb higher among carriers versus non-carriers, $p<0.0001$) and increased but non-significant erythrocyte Cu,Zn-SOD (SOD1) activity (288 U/gHb higher among carriers versus non-carriers, $p=0.127$). In contrast to the other inflammatory biomarkers (CRP, TNF α , and sTNF-rII), the levels of IL-6 were lower by 0.8177 pg/mL among carriers ($p<0.0001$) and there was no significant difference in IL6sR levels between the groups.

Most pollutant interaction models for gene expression showed few interactions between pollutant exposure and the SOD2 polymorphism (not shown). However, models of sP-selectin protein expression showed significant interactions of the SOD2 genotype with EC, primary OC, 5-day average PM_{0.25} and 1- to 3-day average PM_{0.25-2.5} among carriers versus non-carriers (Figure 5.15). Selected estimates in Figure 5.15 are shown for multiple moving average times, as indicated by the number of days on the x-axis. Expression of other protein biomarkers in relation to air pollution exposures was not modified by the SOD2 genotype. The other biomarkers were simply predicted by allele carrier status as stated in results above.

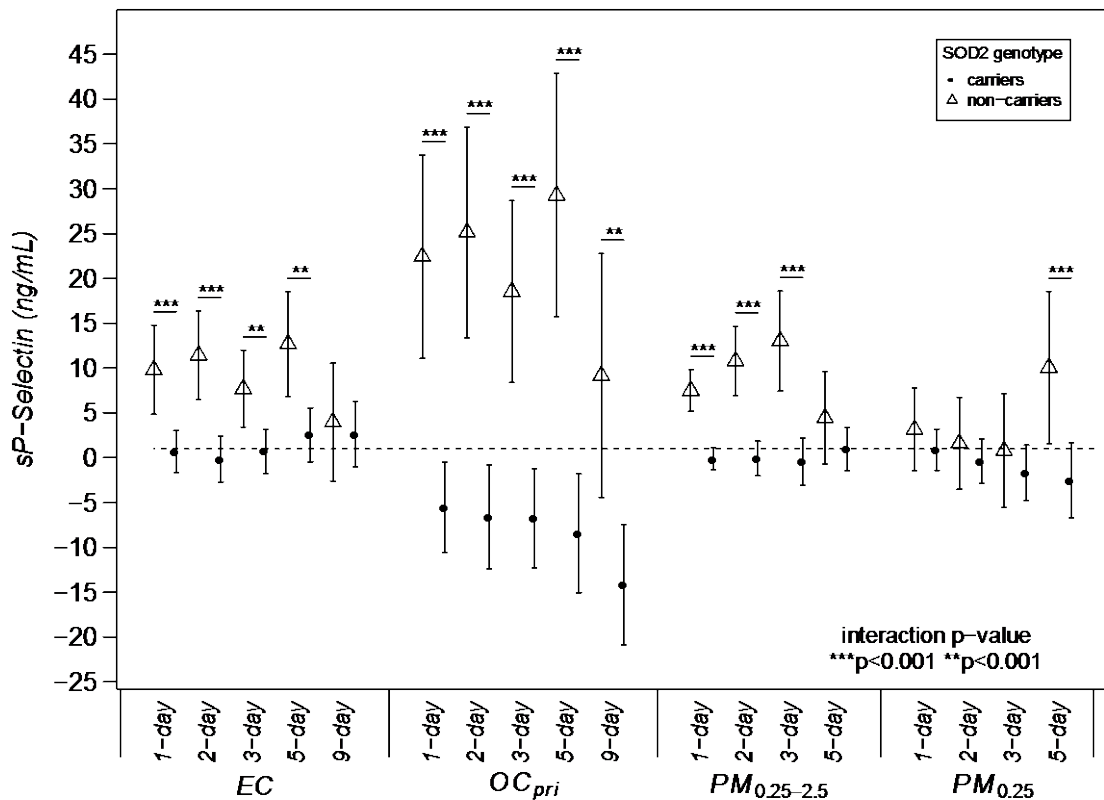


Figure 5.15. Relations between sP-selectin protein expression and selected air pollution exposures: effect modification by SOD2 Val16 risk allele genotype.

Conclusions: We found that being homozygous for the Ala16 variant, and therefore having both higher levels of Mn-SOD import into mitochondria and Mn-SOD enzymatic activity, increases levels of several inflammatory biomarkers (plasma CRP, MPO, TNF α , sTNF-riII, and sP-selectin, but not IL-6), as well as erythrocyte GPx-1 and Cu,Zn-SOD activity. This could be due to the consequent increases in levels of hydrogen peroxide, which can diffuse out of the mitochondria to damage other cellular structures. In addition, models for the interaction between this SOD2 gene variant and air pollution exposure in relation to the circulating levels of sP-selectin showed that carriers of the Val16 allele had significantly lower levels of sP-selectin in association with the air pollutant exposures. We also saw that relationships between both SOD2 and SELP gene expression and air pollutant exposures were increased by the -617A (risk) allele of the gene for Nrf2, an important oxidative stress response mediator (discussed above). This combined evidence of effect modification by SNPs in genes relevant to oxidative stress (SOD2 and Nrf2) could signify that sP-selectin gene and protein expression (which is involved in platelet activation), may be particularly sensitive to the increased oxidative stress thought to be induced by pro-oxidant air pollutant exposures. Overall, the effects of these gene variants were complex and suggested that multiple gene-gene interactions may be involved, including many genes we did not assess.

References

Carter AM, Anagnostopoulou K, Mansfield MW, Grant PJ. Soluble P-selectin levels, P-selectin polymorphisms and cardiovascular disease. *J Thromb Haemost* 2003;1(8):1718-23.

- Crawford A, Fassett RG, Geraghty DP, Kunde DA, Ball MJ, Robertson IK, Coombes JS. Relationships between single nucleotide polymorphisms of antioxidant enzymes and disease. *Gene* 2012;501:89-103.
- Delfino RJ, Staimer N, Tjoa T, et al. Air pollution exposures and circulating biomarkers of effect in a susceptible population: clues to potential causal component mixtures and mechanisms. *Environ Health Perspect* 2009;117(8):1232-8.
- Görling HH, Curran JE, Johnson MP, Dyer TD, Charlesworth J, Cole SA, Jowett JB, Abraham LJ, Rainwater DL, Comuzzie AG, Mahaney MC, Almasy L, MacCluer JW, Kissebah AH, Collier GR, Moses EK, Blangero J. Discovery of expression QTLs using large-scale transcriptional profiling in human lymphocytes. *Nat Genet.* 2007;39:1208-16.
- Marzec JM, Christie JD, Reddy SP, Jedlicka AE, Vuong H, Lanke PN, Aplenc R, Yamamoto T, Yamamoto M, Cho HY, Kleeberger SR. Functional polymorphisms in the transcription factor NRF2 in humans increase the risk of acute lung injury. *FASEB J.* 2007;21(9):2237-46.
- Misra V, Grondin A, Klamut HJ, Rauth AM. Assessment of the relationship between genotypic status of a DT-diaphorase point mutation and enzymatic activity. *Br J Cancer.* 2000;83(8):998–1002
- Siegel D, McGuinness SM, Winski SL, Ross D. Genotype-phenotype relationships in studies of a polymorphism in NAD(P)H:quinone oxidoreductase 1. *Pharmacogenetics.* 1999;9(1):113-21.
- Subramanian H, Gambaryan S, Panzer S, Gremmel T, Walter U, Mannhalter C. The Thr715Pro variant impairs terminal glycosylation of P-selectin. *Thromb Haemost.* 2012;108:963-72.
- Sutton A, Imbert A, Igoudjil A, Descatoire V, Cazanave S, Pessayre D, et al. The manganese superoxide dismutase Ala16val dimorphism modulates both mitochondrial import and mRNA stability. *Pharmacogenet Genomics.* 2005;15(5):311-9. [PMID: 15864132]
- Sutton A, Imbert A, Igoudjil A, Descatoire V, Cazanave S, Pessayre D, Degoul F. The manganese superoxide dismutase Ala16Val dimorphism modulates both mitochondrial import and mRNA stability. *Pharmacogenet Genomics.* 2005;15:311-9.
- Sutton A, Houry H, Prip-Buus C, Cepanec C, Pessayre D, Degoul F. The Ala16Val genetic dimorphism modulates the import of human manganese superoxide dismutase into rat liver mitochondria. *Pharmacogenetics.* 2003;13(3):145-57. [PMID: 12618592]
- Traver RD, Horikoshi T, Danenberg KD, Stadlbauer TH, Danenberg PV, Ross D, Gibson NW. NAD(P)H:quinone oxidoreductase gene expression in human colon carcinoma cells: characterization of a mutation which modulates DT-diaphorase activity and mitomycin sensitivity. *Cancer Res.* 1992;52(4):797-802.
- Volcik KA, Ballantyne CM, Coresh J, Folsom AR, Wu KK, Boerwinkle E. P-selectin Thr715Pro polymorphism predicts P-selectin levels but not risk of incident coronary heart disease or ischemic stroke in a cohort of 14595 participants: the Atherosclerosis Risk in Communities Study. *Atherosclerosis.* 2006;186:74-9.
- Wittkopp S, Staimer N, Tjoa T, Gillen D, Daher N, Schauer JJ, Sioutas C, Delfino RJ. Mitochondrial genetic background modifies the relationship between traffic-related air pollution exposure and systemic biomarkers of inflammation. *PLoS One,* 2013;8:e64444. doi:10.1371/journal.pone.0064444.

6. CHAPTER 6. OVERALL SUMMARY AND CONCLUSIONS

This is the first cohort panel study to report the association of gene expression with exposure to air pollution exposures in an urban home environment. We found increased expression of genes in key biological pathways in association with exposures to traffic-related air pollution in a Los Angeles cohort of elderly subjects with coronary artery disease. Associations were particularly clear for genes that are part of the Nrf2-mediated oxidative stress response pathway. Effect modification by the Nrf2 -617 A risk allele further confirms the importance of this pathway and suggests there is a more genetically susceptible population. This supports our hypothesis that traffic-related air pollutant exposures would be associated with the expression of genes in pathways that are relevant to the adverse effects of pro-oxidant air pollutant exposures. We confirmed our hypothesis that expression levels of key genes would be more strongly associated with markers of primary (combustion-related) organic aerosols than with secondary (photochemically-related) organic aerosols. Also, although there did not appear to be any clear difference in associations by particle size when using total mass concentrations, there were generally stronger associations for PM_{0.25} PAH and/or ROS than for PM_{0.25-2.5} PAH and ROS. Associations with the indoor air pollutant measurements were largely consistent with associations for the outdoor measurements. This is consistent with findings from the source apportionment work using detailed PM chemical speciation showing that although the elderly retirees of the studied communities generally spend most of their time indoors, a sizeable portion of PM_{2.5} particles to which they are exposed likely originate from outdoor mobile sources.

7. CHAPTER 7. RECOMMENDATIONS

Future studies are warranted to examine gene expression associations in other cohorts, including other geographic regions, and younger, more racially diverse, and healthier populations. This would also include other potentially susceptible populations including individuals with other important gene variants and individuals with chronic diseases such as diabetes and asthma. Experimental designs are also needed to further characterize the causal role of the Nrf2-mediated oxidative stress response pathway in cardiovascular responses to traffic-related air pollutant exposure. Our findings in Task 3 using detailed exposure data from Tasks 1-2 support the use of size-fractionated particle composition data in epidemiologic and experimental studies, including ultrafine or quasi-ultrafine PM organic components. This is relevant to potential future regulations. Ambient air quantity standards, do not include ultrafine PM or the general class of organic components from fossil fuel combustion sources that have been associated with gene expression outcomes in this study as well as cardiovascular outcomes in other analyses involving the same cohort, although many of the regulations of the Air Resources Board are designed to reduce traffic pollution. This is important to vulnerable populations because we found that mobile sources were the dominant contributor to both indoor and outdoor PM_{2.5} at all community sites.

8. Presentations and Publications

Presentations:

- Delfino RJ, Staimer N, Tjoa T, Wittkopp S, Gillen D, Shafer M, Schauer JJ, Sioutas C. Peripheral Blood Gene Expression and Traffic-related Air Pollution in Subjects with Coronary Artery Disease. Presented to: American Thoracic Society, International Conference, May 18-23, 2012, San Francisco, CA. *Am J Respir Crit Care Med* 185;2012:A3192.
- Wittkopp S, Staimer N, Tjoa T, Gillen D, Daher N, Schauer JJ, Sioutas C, Delfino RJ. Single nucleotide polymorphism -617 C/A in the Nrf2 gene promoter modifies gene expression-air pollution relationships in subjects with coronary artery disease. Joint ISEE, ISES and ISIAQ Environmental Health Conference 2013 in Basel, Switzerland August 19-23, 2013.
- Wittkopp S, Staimer N, Tjoa T, Gillen D, Shafer M, Schauer JJ, Sioutas C, Delfino RJ. Effect Modification of Associations between Air Pollution and Biomarkers of Inflammation by Mitochondrial Haplogroup. Presented to: American Thoracic Society, International Conference, May 18-23, 2012, San Francisco, CA. *Am J Respir Crit Care Med* 185;2012:A3805.
- Wittkopp S, Staimer N, Tjoa T, Gillen D, Daher N, Shafer M, Schauer JJ, Sioutas C, Delfino RJ. Thr715Pro polymorphism in the platelet selectin gene does not modify effects of air pollution exposure. Submitted to: scientific meeting of the American Heart Association sponsored by the Council on Epidemiology and Prevention and the Council on Nutrition, Physical Activity and Metabolism, March 18-12, 2014, San Francisco.

Publications:

- Wittkopp S, Staimer N, Tjoa T, Gillen D, Daher N, Shafer M, Schauer JJ, Sioutas C, Delfino RJ. Mitochondrial genetic background modifies the relationship between traffic-related air pollution exposure and systemic biomarkers of inflammation. *PLoS One*, 2013;8:e64444. doi:10.1371/journal.pone.0064444.
- Wittkopp S, Staimer N, Tjoa T, Gillen DL, Shafer MM, Schauer J, Sioutas C, Delfino RJ. Associations between peripheral blood gene expression and traffic-related air pollution in subjects with coronary artery disease. For submission to *JESEE* 02/2014.

9. Abbreviations

AER: air exchange rates
BAM: Beta-Attenuation Mass
BC: black carbon
CAD: coronary artery disease
cDNA: complementary DNA
CHAPS: Cardiovascular Health and Air Pollution Study
CI: confidence interval
CMB: chemical mass balance model
CO: carbon monoxide
CPI: carbon preference index
EC: elemental carbon
ER : endoplasmic reticulum
F_{inf}: infiltration factors
G1-4: Groups 1-4HDV: heavy-duty vehicles

I/O: indoor/outdoor ratio
IQR: interquartile range
LDV: light-duty vehicles NO₂: nitrogen dioxide
NO_x: nitrogen oxides
O₃: ozone
OC: organic carbon
OC_{pri}: organic carbon attributed to primary organic carbon
PAH: polycyclic aromatic hydrocarbons
PCR: polymerase chain reaction
PM: particulate matter
PM_{0.25}: quasi-ultrafine particulate matter < 0.25 micrometers in aerodynamic diameter
PM_{0.25-2.5}: accumulation particulate matter 0.25-2.5 micrometers in aerodynamic diameter
PM_{2.5-10}: coarse mode particulate matter 0.25-2.5 micrometers in aerodynamic diameter
PM₁₀: particulate matter < 10 µm in aerodynamic diameter
PM_{2.5}: particulate matter < 2.5 µm in aerodynamic diameter
PN: particle number
POA: primary organic aerosols
RNA: ribonucleic acid
ROS: reactive oxygen species
SOA: secondary organic aerosols
SOC: organic carbon attributed to secondary organic carbon
UFP: ultrafine particles, PM < 0.1 µm in aerodynamic diameter
UPR: unfolded protein response
WIOM: water-insoluble organic matter
WSOC: water soluble organic carbon

10. Appendix. Permutation Analysis Results for *NFE2L2*.

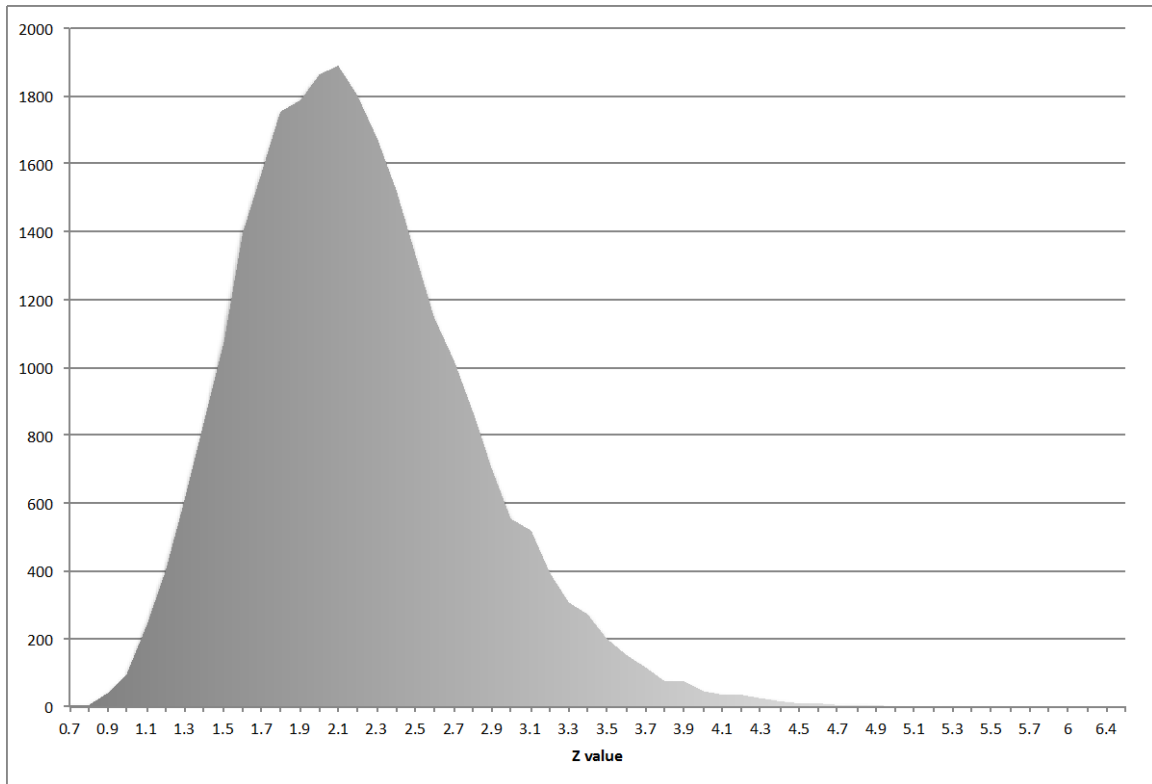


Figure S1. Distribution of simulated Z values from permutation analysis. $Z =$ regression coefficient divided by standard error.

Table S1. Z_{observed} for several *NFE2L2* model coefficients

Pollutant	Regression Estimate	Z observed	Unadjusted p-value	Adjusted p-value
Elemental Carbon				
1-day	1.1604	1.4408	0.1508	0.9007
2-day	1.1840	1.5001	0.1348	0.8710
3-day	1.1841	1.5266	0.1280	0.8619
5-day	1.2152	1.4575	0.1461	0.8938
7-day	1.4922	2.2322	0.0264	0.4006
Black Carbon				
1-day	1.2247	2.3411	0.0199	0.3310
2-day	1.1947	1.9440	0.0529	0.5989
3-day	1.1938	1.6391	0.1023	0.8002
5-day	1.2030	1.2295	0.2199	0.9638
7-day	1.3112	1.4343	0.1526	0.9033
Primary Organic Carbon				
1-day	1.5306	1.7300	0.0848	0.7439
2-day	1.6671	1.8178	0.0703	0.6853
3-day	1.6281	1.7779	0.0765	0.7132
5-day	1.7582	1.6811	0.0938	0.7759
7-day	2.5108	2.4097	0.0166	0.2946
NO _x				
1-day	1.2435	2.2249	0.0269	0.4054
2-day	1.1857	1.6888	0.0923	0.7712
3-day	1.1853	1.5373	0.1253	0.8561
5-day	1.1549	0.9819	0.3270	0.9951
7-day	1.2531	1.2127	0.2262	0.9675
Size Fractionated PM mass				
PM _{0.25}	1.0902	0.4160	0.6777	1.0000
PM _{0.25-2.5}	1.1110	0.9887	0.3236	0.9948
PM _{2.5-10}	1.1473	1.2292	0.2200	0.9639
PM _{0.25} PAH				
Total	1.1173	1.0108	0.3130	0.9934
Low Molecular Weight	1.0998	0.8569	0.3922	0.9987
Medium Molecular Weight	1.1261	1.0172	0.3099	0.9928
High Molecular Weight	1.1205	0.9187	0.3590	0.9977
PM _{0.25} Macrophage ROS	1.1486	1.7282	0.0850	0.7451
PM _{0.25-2.5} PAH				
Total	1.1898	1.9885	0.0477	0.5676
Low Molecular Weight	1.0784	1.2161	0.2249	0.9666
Medium Molecular Weight	1.1040	1.7442	0.0822	0.7345
High Molecular Weight	1.3362	2.0115	0.0452	0.5514
PM _{0.25-2.5} Macrophage ROS	0.9979	-0.0167	0.9867	1.0000

Regression estimates are given as fold-change per IQR increase in pollutant level. NO_x = nitrogen oxides, PM_{0.25} = particulate matter <0.25 μm in aerodynamic diameter, PAH = polycyclic aromatic hydrocarbons.